(10)

WADC TECHNICAL REPORT 59-702
PART II

MECHANICAL PROPERTIES OF SELECTED ALLOYS AT ELEVATED TEMPERATURES

PART II: DESIGN CRITERIA OF SILICON CARBIDE

Harry A. Pearl
John M. Nowak
Harry G. Deban

MARCH 1960

WRIGHT AIR DEVELOPMENT DIVISION

WADC TECHNICAL REPORT 59-702
PART II

MECHANICAL PROPERTIES OF SELECTED ALLOYS AT ELEVATED TEMPERATURES

PART II: DESIGN CRITERIA OF SILICON CARBIDE

Harry A. Pearl
John M. Nowak
Harry G. DeBan

Bell Aircraft Corporation

MARCH 1960

Materials Laboratory
Contract No. AF 33(616)-5760
Project No. 7381

WRIGHT AIR DEVELOPMENT DIVISION
AIR RESEARCH AND DEVELOPMENT COMMAND
UNITED STATES AIR FORCE
WRIGHT-PATTERSON AIR FORCE BASE, OHIO

500 – April 1960 – 31-915

FOREWORD

This report was prepared by the Engineering and Research Laboratories, Bell Aircraft Corporation under USAF Contract No. AF33(616)-5760. This contract was initiated under Project No. 7381, "Materials Application", Task No. 73812, "Materials Information Services". The work was administered under the direction of the Materials Laboratory, Directorate of Laboratories, Wright Air Development Center, with Mr. A. W. Brisbane acting as Project Engineer.

This report covers work conducted from July 1958 to September 1959.

This program was administered at Bell Aircraft Corporation by Mr. Harry A. Pearl, Chief - Materials Section, Mr. John M. Nowak, Materials and Processes Group Engineer, and Mr. Harry G. DeBan, Materials and Processes Engineer. Included among those who cooperated in this program were Mr. F. M. Anthony, Assistant Chief for Leading Edge Projects, Structures Section, Mr. R. W. Buckman, Jr., Metallurgical Engineer and technicians of the Materials and Processes Laboratory and the Metallurgical Laboratory.

ABSTRACT

A study was made of nondestructively testing silicon carbide by density and density uniformity, dynamic modulus by sonic technique, X-ray diffraction under transverse load, electrical resistivity, and internal friction. Dynamic modulus of silicon carbide was experimentally determined at 80 F and 2200 F. Modulus of rupture tests were conducted at 80 F, 2200 F and 2400 F.

The variability of the properties of the silicon carbide and the lack of simple correlations between the properties and geometry require the use of a statistical approach to correlate mechanical properties and geometry. A theoretical analysis is presented on the effect of specimen size, surface finish, and methods of loading on the strength properties of silicon carbide.

Available literature and manufacturers' property data for various types and forms of commercially available silicon carbide are tabulated. Various areas of possible application of silicon carbide in aircraft and missiles and design parameters for leading edge applications are given.

PUBLICATION REVIEW

This report has been reviewed and is approved.

FOR THE COMMANDER:

W. J. TRAPP
Chief, Strength and Dynamics Branch
Metals and Ceramics Division
Materials Laboratory

TABLE OF CONTENTS

TABLE OF CONTENTS (Continued)

TABLE OF CONTENTS (Continued)

LIST OF ILLUSTRATIONS

LIST OF ILLUSTRATIONS (Continued)

LIST OF ILLUSTRATIONS (Continued)

LIST OF ILLUSTRATIONS (Continued)

LIST OF ILLUSTRATIONS (Continued)

LIST OF ILLUSTRATIONS (Continued)

LIST OF TABLES

I INTRODUCTION

Part II of this program (Contract AF33(616)-5760) was a research effort to determine in broad parameters the areas where a brittle, non-metallic body such as silicon carbide might be used in aircraft construction; isolating the design properties required; and establishing methods for obtaining these properties.

Due to the limited effort type of program contracted as Part II, study on non-destructive testing techniques was to be emphasized. The non-destructive tests were to be selected on the basis of usefulness in evaluating silicon carbide as an aircraft and missile leading edge material. KT silicon carbide, a product of the Carborundum Company, was approved by WADC as the material to be used in this study. The test temperature order of priority was room temperature, then 2400 F; and if manhours permitted, some intermediary temperature.

The following program was agreed upon at a conference held on 12 September 1958 at Wright Air Development Center between the personnel of the Materials Laboratory, WADC and of the Engineering and Research Laboratories, Bell Aircraft Corporation.

A. Theoretical and Literature Survey Phase

1. A limited review of literature for various types and forms of commercially available silicon carbide was to be conducted. Available property data of these carbides were to be tabulated.

2. Various areas of possible application of silicon carbide in aircraft and missiles were to be listed. Design parameters were to be listed, if readily available.

3. Design parameters for aircraft and missile leading edge application and reasons for selection of the parameters were to be given.

B. Testing Phase

1. Determination of Density and Density Uniformity

a. Density Determination

The density of the test specimen would be determined by the water displacement method using a Krauss Jolly Balance.

Manuscript released by the authors January 1960 for publication as a WADC Technical Report.

b. Density Uniformity

(1) Industrial X-Ray

Industrial X-ray would be utilized to enable visual inspection of uniformity; detection of flaws; etc.

(2) Densitometer Comparator

The densitometer comparator would be used to scan the industrial X-ray photographs and automatically record the density variance.

(3) Ultra-Sonic Inspection

Ultra-sonic inspection for density uniformity would be limited to an extremely low level of effort since the University of Illinois was performing a WADC program for the development of such non-destructive inspection method for ceramics, cermets, and graphite.

2. Dynamic Modulus - Sonic Technique

Dynamic modulus would be determined by a sonic technique at room temperature and then at 2200 F.

3. X-Ray Diffraction Under Transverse Load

X-ray diffraction of KT silicon carbide under transverse load would be examined in an effort to determine whether non-linear areas exist in the stress strain curve when strain is measured in Angstrom units. It was emphasized that this test was theoretical in nature. It was anticipated that insight may be gained in the nature and manner of failure of the material. Experimental work would be limited to indicating feasibility.

4. Electrical Resistivity

An attempt would be made to determine the change of electrical resistivity of the silicon carbide due to compression or bending stresses. A meaningful relation would enable correlating the change in electrical resistivity with mechanical stress-strain.

5. Internal Friction

A limited amount of testing would be initiated to investigate the internal friction of silicon carbide.

6. Modulus of Rupture

Modulus of rupture would be the only destructive test to be conducted. One and two point loading systems would be used.

C. Test Specimen Geometry

The various types of test specimen geometry to be utilized would be dependent on allocated manhours. The immediate program would utilize rectangular bars, unpolished (as fabricated) and polished to a nominal finish of 60 microinches.

This program was exploratory in nature and the results may or may not be conclusive.

The following materials, considered to be off the shelf items by the manufacturer, were ordered:

- 25 KT silicon carbide test bars 6" x 1/2" x 1/4" ±0.003" ground to at least 60 microinches.

- 25 KT silicon carbide test bars 6" x 1/2" x 1/4" ±0.003" "as fabricated".

Throughout the body of this report the following code letters are used to identify the specimen:

D = 6" x 1/2" x 1/4" ground to at least 60 microinches.

H = 6" x 1/2" x 1/4" "as fabricated", surface finish approximately 350 microinches.

G = 5" x 1/4" x 1/4" ground to at least 60 microinches.

II LITERATURE REVIEW

A. General

A literature survey and direct vendor contacts for the various types, forms, and properties of commercially available silicon carbide were conducted. Although the emphasis was on commercially available materials, limited available data on new developments or items in the research phase were also collected.

Detailed technical data on various silicon carbide bodies are given in Table I. High temperature erosion test data on silicon carbide-bonded graphite are given in Table II. Ablation test data for KT silicon carbide and silicon carbide bonded graphite is given in Figure 1.

With the exception of single crystal growths, silicon carbide bodies are usually silicate-bonded, silicon nitride-bonded, silicon-bonded, and self bonded (densified).

A general comparison of the various bonded silicon carbides follows.

1. Silicate-Bonded

   a. Also called ceramic or clay bonded

   b. Oldest and most widely used

   c. Bond softens at 2200 to 2750 F

   d. Bond attacked by certain chemicals

   e. Produces excellent refractory for many purposes but less refractory than pure SiC

   f. Bonded SiC materials are porous

   g. Undergoes volume change during firing (prevents close dimensional tolerances)

   h. Lacks resistance to thermal shock

2. Silicon Nitride-Bonded

   a. Higher strength at high temperatures than silicate-bonded SiC

   b. Nitride bond more refractory than silicate bond, does not soften but decomposes at 3450 F (inert atmosphere).

   c. Can be made to closer tolerances than silicate bonded SiC since volume does not change during firing

d. Formed by compacting, pressing, or casting

e. Superior in thermal shock resistance to the silicate bonded SiC

f. More resistant to certain materials than silicate-bonded SiC (e.g., molten Al, molten cryolite)

g. Less refractory than pure SiC and less chemically inert

h. Porous, somewhat permeable refractory (to a lesser degree than the silicate bonded SiC)

3. Silicon-Bonded

a. Some are quite dense

b. High strength and excellent oxidation resistance at moderate temperatures

c. Use limited by the 2600 F melting point of silicon

4. Self Bonded (Densified)

a. Flexural strength is 2 to 3 times that of other types of bonded SiC at room temperature. At high temperatures, e.g., 2700 F, the difference is more marked.

b. Modulus of elasticity is much higher than that of silicate - or nitride-bonded wares, the difference being greater at elevated temperatures.

c. Thermal conductivity appears to be higher than that of any other ceramic material at elevated temperatures (exception - graphite). Thermal conductivity is better than 2-1/2 times that of stainless steel at 1100 F.

d. Thermal expansion is low

e. Thermal shock characteristics should be good due to high thermal conductivity and low thermal expansion

f. Abrasion resistance is 2 to 4 times better than silicate - or nitride-bonded SiC

g. Densified silicon carbide is a semiconductor having a negative temperature-resistivity characteristic. At room temperature its resistivity is about 0.05 ohm-inches, decreasing to about 0.02 ohm-inches at 2000 F

h. Inert to most chemicals at room temperature. Excellent resistance to oxidation at temperatures up to 3000 F (protective silica coating forms at high temperatures of about 2560 F).

i. Attacked at moderate or high temperatures by fused alkalies, iron, iron oxide, copper oxide, chlorine

j. Resistance to chemical attack at moderate or high temperatures is superior to that of granular silicon carbide.

k. Silicate or silicon nitride-bonded SiC disintegrates in $HF-HNO_3$ mixture, the mixture produces no dimensional changes in self-bonded SiC.

l. Self-bonded SiC has high emissivity, low absorption of thermal neutrons, possesses excellent resistance to spark erosion.

m. Formed by conventional methods (pressing, casting, extruding)

n. Formed parts are subjected to a special high temperature treatment that produces a dense self-bonded body

o. Surface is rather rough due to crystal growth during heat treatment.

p. Smooth, dense surface produced by rough grinding or polishing

q. Grinding and polishing can produce a surface finish as low as 5 micro-inches.

r. Hot pressed SiC not commercially available

B. New Developments

Charmotte-Industries Hagenburger Schwalb A. G. of Pfalz, West Germany report (Reference 18) the development of a coating for the protection of silicon carbide at 3000 F. Known as Vanal linings, these materials are said to take advantage of surface and interface tension as a means of repelling corrosive liquids and gases and to "neutralize the capillary action in such porous materials as silicon carbide, preventing oxidation without altering heat conductivity". The coating was developed for furnace use and it is claimed that coatings a few thousandths of an inch thick are effective in providing "many years" of protection. Correspondence was initiated twice with Charmotte-Industries for more detailed technical data, however, no replies were received. The publisher of Reference 18 was unable to furnish further details than those appearing in the publication. (Reference 19)

A new development recently announced by the Carborundum Company is KT silicon carbide foam. The foam is in an open cellular form of self-bonded silicon carbide and is available in two density ranges, 0.2 to 0.3 gram/cc and 0.5 to 0.6 gram/cc. Detailed property data are given in Table I. Figure 2 is a photograph of various shapes and applications of the foam. Experimental work with this foam is currently being conducted by the Engineering and Research Laboratories of Bell Aircraft Corporation under Air Force Contract Number AF33(616)-5930 Refractory Inorganic Materials for Structural Applications.

The American Lava Corporation has developed a fine grain silicon carbide body designated as Alsimag 687 (Reference 12 and 13). Available data are given in Table I. The material is still considered to be a research item and the information presented should not be construed as being conclusive.

The effect of nuclear radiation on silicon carbide is reported in Reference 20.

Horizons, Incorporated, have developed a method for the vapor deposition of silicon carbide. Published technical data on this vapor deposited silicon carbide is not currently available.

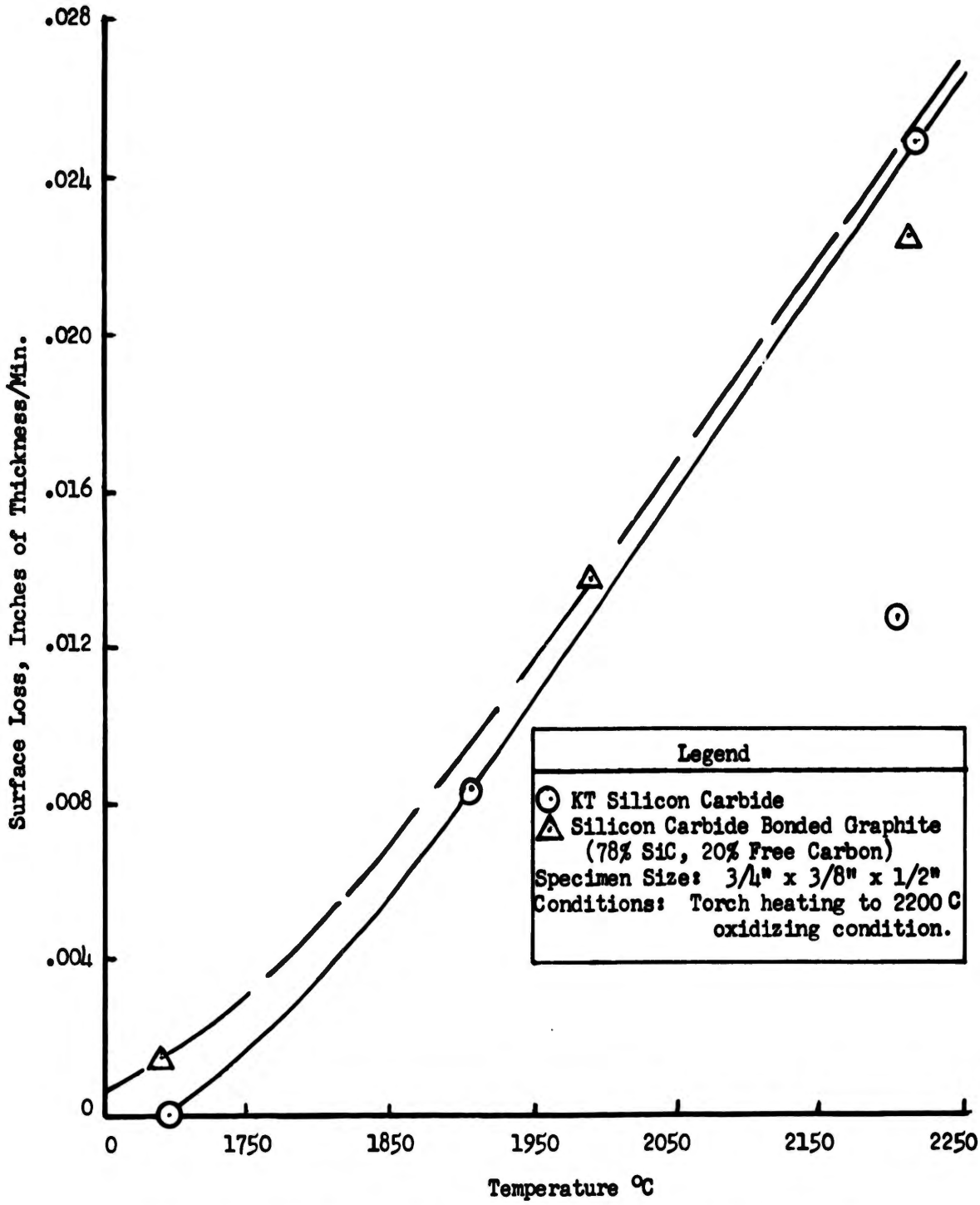

Figure 1. Ablation Test Data on KT Silicon Carbide and Silicon Carbide-Bonded Graphite After 10 Minute Exposure Time (Source: Reference 22)

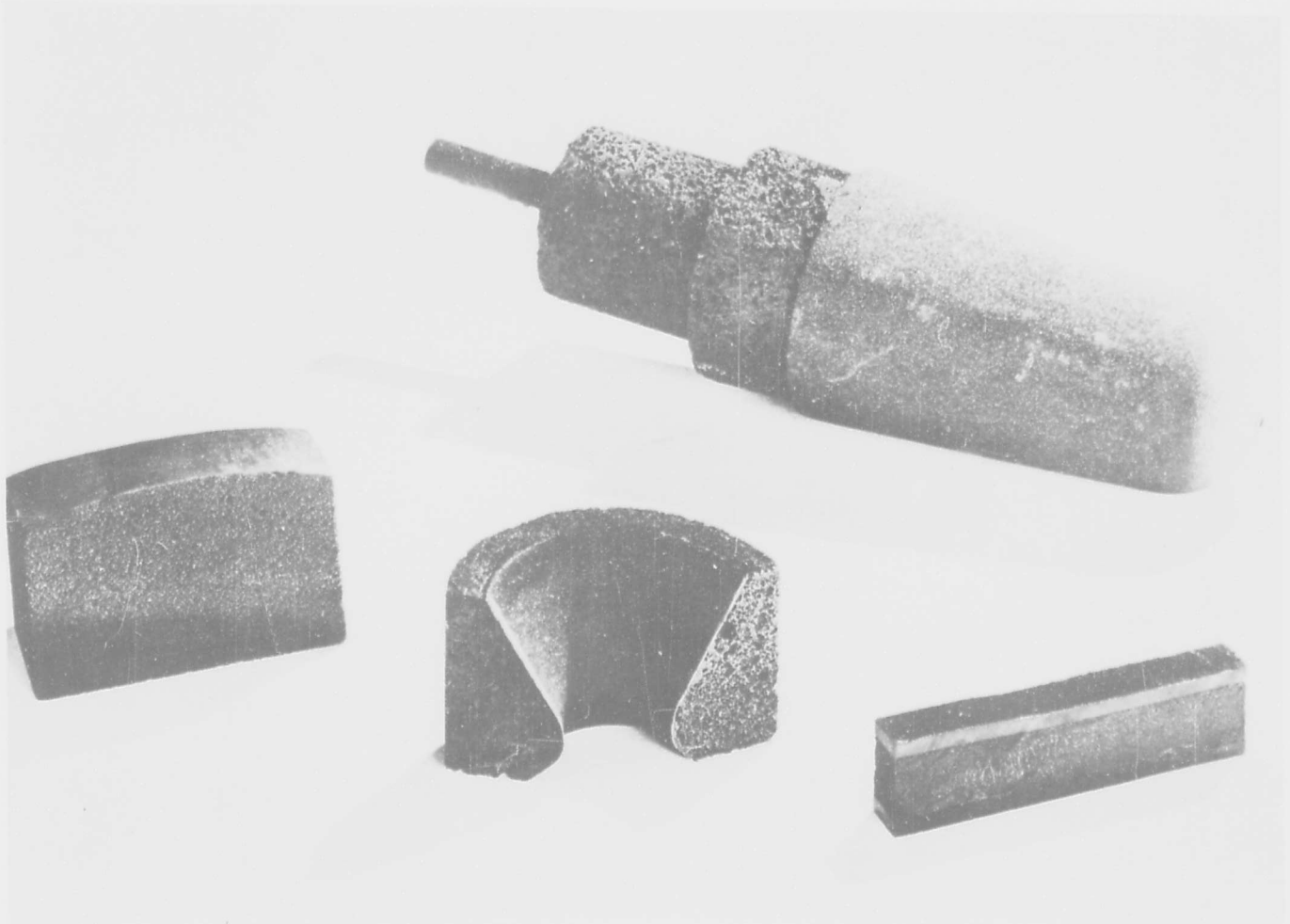

Figure 2. Silicon Carbide Foam - Coated and Laminated Surfaces of Dense, Self Bonded Silicon Carbide (Photo Courtesy of Research and Development Division, Carborundum Company)

TABLE I

LITERATURE AND MANUFACTURERS' DATA ON SILICON CARBIDE FORMULATIONS

MATERIAL / Property	SILICATE BONDED	SILICON NITRIDE-BONDED		SILICON-BONDED	SELF-BONDED			GRANULAR		FOAM		COATING	SILICON CARBIDE BONDED GRAPHITE	
	Carborundum	Carborundum	Norton	Carborundum	Carborundum RT SiC		Norton	American Lava		Carborundum		Norton	Carborundum GRB	
	Carbofrax	Refrax	Crystolon N	Durig	Coarse Grit	Fine Grit	Crystolon R	Alsimag 539 Coarse Grain	Alsimag 687 Fine Grain	SiC Foam		Crystolon C	High Free Carbon	Low Free Carbon
Density grams/cc	2.6(2)	2.9(2)	2.6	2.4		3.1(16)	2.4 - 2.6	2.2	3.0	0.25-0.30	0.50-0.60	1.7	2.3	2.8
Sustained Working Temperature - maximum														
Oxidising Atmosphere	2900 F	3000 F	2900 F	2450 F (2730 F short time)		3000 F(16)		2642 F	2700 F	3000 F	3000 F	Varies, above 4000 F in some cases	1500 F	2800 F
Inert Atmosphere	3200 F	3200 F	-	-		4000 F	4200 F			4000 F	4000 F		4000 F	4000 F
Porosity percent	9 - 17	6 - 10	18 - 20	6		Negligible (16)	18 - 25	Highly Porous	Non Porous	90	80			
Modulus of Rupture psi x 10^{-3}	2.2 : 77 F (2) .8 to 3. : 2370 F (6)	5.5 : 77 F(2) 5.5 : 1292 F 7.0 : 1832 F 5.9 : 2462 F 3.0 : 2732 F	6.0 : 70 F 7.0 : 2300 F	3.0 : 70 F 12 : 2450 F	15 : 77 F(6) 16 : 2192 F 13 : 2732 F	24 : 77 F(6) 25 : 2192 F 18 : 2732 F	10 linear from 70 F to 2650 F	4.0 : 77 F	20 : 77 F				7.1 : 2730 F	8.7 : 1830 F 12 : 2730 F
Modulus of Elasticity psi x 10^{-6}	13.2 : 77 F (2)	17 : 77 F(2) 16 : 1292 F 9.5 : 1832 F	20 : 70 F		38.8 : 77 F (6) 61.4 : 2192 F 66.7 : 2732 F	68.5 : 77 F (6) 61.5 : 2192 F 49.4 : 2732 F	2.3 : 70 F							30 : 1830 F
Thermal Conductivity BTU/(hr)(ft²)(F/in)	109 : 2200 F	113.5 : 2200 F	66.7 : 494 F 74.9 : 1304 F	>110		710 : 392 F (6) 500 : 752 F 400 : 1112 F 333 : 1472 F 293 : 1832 F	130	87	1162 : 77 F 174.2 : 1832 F	6 to 8 : 800 to 1900 F	11 to 14 : 800 to 1900 F	100 : 1800 F mean		700 : 400 F 470 : 1000 F 350 : 1600 F
Specific Heat BTU/lb/F	0.2875 : 0 F to 2500 F(2)	0.197 : 32 F (2) 0.297 : 1832 F 0.372 : 2552 F				0.331 : (16) 0 F to 2550 F								
Poisson's Ratio						0.27(17)								
Softening Temperature								3272 F	>4000 F					

TABLE I (Continued)

LITERATURE AND MANUFACTURERS' DATA ON SILICON CARBIDE FORMULATIONS

MATERIAL / Property	SILICATE BONDED	SILICON NITRIDE-BONDED		SILICON-BONDED	SELF-BONDED			GRANULAR		FOAM		COATING	SILICON CARBIDE BONDED GRAPHITE	
	Carborundum	Carborundum	Norton	Carborundum	Carborundum RT SiC		Norton	American Lava		Carborundum		Norton	Carborundum GRB	
	Carbofrax	Refrax	Crystolon N	Durity	Coarse Grit	Fine Grit	Crystolon R	Alsimag 539 Coarse Grain	Alsimag 687 Fine Grain	SiC Foam		Crystolon C	High Free Carbon	Low Free Carbon
Coefficient of Linear Thermal Expansion x 10^6/F	2.44 : 0(2) to 2500 F	1.81 : 77 to 392 F 2.09 : 77 to 752 F 2.26 : 77 to 1112 F 2.38 : 77 to 1472 F 2.48 : 77 to 1832 F 2.61 : 77 to 2282 F	2.8 : 70 to 2700 F	1.55 : 70 to 212 F 2.22 : 76 to 1470 F	1.64 : 77 to (6) 572 F 2.27 : 77 to 1292 F 2.62 : 77 to 1832 F 2.80 : 77 to 2192 F	2.05 : 77 to (6) 572 F 2.18 : 77 to 1292 F 2.23 : 77 to 1832 F 2.17 : 77 to 2192 F	2.80 : 20 to 2700 F	2.88 : 77 to 1292 F	2.33 : 77 to 1832 F	1.99 : 800 F 2.43 : 1470 F 2.80 : 2200 F 2.91 : 2450 F				1.55 : 70 to 390 F 2.55 : 70 to 1830 F 2.70 : 70 to 2460 F
Hardness			9 to 9.5 (Moh) 2500 (Knoop at 100 grams)	9.1 (Moh)			9 to 9.5 (Moh) 2500 (Knoop at 100 grams)	Very hard				2500 (Knoop at 100 grams)		
Impact Resistance				Low				2.2 in-lbs (Charpy, 1/2" rod)	4 in-lbs					
Oxidation Resistance				2.5% gain in wt at 2000 F after 9 weeks in air										
Tensile Strength psi x 10^{-3}	Very low:(2) 77 F	3.5 : 77 F(2) 3.5 : 1292 F 4.5 : 1832 F 3.7 : 2462 F 1.9 : 2732 F	3 to 4				5 to 6		10	.030 psi : 68 F	.070 psi : 68 F			
Compressive Strength psi x 10^{-3}	15 psi : 68 F(2)	20 : 77 F(2) 20 : 1292 F 25.5 : 1832 F 21.5 : 2462 F 11.9 : 2732 F	25 : 70 F			150 : 77 F (6)	25 : 70 F	25		.085 psi : 68 F	.750 psi : 68 F			62.8 : 70 F
Total Emissivity		0.93 : 1500 F(10)										0.9		
Notes ( )	Data from Ref. 2, 6, 16	Data from Ref. 2, 10, 16	All data from Ref. 14	All data from Ref. 1	Data from Ref. 6, 16, 17		All data from Ref. 14	All data from Ref. 11	All data from Ref. 12, 13	All data from Ref. 15		All data from Ref. 14	All data from Ref. 3	

TABLE II

HIGH TEMPERATURE EROSION TEST DATA (1)
SILICON CARBIDE BONDED GRAPHITE

Specimen Size: 1/2 inch diameter hemispheres - cylinders

Conditions: High intensity electric arc, 4500 F for 60 seconds

% Free Carbon In Body (Approximate)	% Weight Loss
20	0.10
30	0.63
35	0.90
40	1.61
100 (Special Graphite)	5.80

Specimen Size: 1 inch diameter hemisphere - cylinders

Conditions: High intensity electric arc, 4800 F for 20 seconds

% Free Carbon In Body (Approximate)	Length Loss (cm)	Weight Loss Mg/kw/sec
0.4	cracked	cracked
10	0.014	0.004
25	0.05	0.13
45	0.20	0.41
100 (Special Graphite)	0.12 (2)	0.60

Note (1) Data from Reference 21

(2) Erosion characteristics of graphite show a reduction of diameter rather than length.

III AREAS OF APPLICATION AND DESIGN PARAMETERS FOR SILICON CARBIDE

The major problems confronting designers of aircraft and missiles who desire to use silicon carbide or other brittle non-metallic materials are:

a. Rules for design have not been established.

b. The safety factor used by industry for brittle materials is too high for aircraft and missiles. Industry uses a safety factor in the order of 3 to 5 or higher whereas a safety factor of 1.25 is used by the aircraft industry for materials such as aluminum alloys.

c. Insufficient design and fabrication technology to build with engineering integrity, an all silicon carbide aircraft structural element such as a wing.

d. The majority of the design of silicon carbide parts has been on a trial and error basis.

e. Insufficient technology for attaching brittle to non-brittle materials.

In the sections which follow, an attempt has been made to demonstrate the influence of thermal stress and other thermal factors on the selection of materials for use in hypersonic aircraft. The methods for determining temperature and thermal stresses have been developed by Bell Aircraft structural engineers under Air Force Contract Number AF33(616)-6034, Investigation of Feasibility of Utilizing Available Heat Resistant Materials for Hypersonic Leading Edge Applications.

A. Leading Edge

1. Compressive Strength, Tensile Strength, Modulus of Elasticity

These properties are of major importance in a brittle material exposed to thermal stress conditions. Thermal stresses are influenced by thermal conductivity, modulus of elasticity, and coefficient of thermal expansion. The maximum and minimum temperatures of a leading edge wedge subjected to heat flux are a function of the density, emissivity, thermal conductivity and specific heat of the material; geometry and diameter of the wedge; and the angle of sweep of the wedge.

a. Assuming a thermal emissivity of 0.9, steady state conditions (in order that specific heat need not be considered), and specific flight conditions, the following calculated data indicate the influence of thermal conductivity and wedge diameter on anticipated maximum and minimum temperatures of a selected theoretical design.

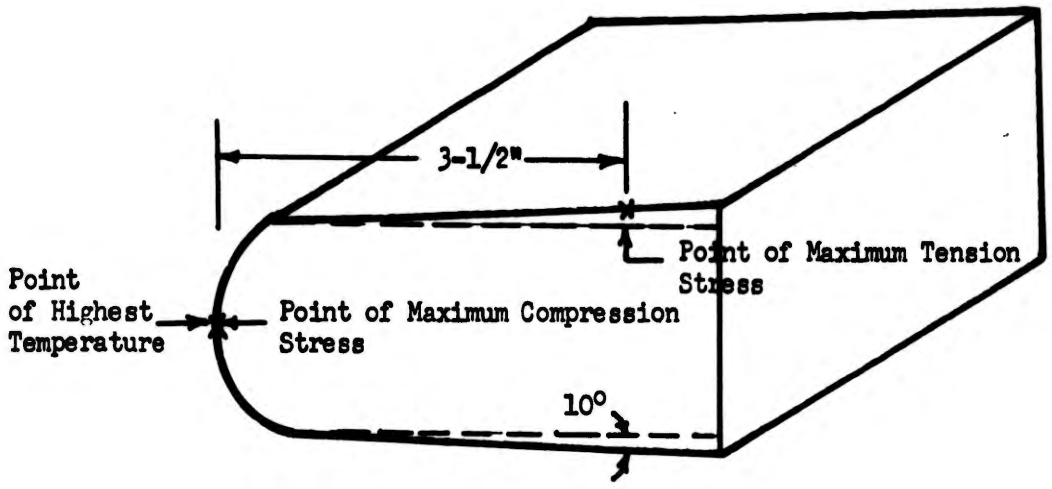

Figure 3. Leading Edge Wedge (Solid)

Thermal Conductivity $\frac{BTU\text{-}in}{ft^2 \cdot hr \cdot {}^oF}$	Temperature	
	Leading Edge Point	3-1/2" Back from Point of Leading Edge and Perpendicular to Leading Edge
1" Diameter, 10° Wedge		
200	2920 F	1910 F
400	2750 F	2030 F
800	2590 F	2140 F
1000	2520 F	2150 F
3" Diameter, 10° Wedge		
200	2720 F	1990 F
400	2590 F	2110 F
500	2550 F	2140 F

b. Maximum thermal stress parameters $\frac{\sigma}{\alpha E}$, for compression and tension, are a function of thermal conductivity and flight parameters $\frac{K}{\sqrt{\frac{W}{SC_L}}}$ for a given emissivity and steady state conditions.

σ = Stress, psi

α = Coefficient of expansion of the material

E = Modulus of elasticity of the material

K = Thermal conductivity of the material

W = Weight of the vehicle

S = Area of the wing

C_L = Lift coefficient

For the purpose of illustration, let us assume a hypothetical case where the flight parameter $\frac{K}{\sqrt{\frac{W}{SC_L}}}$ is 40 and the temperature of interest is 2750 F at a given thermal emissivity. A graphic parametric presentation of maximum thermal stresses for 1" diameter 10° leading edge wedge indicates a tension thermal stress parameter $\frac{\sigma_t}{\alpha E}$ of 80 and a compression thermal stress parameter $\frac{\sigma_c}{\alpha E}$ of 260.

From a property data sheet on the hypothetical material selected, we find at 2750 F the coefficient of thermal expansion to be 2.2×10^{-6} in/in/°F and the modulus of elasticity to be 49×10^6 psi. Substituting these values in $\frac{\sigma_t}{\alpha E} = 80$ and $\frac{\sigma_c}{\alpha E} = 260$ we find that the thermal stress in tension σ_t to be 8,624 psi and the thermal stress in compression σ_c to be 28,028 psi. Again referring to the property data sheet we find that at 2750 F the hypothetical material has an allowable tensile strength of 7000 psi and an allowable compression strength of 25,000 psi. Therefore, the material would not be satisfactory for leading edge use at 2750 F since the thermal stresses exceeded the allowable tensile and compression strengths.

2. Poisson's Ratio

Although Poisson's ratio has been listed as a desired property for preliminary design data for leading edge application, it is not considered an item of primary interest. However, for specific cases, Poisson's ratio may be of utmost importance.

3. Shear Strength

Shear strength data are desired for design of attachments and areas where air loading may induce shear stresses.

4. Torsion Strength Including Modulus of Rigidity

To date, thermal stress calculations do not indicate torsion data to be of prime importance. However, depending on design it is believed possible that stresses in torsion may be induced by air loads.

5. Creep and Rupture Strength in Tension and in Compression

Data of this nature are desired in calculations where long time usage is to be anticipated.

6. Erosion

Erosion characteristics are desired for predicting the life expectancy of the material under specific flight conditions for a single or repetitive flights.

7. Notch Sensitivity

Most brittle materials have a notch sensitivity factor close to 1.0 at room temperature. This results in a large strength reduction. It is believed that as the temperature increases there probably may be some plastic flow which would tend to reduce the notch sensitivity factor and also reduce the stresses.

B. Fuselage - Outer Wall Panels

It is anticipated that under normal flight conditions non-metallic outer wall panels of a fuselage would be exposed to a lower heat flux than the leading edge. The effect of thermal conductivity is not as important as with the leading edge because of smaller thermal gradients.

Since the heating intensity is less, materials having a low thermal conductivity could be used for outer wall panels. However, materials of a high thermal conductivity could be used provided some other advantage was gained, such as improved erosion resistance.

The low thermal conductivity material used should have a lower specific heat than for the leading edge in order to heat more rapidly and minimize thermal stresses. A high thermal emissivity is desirable to keep the overall temperature at a minimum.

C. Nose Cones

Nose cones are generally of two types; "glide" and "ballistic". The ballistic type is further subdivided into "heat sink" and "insulated". One example of the insulated is the ablative nose cone.

The design problems for the glide type nose cone are similar to those for the leading edge because heat inputs are generally of the same order of magnitude.

The major problem encountered with the ballistic nose is thermal shock. With the heat sink nose a high thermal conductivity and a high specific heat is desirable. The insulated nose requires a material having a low thermal conductivity and a high specific heat. The high specific heat will tend to retard the heat entry.

D. Rocket Nozzles

The selection of a material for rocket nozzle applications is governed to a large extent by erosion resistance, compatibility with fuels employed, and thermal shock. The thermal shock parameter should take into consideration expansion, specific heat, and modulus of elasticity.

E. Other Areas

Other areas where silicon carbide may possibly find application are:

1. Wearing parts in high temperature areas

2. Jet vane controls

3. Flame holders and ram jets.

IV DETERMINATION OF DENSITY AND DENSITY UNIFORMITY

A. General

The determination of density and density uniformity are of prime concern in the inspection of any material. A marked difference in the density from one part to an identical part and a marked variance of density distribution throughout a part would undoubtedly have an adverse effect on the design criteria and the functional use of the part.

Brittle materials such as silicon carbide are more susceptible to change in properties due to variation in density than non-brittle materials. The latter can distort under stress to a greater degree.

The following approaches to the determination of density uniformity were taken during this program: (1) industrial X-rays on photosensitive glass plates, (2) scanning of the X-rays by a densitometer comparator, and (3) a limited exploratory examination by ultra-sonic means.

B. Density Determination

1. General

The manufacturer reports the nominal density of KT silicon carbide to be 3.10 grams/cc minimum. The theoretical density of SiC is 3.22.

2. Test Apparatus and Method

The density of each test specimen was determined using a Krauss Jolly Balance shown in Figure 7. The specimen was weighed in air and then in water. The density was read directly from the vernier of the Balance. The instrument was standardized using a standard of pure nickel having approximately the same weight as the silicon carbide specimens.

3. Results

The density data collected are given in Table III.

4. Conclusions

The density determinations made by use of the Krauss Jolly Balance coincide with the manufacturer's reported density.

C. Density Uniformity

1. Industrial X-Ray

a. General

The use of X-rays is one of the oldest and most commonly used non-destructive methods of inspection. X-rays are electromagnetic waves which can penetrate matter and have properties similar to light waves in regards to propagation and effecting photographic materials. In addition to the normal factors which affect photographic presentations (source of light, distance from object, exposure time, speed of film, etc.), the density, thickness, and length of specimens are factors of X-ray presentation.

b. Test Apparatus and Method

The X-ray presentations were obtained on photosensitive glass plates used for spectrographic analysis. The X-rays were obtained on glass plates so they could be scanned by a photoelectric densitometer comparator described later in this report. Obtaining the X-rays directly on the glass plates greatly minimized the human error which would have been present by X-raying on a celluloid film and then obtaining a positive on the glass.

The test specimens were X-rayed using a Westinghouse 220KV unit. The exposure time, voltage, amperage, and source to glass plate distance were varied for optimum presentations. The angle of the beam to the glass plate was maintained at 90 degrees and no filters were used.

The 6" x 1/2" x 1/4" specimens were X-rayed through the 1/2" thickness and through the 1/4" thickness. The 5" x 1/4" x 1/4" specimens were X-rayed through two faces 90 degrees to each other.

c. Results

By X-raying the test specimens through two directions, a better indication of density uniformity was possible. Some bars showed the same areas of higher density in both exposures. Other bars having areas of higher density in one direction did not show the higher density area when viewed from the other direction. It was observed that there was a difference in intensity and width and also a difference in length of the more dense areas when viewed through the two different thicknesses.

Figures 8 through 21 are specimen X-ray photographs taken 90 degrees from each other. The figures depicting the exposures through the 1/4" thickness of the D and H series of specimens are composite photographs. For example, bar D-1 X-rayed with

the first set was selected as the standard for the subsequent exposure of the D series. The first exposure contained bars D-1 through D-4. The second exposure contained bars D-1, D-5, D-6 and D-7, etc. The X-rays were taken in this manner due to the size limitations of the glass plates and also for comparison on the densitometer.

Attention is directed to bar D-4 in Figures 8 and 9. As the bars were being turned (two at a time) from the 1/2" face to the 1/4" face during the X-ray process, bar D-4 cracked when forceful contact was made with another bar. During handling the bar was inadvertently dropped and cracked again. Examination of the broken bar and the X-rays revealed that the break occurred on each side of the dense area which can be noted in Figures 8 and 9. The over-all density of D-4 was 3.13 grams/cc. The density of the broken section having the more dense area was 3.14 grams/cc.

d. Conclusions

At present, no definite conclusions can be made as to what effect these variations in density may have on mechanical strength. Many factors must be considered and studied. A few of these factors are the nature, location, depth, and size of the areas, the direction of the load, etc. Modulus of rupture tests (Section IX Modulus of Rupture) conducted on SiC specimens indicate that under transverse load the break did not always occur at points of marked variance of density.

2. Densitometer Comparator

a. General

It has been demonstrated that X-ray inspection will detect areas of density variation. X-rays can not tell us how much the variation in density is from one point to another throughout the specimen.

In an attempt to detect the amount of density variation, a densitometer comparator normally used for spectrographic analysis was employed. A densitometer comparator is an instrument for measuring the blackness of an exposed photographic plate by observing the relative amount of light which is transmitted. The ratio of the light intensity transmitted by an exposed plate to that transmitted by a clear plate is defined as the transmission T. Density D, is by definition the negative logarithm of the transmission.

$$D = -\log_{10} T = \log_{10} 1/T$$

In addition to being able to determine the amount of density variation within a specimen, it was anticipated that standard traces could be obtained for various uniform densities. By having a series of traces, the unknown density of a silicon carbide body could be readily and accurately obtained by photo-electric scanning of the X-rays and comparing the traces with the standards.

b. Test Apparatus and Method

The instrument used was a Baird Associates double beam densitometer comparator which utilizes a two-beam optical null method employing a servo-type automatic balancing system. The use of variable precision logarithmic apertures with a range of density units from 0 to 2.00 as the ultimate standard for measurements, provides an instrument which reads density directly on a linear scale. The densitometer comparator used, is both a visual and automatic recording type.

The optical system includes two light sources and two projection lenses, thus the images of the specimen and comparison plates are projected simultaneously on a viewing screen at 10X magnification. A schematic diagram of the optical system is given in Figure 22. A general view of the densitometer comparator is given in Figure 23.

As stated previously, the specimens were X-rayed on glass plates and one specimen was selected as a standard for the subsequent exposures. This was done in order that a standard for comparison could be had which would eliminate the variables such as time of exposure, strength of developing solutions, etc.

After visual observation of several plates, it was decided that specimens D-1 (ground surface) and D-23 (ground surface) would be scanned and recorded automatically. Bar D-1 had a density of 3.12 grams/cc and areas of marked density variation. Bar D-23 had a density of 3.11 grams/cc and relatively uniform. It was believed that these two bars would indicate the following: (1) the amount of density variation within the specimen, and (2) whether the difference in density (as determined by the Krauss Jolly Balance) from one specimen to another would be adequately detected and recorded.

The X-rays through the 1/4" thickness of bars D-1 and D-23 were scanned lengthwise three times, at three different heights from the base. The recorder and instrument were zeroed for the first scan. For the subsequent scans of the same bar, the recorder was adjusted so that the traces would not be superimposed on each other on the chart paper.

The ground specimens were used for the automatic scanning because the X-rays revealed them to have more defined areas of density variation than the "as fabricated" specimens. Another factor for the selection of the ground bars was the warpage of the "as fabricated" bars.

c. Results

The following observations are made based on the examination of Figure 24 which shows the densitometer comparator traces of specimens D-1 and D-23:

(1) The slight bow in the traces from one end to the other are attributed to the difference in the intensity of the X-rays which were affected by the length of the specimens. With the X-ray beam being 90 degrees to the specimen and centered, the X-rays are passing through 1/4" thickness at the center portion of the specimen. Near the ends of the specimen, the X-rays are entering at an oblique angle and thus a greater thickness.

(2) Traces are jagged instead of smooth lines. This is due to the grain of the exposed photographic plates.

(3) Traces ① are for the top portion of the bars, ② for the center, and ③ for the bottom portion.

(4) In the relatively uniform portions of the two bars, it can be seen at Stations 1, 2, and 3, that bar D-23 has a higher numerical reading than D-1 by approximately two units. Since D-23 has a density of 3.11 grams/cc and D-1 has a density of 3.12 grams/cc, the assumption is therefore made that two units on the chart are equivalent to 0.01 gram/cc. As stated previously, the densitometer is measuring the blackness of the exposed photographic plate.

(5) Observing trace ① bar D-1 at Stations 2 and 3, we have a reading of 70. Assuming that at 70, the density is 3.12 grams/cc. Then at point A between Stations 4 and 5, we have a reading of 74 or 4 units of more blackness. Since in (4) above we state that two units are equivalent to 0.01 gram/cc, then four units are equivalent to 0.02 gram/cc. Therefore, it can be assumed that the density of the bar at point A is 3.10 grams/cc. Proceeding to point B between Stations 6 and 7, and using 70 as the 3.12 grams/cc base line, we have a difference of 12 units or 0.06 grams/cc. Therefore, point B has an assumed density of 3.18 grams/cc.

Efforts to establish standard traces for various uniform densities of silicon carbide were thwarted because specimens of the desired densities and uniformity were not obtainable.

d. Conclusions

The feasibility of non-destructively determining the quantitative density variation within a silicon carbide body has been demonstrated. The technique should be suitable for other materials. More accurate density measurements can be made by use of standard density bars. Corrections can be made for sample thickness variations where greater accuracy is desired.

3. Ultrasonic Inspection

a. General

The ultrasonic method of flaw-detection is based on the effect caused by applying alternating current across certain types of crystals. As the current is applied, the crystal contracts and dilates - the piezoelectric effect - which in turn causes longitudinal waves to be set up in the surrounding media in a direction perpendicular to the crystal. The piezoelectric effect is reversible; therefore, any energy waves returned to the crystal are transformed into electrical energy known as the inverse piezoelectric effect. (Reference 23)

The four main methods of ultrasonic examination for uniformity and/or defects are the (1) reflection method, (2) transmission method, (3) resonance method, and (4) energy-decay method. The reflection and transmission methods are usually employed for detection of internal defects. The resonance method is used for measuring thickness and locating laminar separation. The energy-decay method is used to determine the grain size of a material and detection of discontinuities in sections which are relatively thin.

The reflection method was used by Bell Aircraft Corporation during this study on silicon carbide. The principles of the reflection method of ultrasonic inspection presented below have been extracted in part from Reference 23.

Ultrasonic waves or beams are similar to sound waves in that they require an elastic medium for propagation. The waves can be refracted or reflected. The four main methods of ultrasonic inspection make use of one or more of three ways of introducing energy into a specimen. They are longitudinal waves, transverse waves, and surface waves. When energy enters one medium from another, normal to the interface, it is reflected and not refracted, producing longitudinal waves. As the angle of incidence increases, the longitudinal waves decrease, and the transverse waves (shear waves) due to refraction begin to develop. As the angle of incidence increases still further, the transverse waves disappear and surface waves are produced.

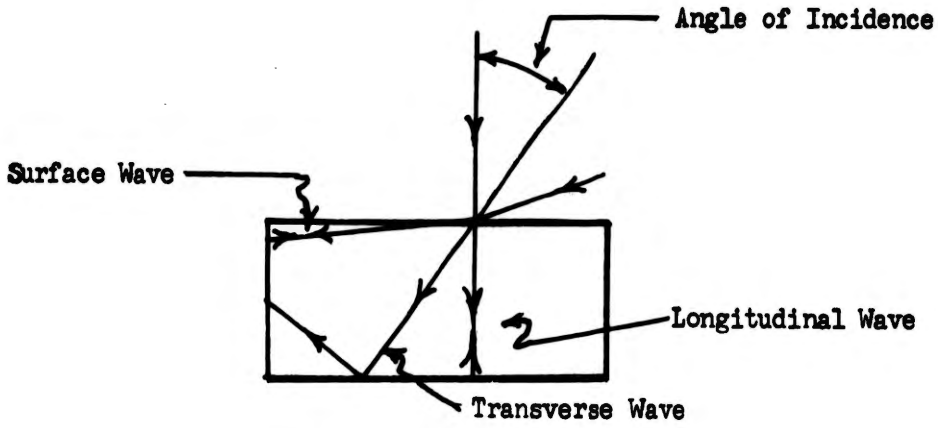

Figure 4. Examples of Ultrasonic Waves

The penetration and absorption of ultrasonic energy is affected by the structure of the material, the frequency of the energy, and the interface coupling material. Penetration is largely dependent on uniformity of structure. If the grain structure varies in size and direction, there is less chance of obtaining maximum penetration of the energy (which, in form is a conical beam, of which the axis lies along a line normal to the center of the crystal) than is possible with a uniform grain size. A coarse grained structure will absorb more energy than a fine grain structure. The angle of spread of the energy depends on several factors, and in the ideal case, upon the ratio between the radius of the generating crystal and wave length of the beam. The choice of frequency has an important bearing on sensitivity. The higher the frequency the more sensitive is the test, but less penetrating. Therefore, the selection of frequency is dependent upon the surface finish of the specimen, grain size of structure, and kind of defect expected.

Ultrasonic energy of the frequencies used for this type of investigation will not pass through an air gap or vacuum efficiently, therefore any discontinuity will act as a reflecting surface, and the amount of energy reflected by it is an indication of the size of the gap. To overcome this situation, a coupling medium between the probe crystal and the specimen must be employed. The coupling medium is generally a liquid, thin oil or water, according to the conditions of the test. The surface finish of the specimen has considerable bearing on the

final choice of liquid. On a rough mechanical surface, it is necessary to use a heavy oil while in extreme cases, a combination of oil and glycerine is used. The couplant fills any air gaps between the two surfaces to produce a clean interface. Couplants have the effect of inducing a slight loss in energy.

The transmitted and reflected waves are triggered on a time-base and they are presented on a cathode ray tube of an oscilloscope in such a way that they do not interfere with one and another. This effect is obtained by a system whereby the cathode ray time base is first set in operation, and a short time later a transmission is made. The resultant echo and reflection of the signal cause vertical deflection of the trace and from these "blips" it is possible to establish the existance of a defect between the upper and lower surfaces of the part being investigated. A defect causes an interface in the medium which reflects some of the ultrasonic energy in a manner similar to that of an optical reflection from a polished surface.

Under ideal conditions of ultrasonic testing, sound energy is transmitted from the upper face of the material at A, and reflected from face B, to the transreceiver crystal, see Figure 5. The time base of this sequence, is given along the X-axis of the oscilloscope on the right of the illustration. The time scale A_1 - B_1, represents the distance the energy has travelled in the material from A to B; that is, it is representative of the thickness of the specimen. The reflection from the defect is shown by C_1, where the distance A_1 - C_1, represents the depth that the defect is below the interface. As the size of the defect increases, it reflects more energy and correspondingly less is reflected from the underface - echo at B. Thus as the flaw - echo amplitude increases, the bottom - echo decreases.

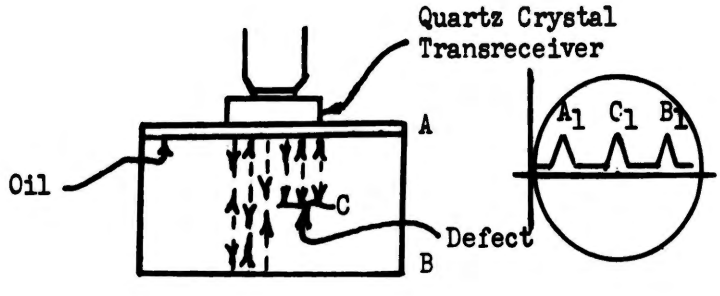

Figure 5. Reflection of Energy From Top and Bottom Faces and From Defect

If the defect is orientated in the manner shown in Figure 6 below where it is no longer normal to the ultrasonic energy, it is possible that no defect - echo would occur owing to the reflection of the beam, but its presence would be suggested by a noticeable loss of the bottom - echo obtained when the probe was over a sound portion of the material. If such a defect occurred in a rectangular section bar and the scanning was done from three or more faces, it would be possible to obtain a reasonably accurate assessment of the orientation of the defect. The energy could then be directed into the material in a plane normal to the greatest surface of the defect for a more complete appraisal of its extent.

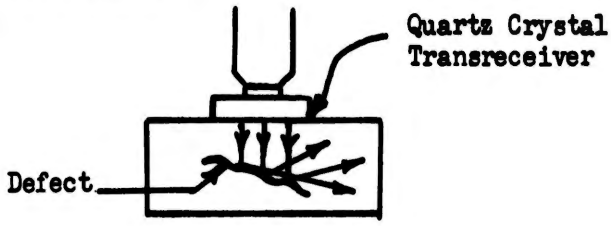

Figure 6. Scatter Effect of Energy When Defect Is Not Normal to Ultrasonic Beam

b. Test Apparatus and Method

The equipment used was a Sperry Reflectoscope Model 50E-383 and a 5Mc crystal. Figure 25 is a general view of the equipment and Figure 26 is a block diagram of the functions of the components of the Reflectoscope.

The specimens selected for this study were D-1 and D-15. The selection was on the basis of X-ray inspection which showed D-1 to have areas of marked density variation and D-15 to be relatively uniform. The ultrasonic inspection of the specimen was through the lengthwise (6 inch) direction. Glycerine was used as the couplant medium.

c. Results

The results of this limited study are shown in Figures 27 and 28 which are photographs of the reflectoscope traces.

The differences in the amplitudes of the flaw - echoes and the bottom echoes verify the X-ray inspection in that D-15 was more uniform than D-1. However, the traces indicate that both bars contained numerous discontinuities. The difference in the amplitudes of the echoes on the reflectoscope examplifies the principles of ultrasonic inspection previously discussed.

d. Conclusions

The low level of effort expended and the lack of a standard uniform test specimen of KT silicon carbide precludes any critical interpretation of the results obtained. What has been designated in the Results above as flaw - echoes cannot be construed as cracks or defects per se. These echoes are believed to have been returned by the areas of different densities. Therefore, in the case of silicon carbide, until such time as a standard uniform bar is producible, ultrasonic inspection may be best utilized for comparison of uniformity rather than an accurate detector of flaws.

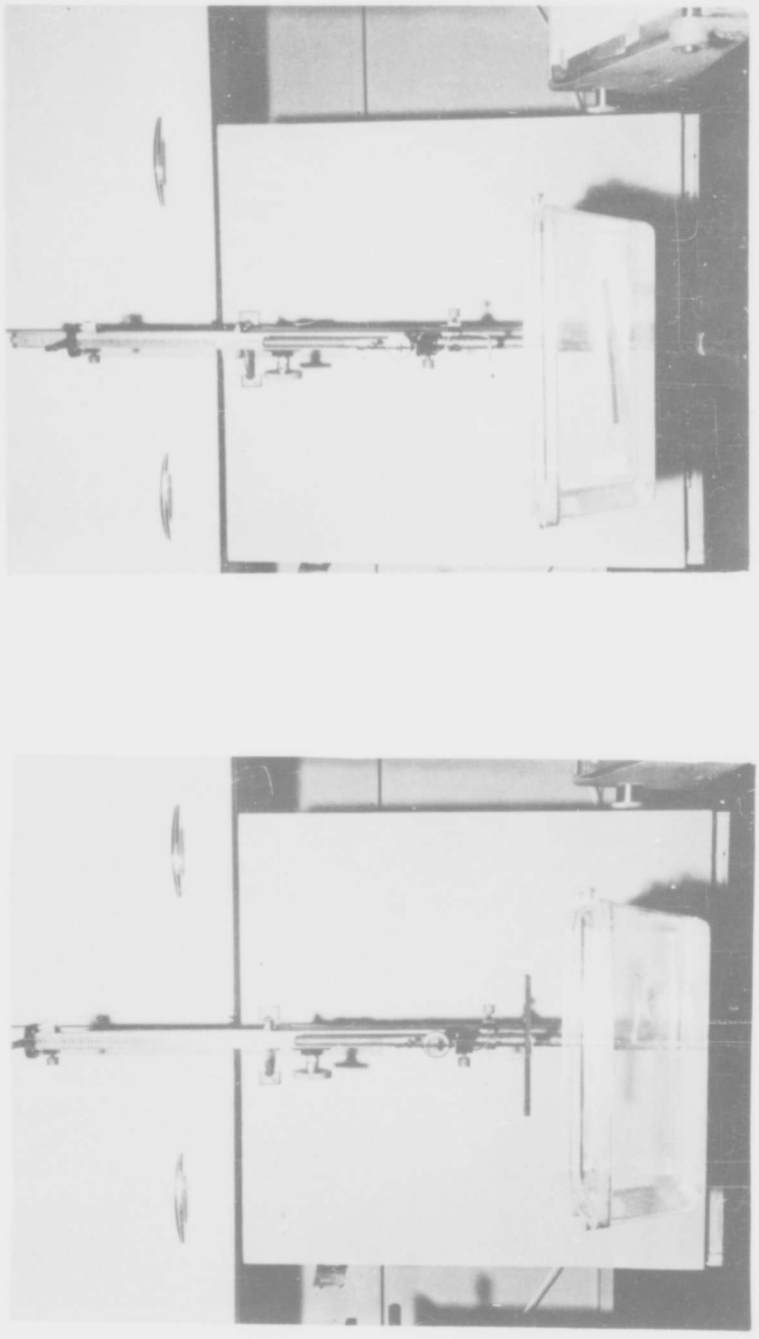

Figure 7. KT Silicon Carbide Specimen Being Weighed In Air And In Water On Krauss Jolly Balance

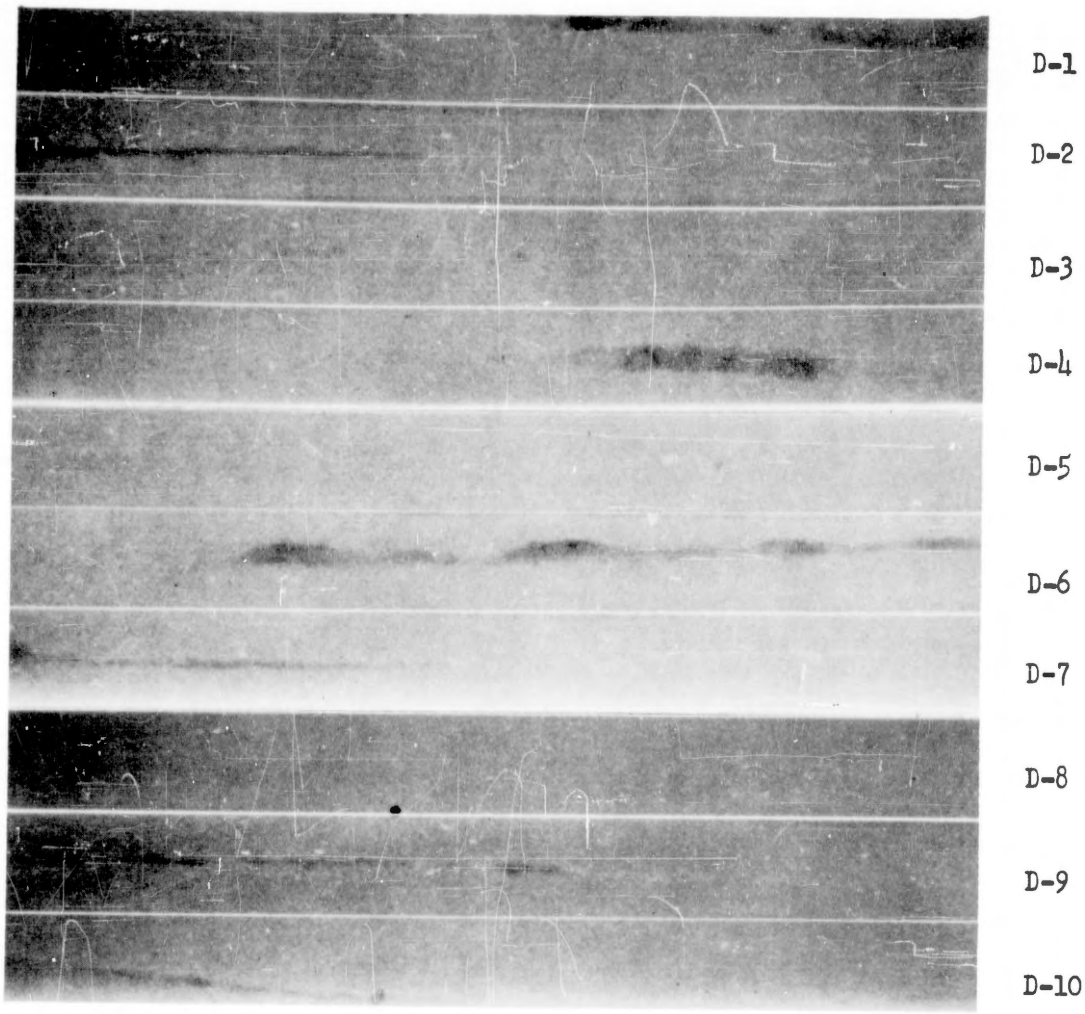

Figure 8. X-Ray Photograph: KT Silicon Carbide Test Bars D-1 to D-10, 6" x 1/2" x 1/4" Ground, X-Ray through 1/4" Thickness

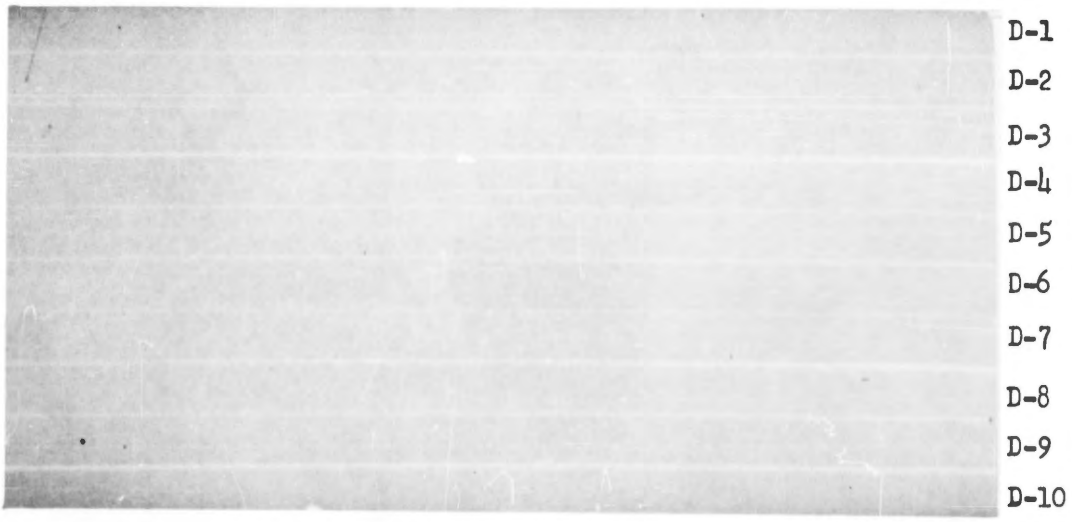

Figure 9. X-Ray Photograph: KT Silicon Carbide Test Bars D-1 to D-10, 6" x 1/2" x 1/4" Ground, X-Ray through 1/2" Thickness

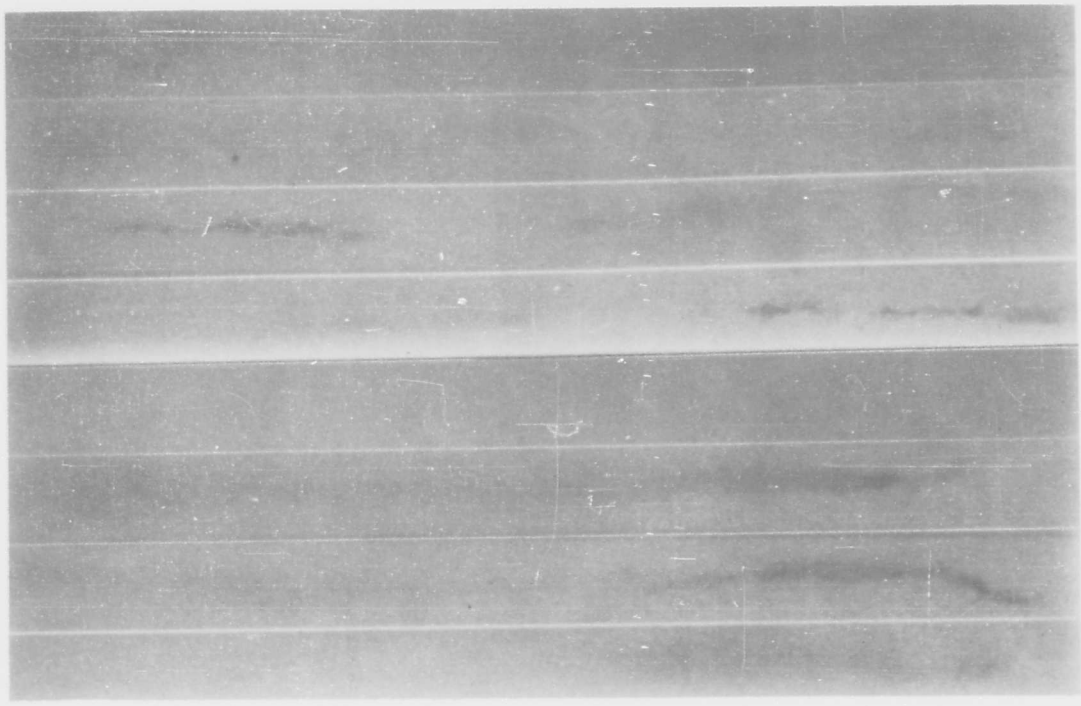

Figure 10. X-Ray Photograph: KT Silicon Carbide Test Bars, D-11 to D-18
6" x 1/2" x 1/4" Ground, X-Ray through 1/4" Thickness

Figure 11. X-Ray Photograph: KT Silicon Carbide Test Bars, D-11 to D-18
6" x 1/2" x 1/4" Ground, X-Ray through 1/2" Thickness

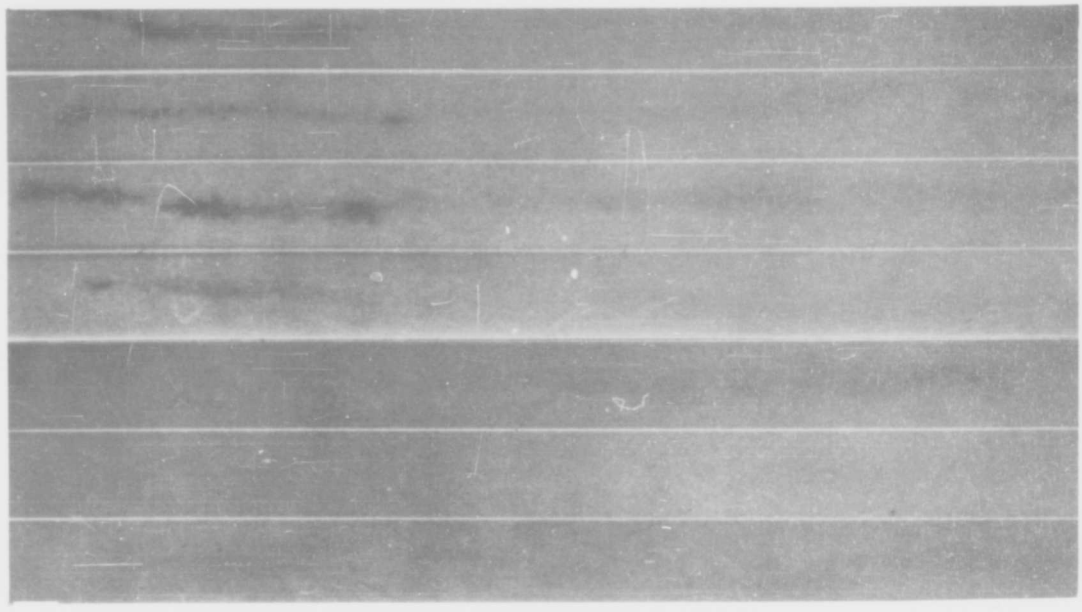

Figure 12. X-Ray Photograph: KT Silicon Carbide Test Bars D-19 to D-25, 6" x 1/2" x 1/4" Ground, X-Ray through 1/4" Thickness

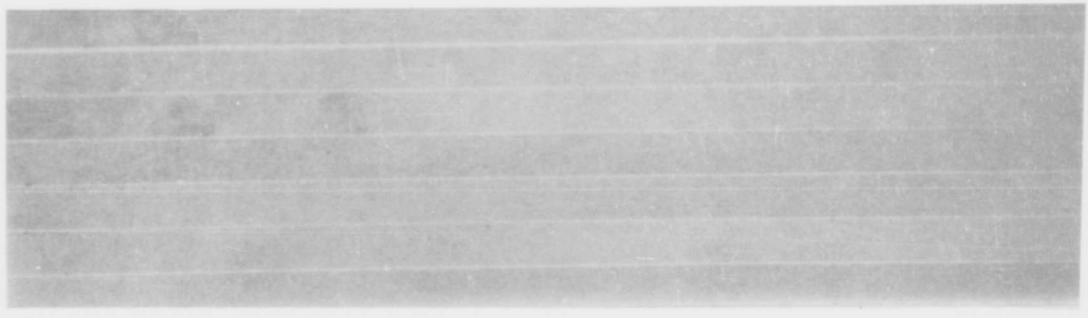

Figure 13. X-Ray Photograph: KT Silicon Carbide Test Bars, D-19 to D-25, 6" x 1/2" x 1/4" Ground, X-Ray through 1/2" Thickness

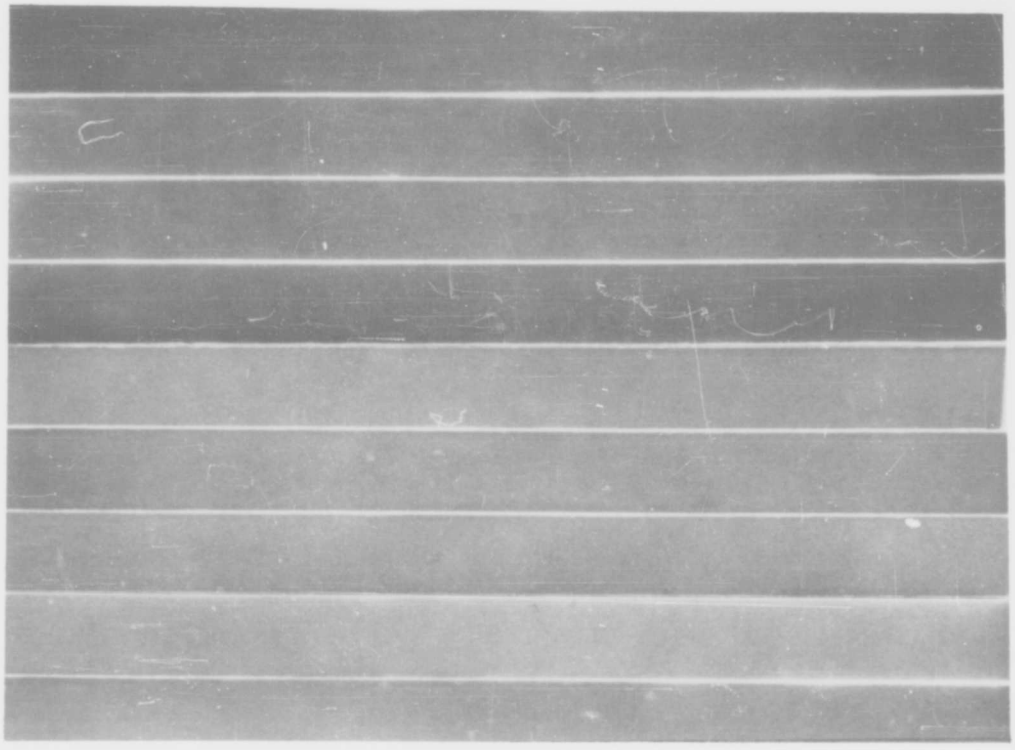

Figure 14. X-Ray Photograph: KT Silicon Carbide Bars, H-2 to H-10, 6" x 1/2" x 1/4" "As Fabricated", X-Ray through 1/4" Thickness

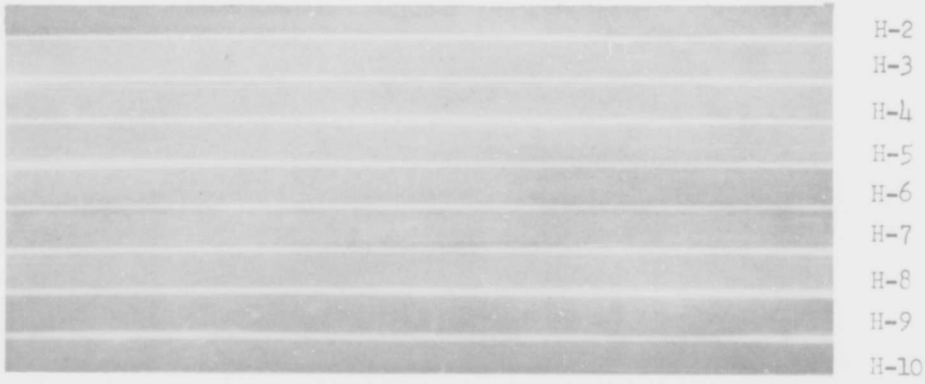

Figure 15. X-Ray Photograph: KT Silicon Carbide Test Bars, H-2 to H-10, 6" x 1/2" x 1/4" "As Fabricated", X-Ray through 1/2" Thickness

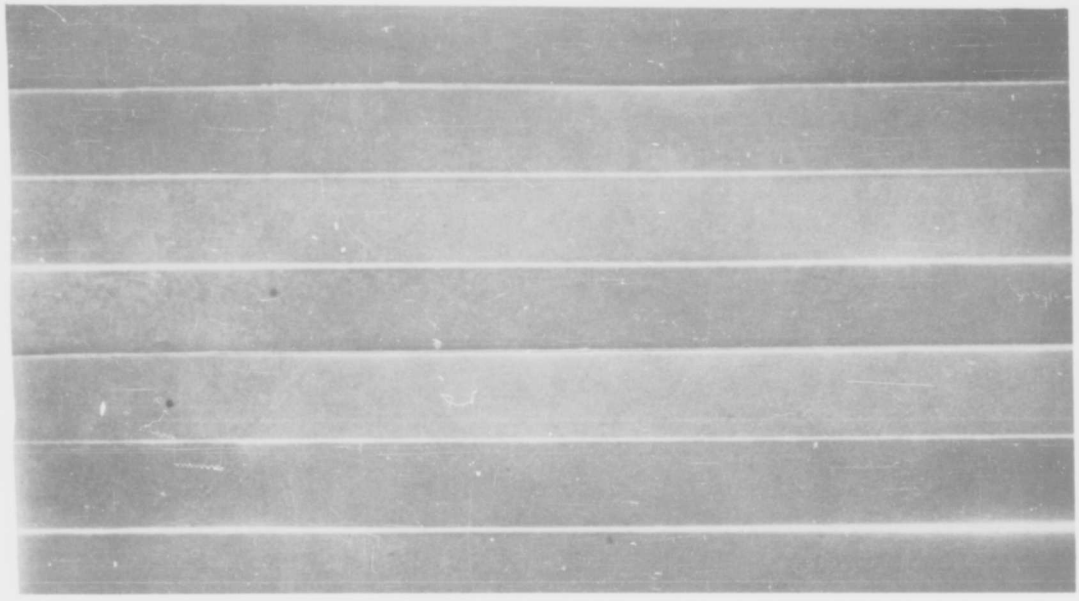

Figure 16. X-Ray Photograph: KT Silicon Carbide Bars, H-12 to H-14, H-16 to H-17, H-20 to H-21, 6" x 1/2" x 1/4" "As Fabricated", X-Ray through 1/4" Thickness

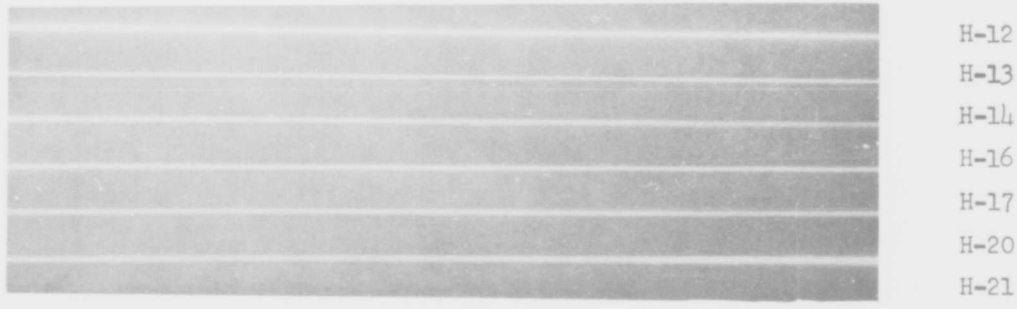

Figure 17. X-Ray Photograph: KT Silicon Carbide Test Bars, H-12 to H-14, H-16 to H-17, H-20 to H-21, 6" x 1/2" x 1/4" "As Fabricated", X-Ray through 1/2" Thickness

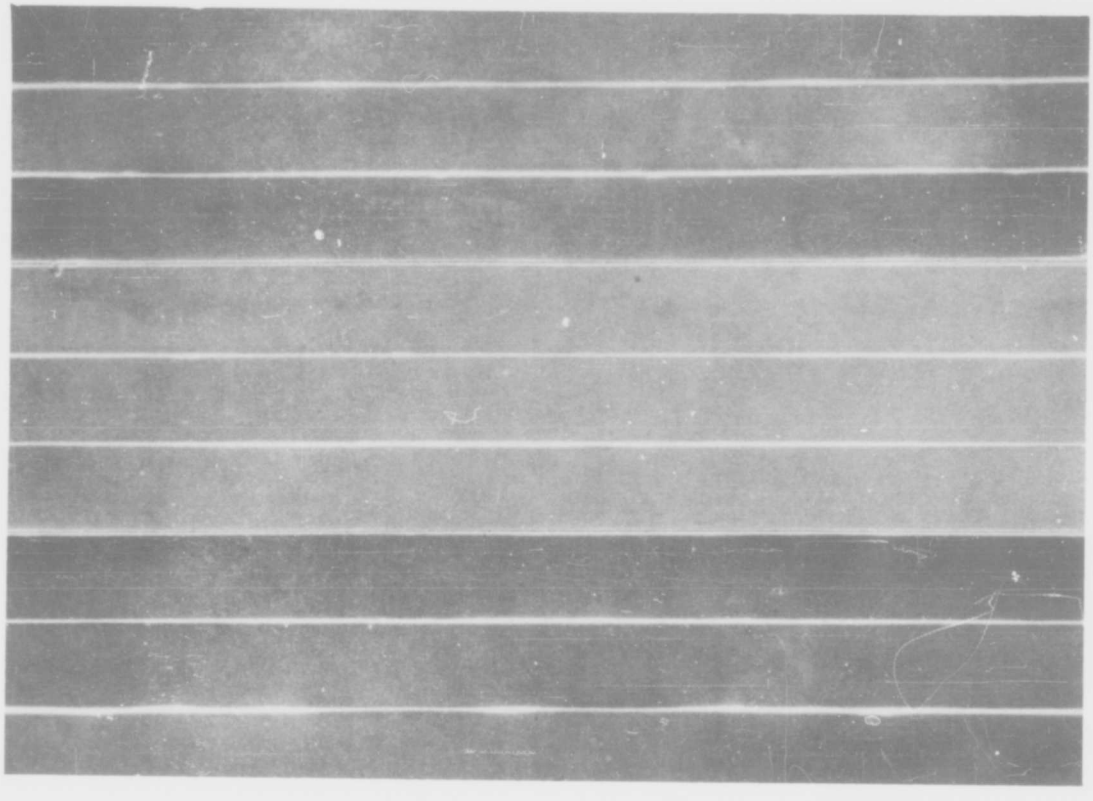

Figure 18. X-Ray Photograph: KT Silicon Carbide Test Bars H-22 to H-30, 6" x 1/2" x 1/4" "As Fabricated", X-Ray through 1/4" Thickness

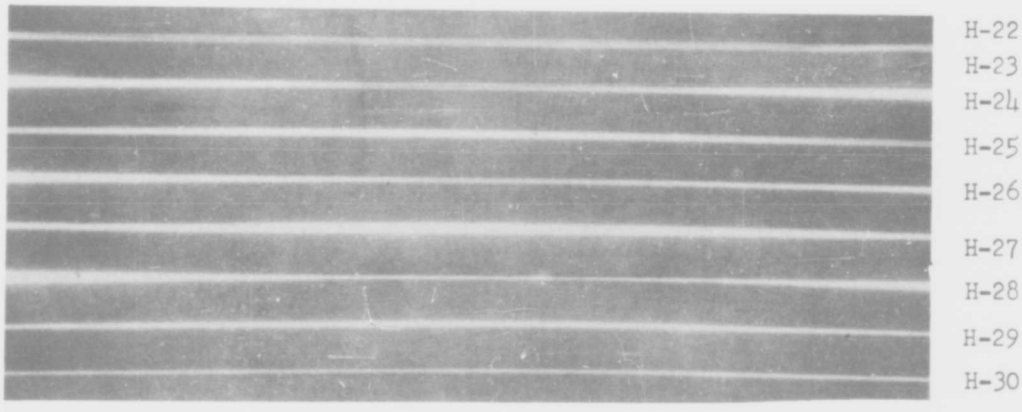

Figure 19. X-Ray Photograph: KT Silicon Carbide Test Bars H-22 to H-30, 6" x 1/2" x 1/4" "As Fabricated", X-Ray through 1/2" Thickness

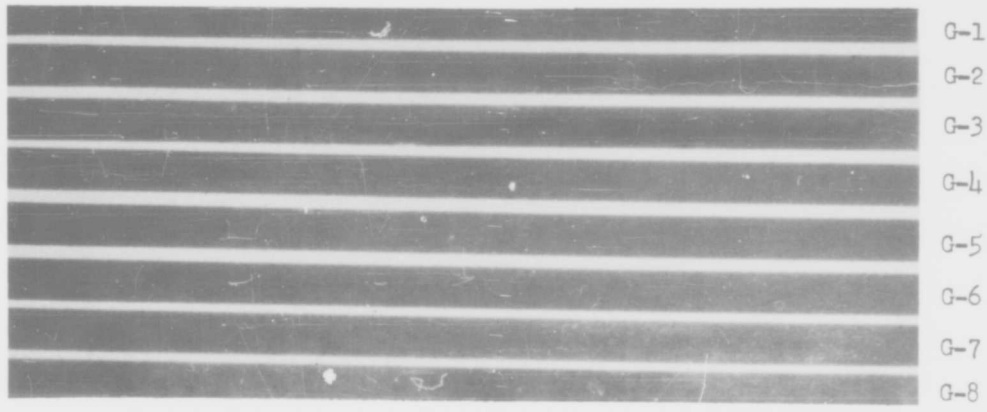

Figure 20. X-Ray Photograph: KT Silicon Carbide Test Bars, G-1 to G-8, 5" x 1/4" x 1/4" - Ground, "A" Side

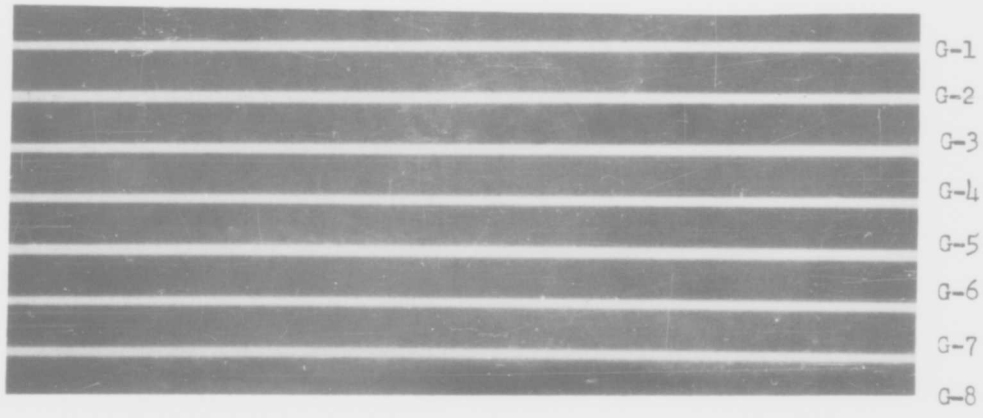

Figure 21. X-Ray Photographs: KT Silicon Carbide Test Bars, G-1 to G-8, 5" x 1/4" x 1/4" - Ground, "B" Side (90° to "A" Side)

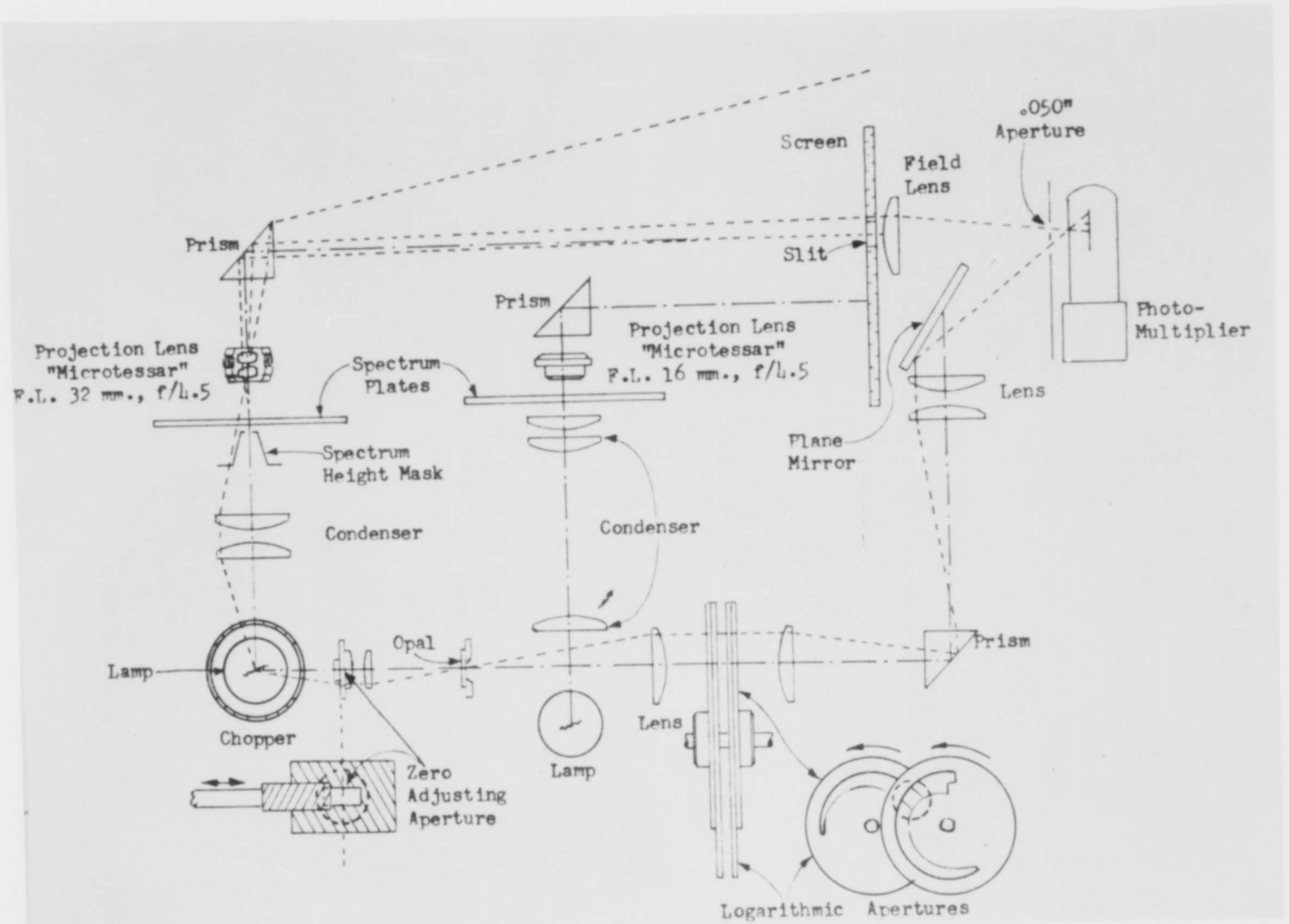

Figure 22. Optical Schematic Of Densitometer Comparator

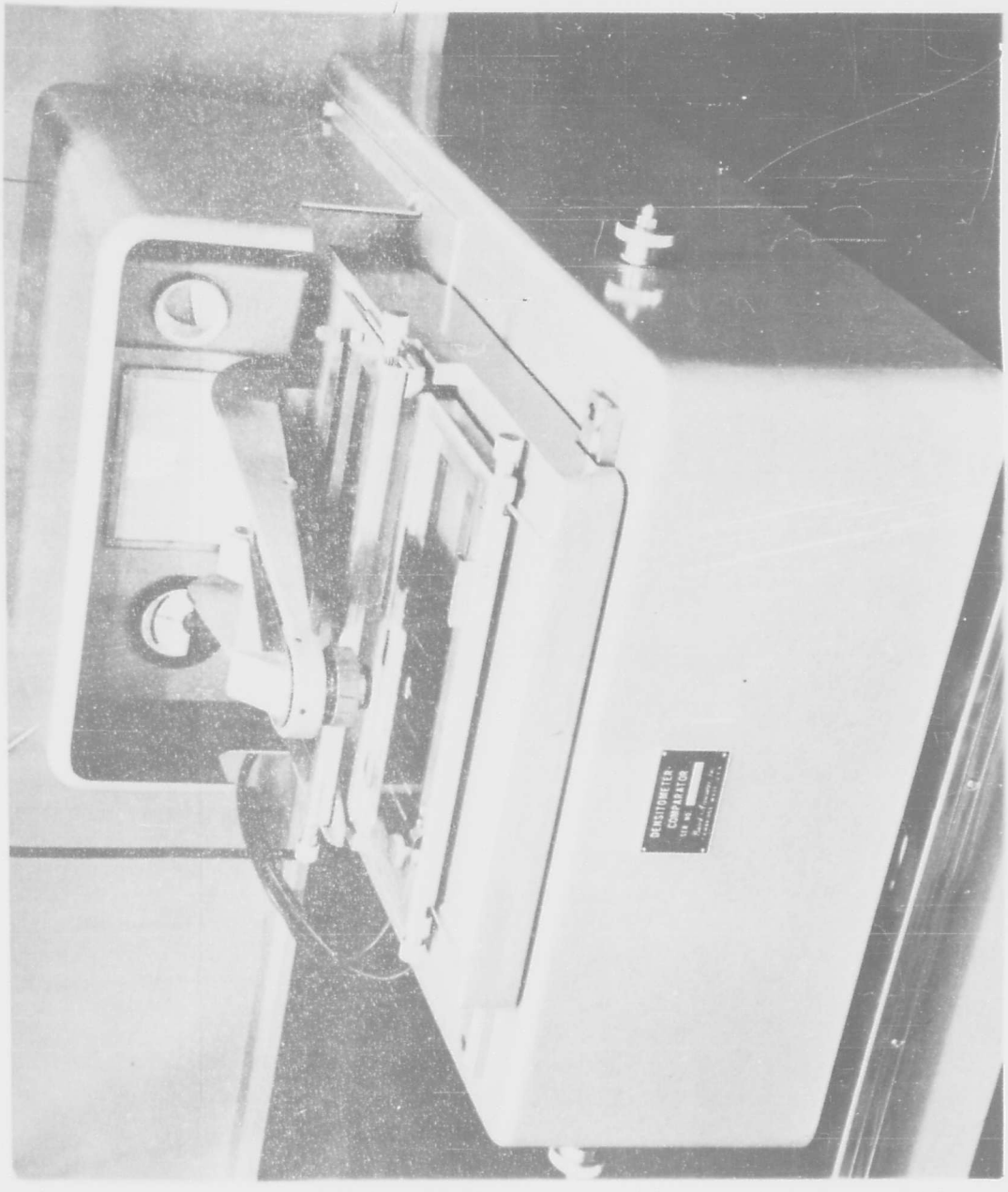

Figure 23. Densitometer - Comparator

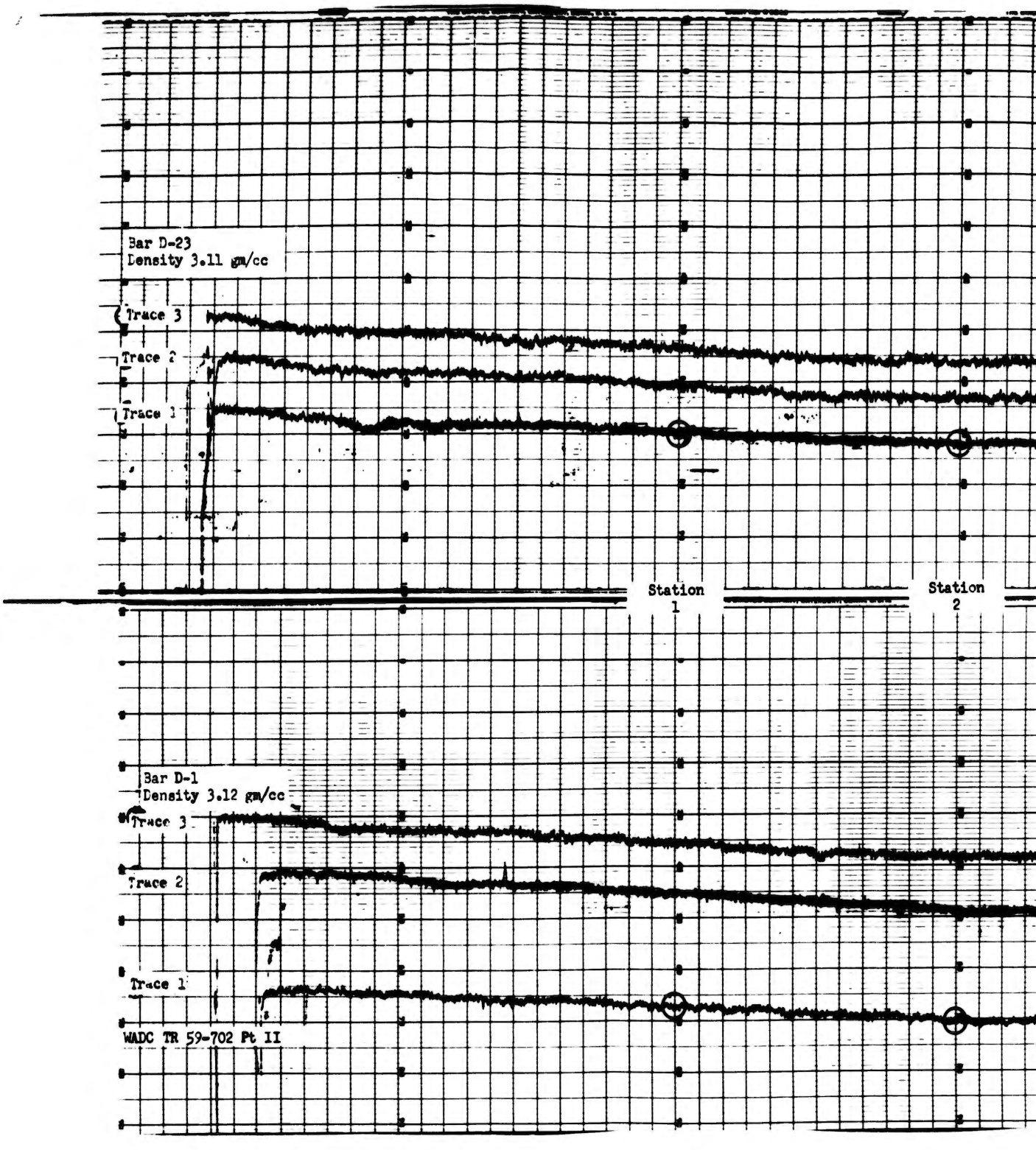
Bar D-23
Density 3.11 gm/cc
Trace 3
Trace 2
Trace 1
Station 1
Station 2
Bar D-1
Density 3.12 gm/cc
Trace 3
Trace 2
Trace 1

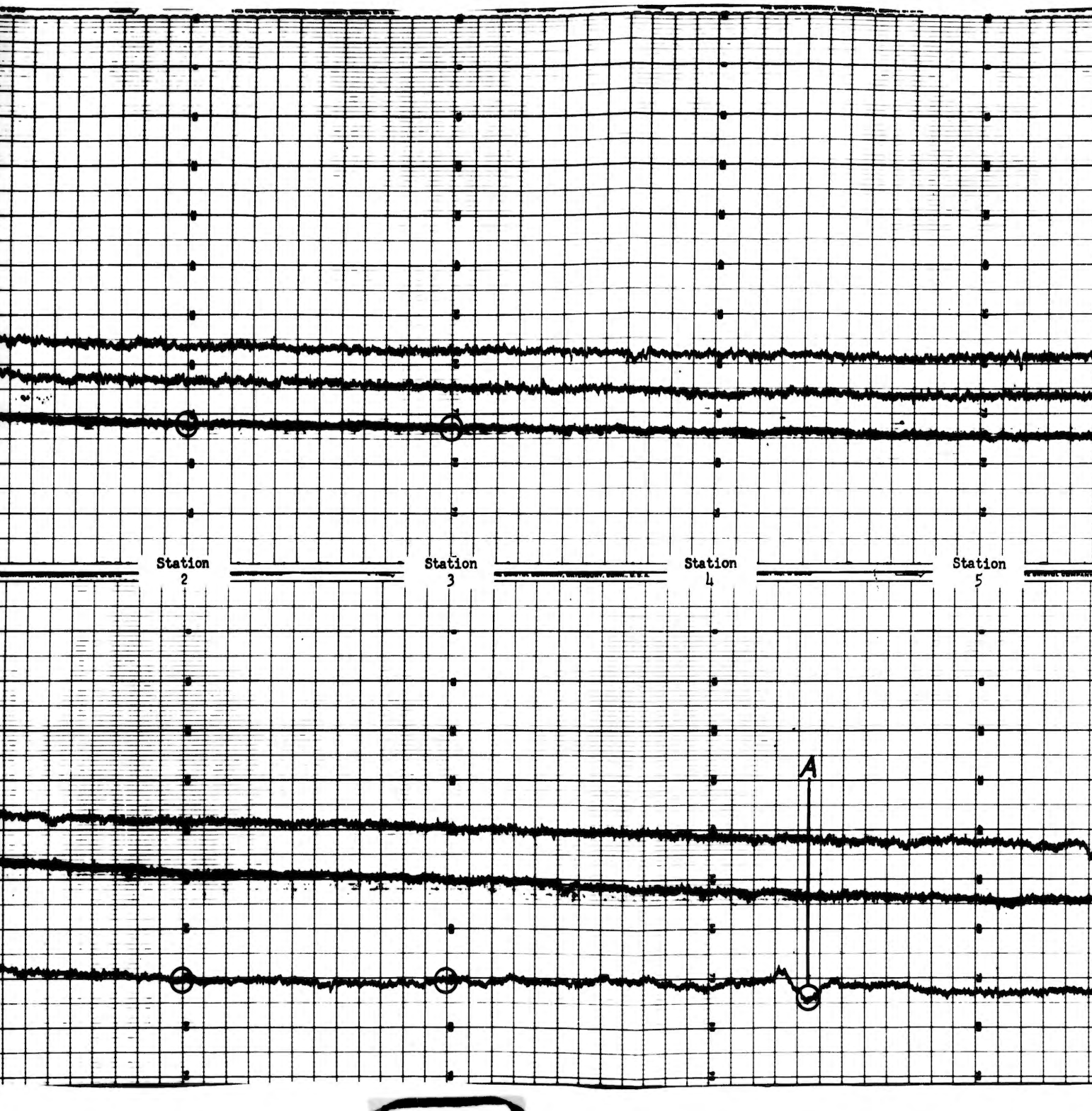

2

3

4

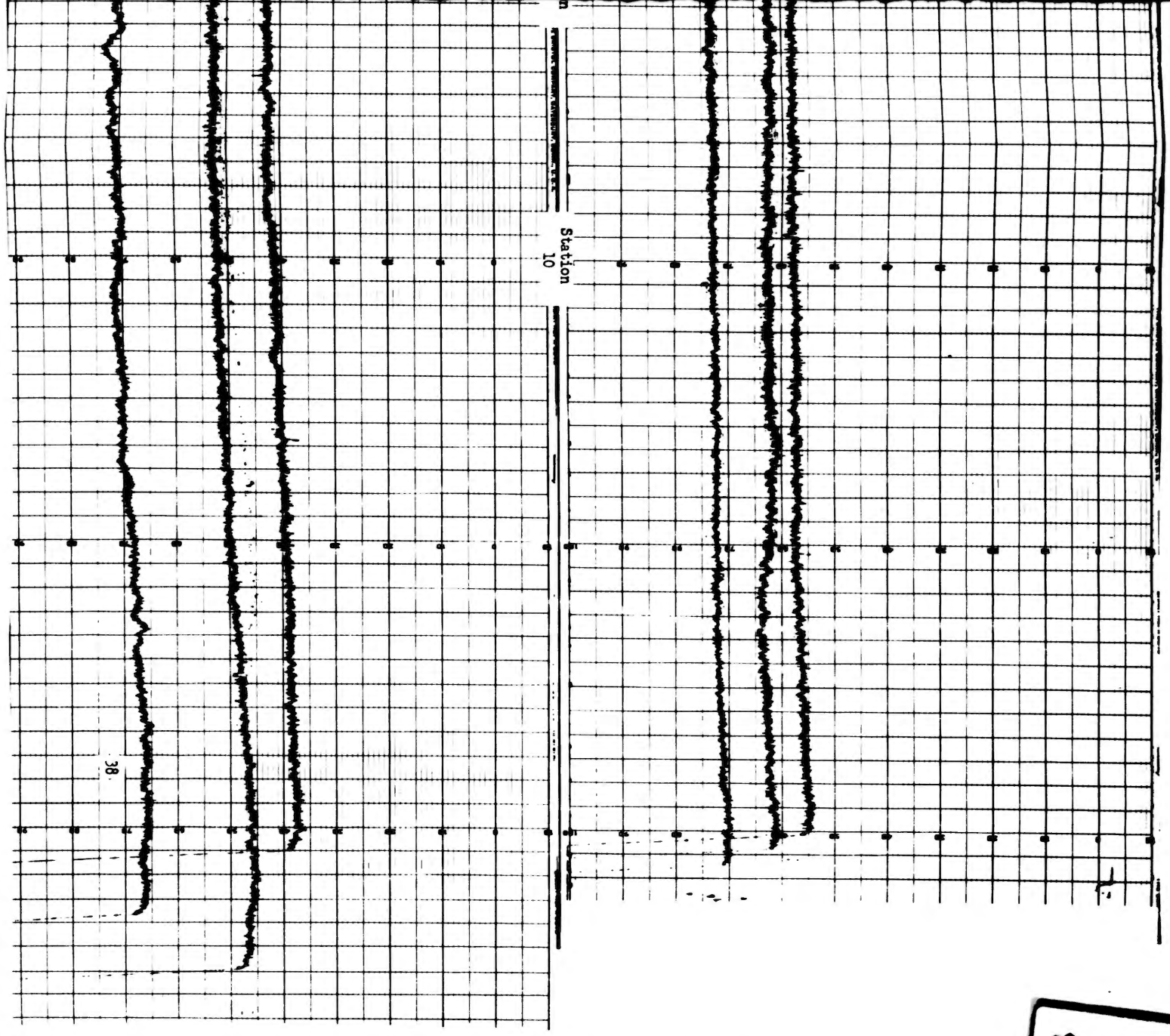

Figure 24. Densitometer-Comparator Traces Of KT Silicon Carbide Bars D-1 and D-23 X-Rays through 1/4" Thickness

Figure 25. Reflectoscope Ultrasonic Inspection Apparatus

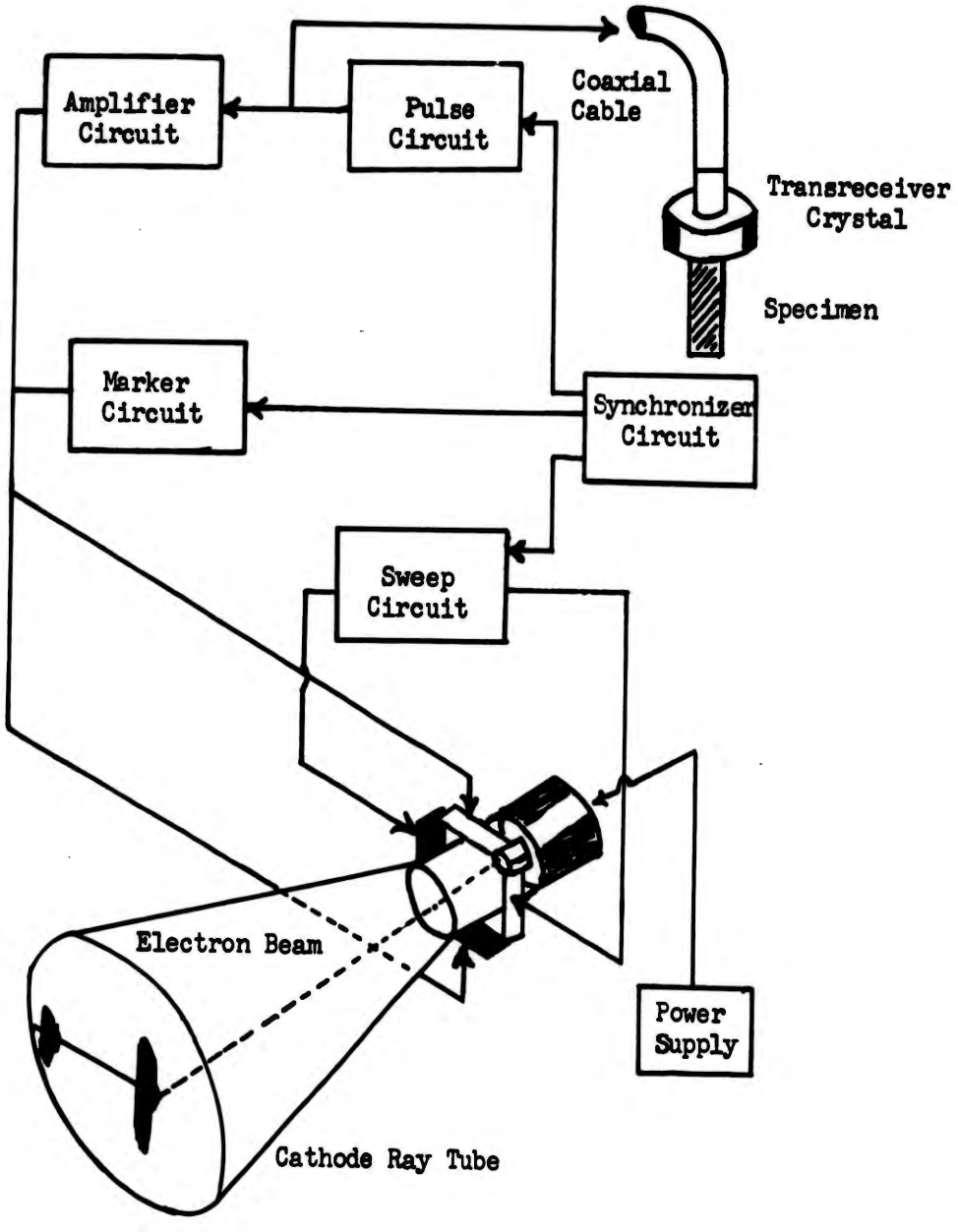

Figure 26. Block Diagram of the Functions of the Components of the Reflectoscope

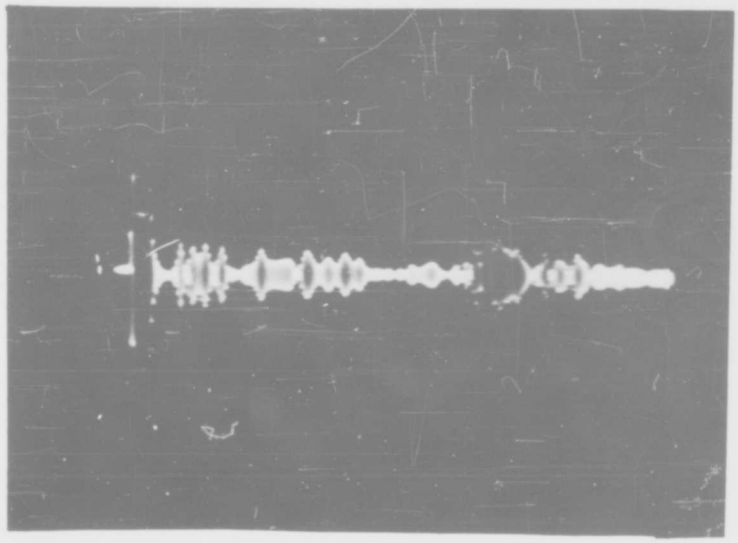

Figure 27. Reflectoscope Trace for KT Silicon Carbide Specimen D-1

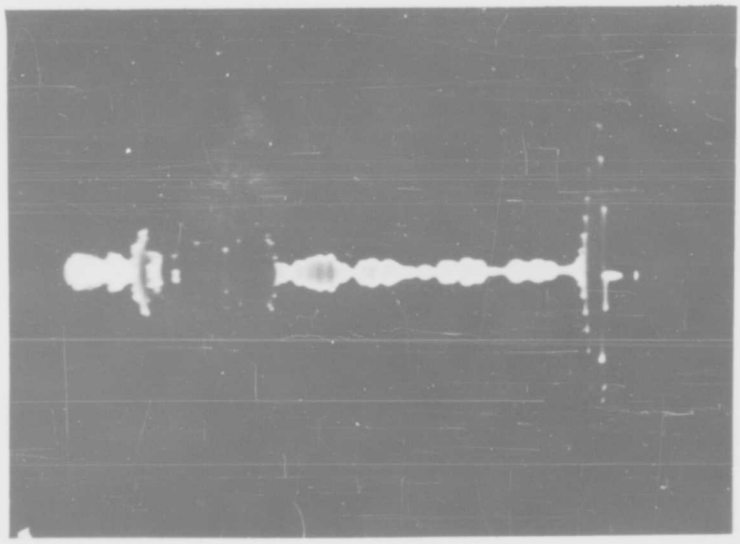

Figure 28. Reflectoscope Trace for KT Silicon Carbide Specimen D-15

TABLE III

DENSITIES OF KT SILICON CARBIDE TEST SPECIMENS

Specimen Number ①	Density grams/cc	Specimen Number ②	Density grams/cc	Specimen Number ③	Density grams/cc
D-1	3.12	H-2	3.10	G-1	3.12
D-2	3.09	H-3	3.12	G-2	3.11
D-3	3.10	H-4	3.12	G-3	3.12
D-4	3.13	H-5	3.10	G-4	3.12
D-5	3.10	H-6	3.10	G-5	3.11
D-6	3.09	H-8	3.11	G-6	3.14
D-7	3.09	H-9	3.10	G-7	3.12
D-8	3.11	H-10	3.11	G-8	3.11
D-9	3.10	H-11	3.12		
D-10	3.10	H-12	3.11		
D-11	3.12	H-13	3.10		
D-12	3.11	H-14	3.08		
D-13	3.11	H-16	3.15		
D-14	3.10	H-17	3.12		
D-15	3.11	H-20	3.11		
D-16	3.12	H-21	3.09		
D-17	3.11	H-22	3.11		
D-18	3.10	H-23	3.11		
D-19	3.11	H-24	3.12		
D-20	3.10	H-25	3.13		
D-21	3.10	H-26	3.11		
D-22	3.11	H-27	3.12		
D-23	3.11	H-28	3.11		
D-24	3.10	H-29	3.11		
D-25	3.11	H-30	3.10		
Average	3.11	Average	3.11	Average	3.12

Note: ① D = 6" x 1/2" x 1/4" Ground

② H = 6" x 1/2" x 1/4" As Fabricated

③ G = 5" x 1/4" x 1/4" Ground

V X-RAY DIFFRACTION UNDER TRANSVERSE LOAD

A. General

When a bar of uniform cross-section is subjected to an uniaxial load, the bar is lengthened and its cross-sectional area is decreased in direct proportion to the resultant applied stress, providing the elastic-limit of the material has not been exceeded. The resultant effect on each individual crystallite in the bar is an extension of the crystallite in the direction parallel to the bar axis and a compression in directions normal to the applied load. Crystallites whose crystallographic planes are perpendicular to the extension or compressive forces will have their interplanar spacings changed by an amount $\pm\Delta d$. Measurement of this change yields a measure of the elastic strain.

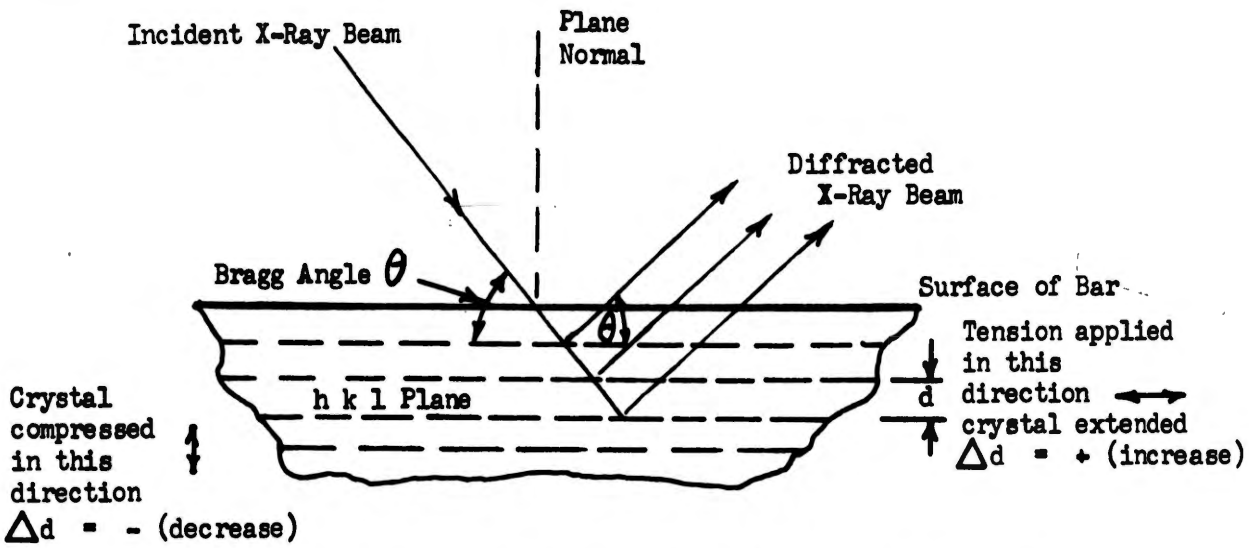

Figure 29. Diffraction of X-Ray Beam (Source: Reference 24)

The principle used in measuring these elastic strains by X-ray diffraction is based on the fact that, if the interplanar spacing "d" is altered by application of a load, the Bragg angle θ will change. Once the change in θ is known, the strain of those particular lattice planes can then be calculated from the differential of the Bragg equation

$$(1)\quad \frac{\partial d}{d} = -\cot\theta\partial\theta \qquad \text{(Reference 25)}$$

If the material is elastically isotropic and the lattice planes lying parallel to the surface are altered in spacing by an amount δd due to a biaxial stress ($\sigma x + \sigma y$) lying in the plane of the surface, the strain normal to the surface is

$$(2) \quad e_z = -\frac{\gamma}{E} (\sigma x + \sigma y) = \frac{\delta d}{d}$$

γ = Poisson's Ratio

E = Young's Modulus

Combining equations (1) and (2)

$$(3) \quad \sigma x + \sigma y = \theta (\tan \theta \cdot \gamma / E)$$

For a flat bar subjected to a uniaxial load $\sigma y = 0$ and thus

$$(4) \quad \delta\theta = \gamma \tan \theta \cdot \epsilon_x$$

$\delta\theta$ is in radians

The fundamental relationships discussed above are satisfied when the following assumptions hold true.

1. The material is a perfectly elastic, homogenous, and isotropic body.

2. The elastic constants are the same in compression and in combined stress systems as in simple tension.

3. The lattice planes under study are parallel to the surface of the bar.

4. Loading is uniaxial.

B. Test Apparatus and Method

The X-ray diffraction apparatus at Bell Aircraft uses a counter tube, instead of a special film camera, as the detector for indicating the intensity of the diffracted radiation. The detector, fitted with a goniometer, is made to move in a circle around the specimen at twice the angular speed of the specimen to allow the angle between the incident and reflected beams to be measured accurately.

Pulses from the detector are conveyed via an amplifier to a recording apparatus, which traces the pulse rate or X-ray intensity on calibrated graph paper.

Figure 30 is a general view of the X-ray diffraction apparatus and Figure 31 is a block diagram of the apparatus. Figure 32 is a close up view of the transverse loading fixture which was fabricated at Bell Aircraft. The loading fixture was patterned after the fixture developed by the Springfield Armory, Research and Development Division, Springfield, Massachusetts (Reference 26).

The load was applied by advancing a screw with a pitch of 1/32 of an inch in 1/100 increments of a complete turn. A diffraction pattern was recorded at each load application and the interplanar spacing calculated for the Bragg angle measured for the recorded reflection using the basic Bragg equation. The readings were taken using a Norelco Wide Range Goniometer, scanning at a rate of 1° per minute with the peak intensity kept constant.

C. Results

Tests were conducted on silicon carbide to explore the possibility of obtaining stress strain relationship for this material measured in Angstrom units. It is believed this data may be useful in determining whether nonlinear areas exist before rupture, and whether crystal lattice slippage occurs before rupture. KT silicon carbide exhibits polymorphism and is known to be anisotropic. The predominant crystallographic species are hexagonal and rhombohedral. This phase of the investigation was directed toward exploring a simple technique to probe whether strain and crystal lattice changes may be detected in brittle materials such as silicon carbide. The ultimate objective would be to ascertain by non-destructive methods the degree of strain in a silicon carbide system. This information would in effect determine the degree of useful strength that may be left in a system fabricated from brittle materials.

The data obtained on two KT silicon carbide bars 6" x 1/2" x 1/4" is given in Tables IV and V. Figure 33 is the load deflection curve for the loading apparatus used in the test.

As shown in Table IV and Table V indications are that there is a measurable effect in interplanar spacing with an increase in transverse load. The apparent non-increase in some of the readings with an increase in load may be due to partial seizure of the movable part of the test fixture. A more sophisticated loading device may be necessary but is beyond the scope of this contract. It is probably desirable for future consideration to spot check the effect on single crystals before any extensive studies are initiated on polycrystalline materials.

The calculations made for establishing Figure 33 were derived as follows:

Using Young's modulus, $E = 54.78 \times 10^6$, determined using sonic techniques, the load P, is calculated from the following relationship

$$P = \frac{48\,\delta\,EI}{l^3} \quad \text{(Reference 27)}$$

P = load in lbs

δ = Deflection in inches

E = Young's Modulus, 54.78×10^6

I = Moment of Inertia, $\frac{bd^3}{12}$

l = Span length, 5 inches

$$P = \frac{48 \times 54.78 \times 10^6 \times 0.502 \times 1.5625 \times 10^{-2} \times \delta}{12 \times 125}$$

$$P = \frac{4 \times 54.78 \times 10^6 \times 0.502 \times 1.5625 \times 10^{-2} \times \delta}{125}$$

$$P = 13{,}750\delta$$

thus for a deflection $\delta = .0013"$

$$P = 13{,}750 \times .0013$$

$$P = 17.9 \text{ lbs}$$

The stress in the outermost fiber $S_{max} = \frac{M}{Z}$

M = bending moment, $\frac{Pl}{4}$

Z = Section Modulus, $\frac{bd^2}{6}$

thus at P = 17.9 lbs, $\delta = .0013"$

S_{max} = 4,278 psi

Calculation of interplanar spacing d -

$n\lambda = 2\,d\,\sin\theta$

$\lambda = 1.5405A \quad n = 1$

Ex - Using data for specimen #2 at Reading 16

$2\theta = 134.038^\circ$

$\theta = 67.019^\circ$

$1 \times 1.5405 = 2d \sin 67.019$

$$d = \frac{1.5405}{2 \times \sin 67.019}$$

$d = .836740$ Angstroms

D. Conclusions

Based on this preliminary study it appears possible to determine the stress-strain relationship of brittle materials such as silicon carbide using the technique and equipment previously described.

A comprehensive study to establish the strain and crystal lattice changes occurring in brittle materials should be the subject of a study under a separate contract.

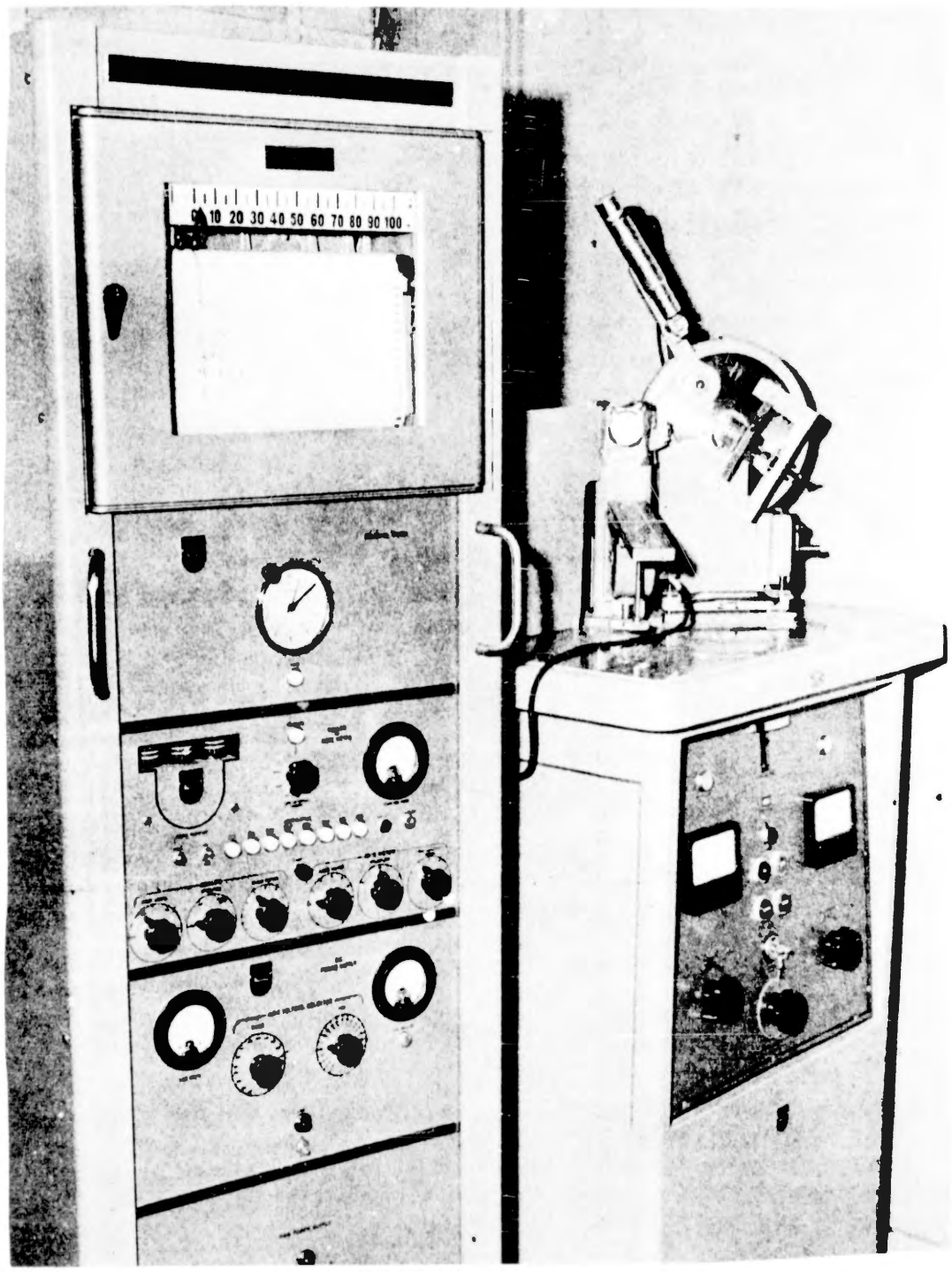

Figure 30. X-Ray Diffraction Test Apparatus

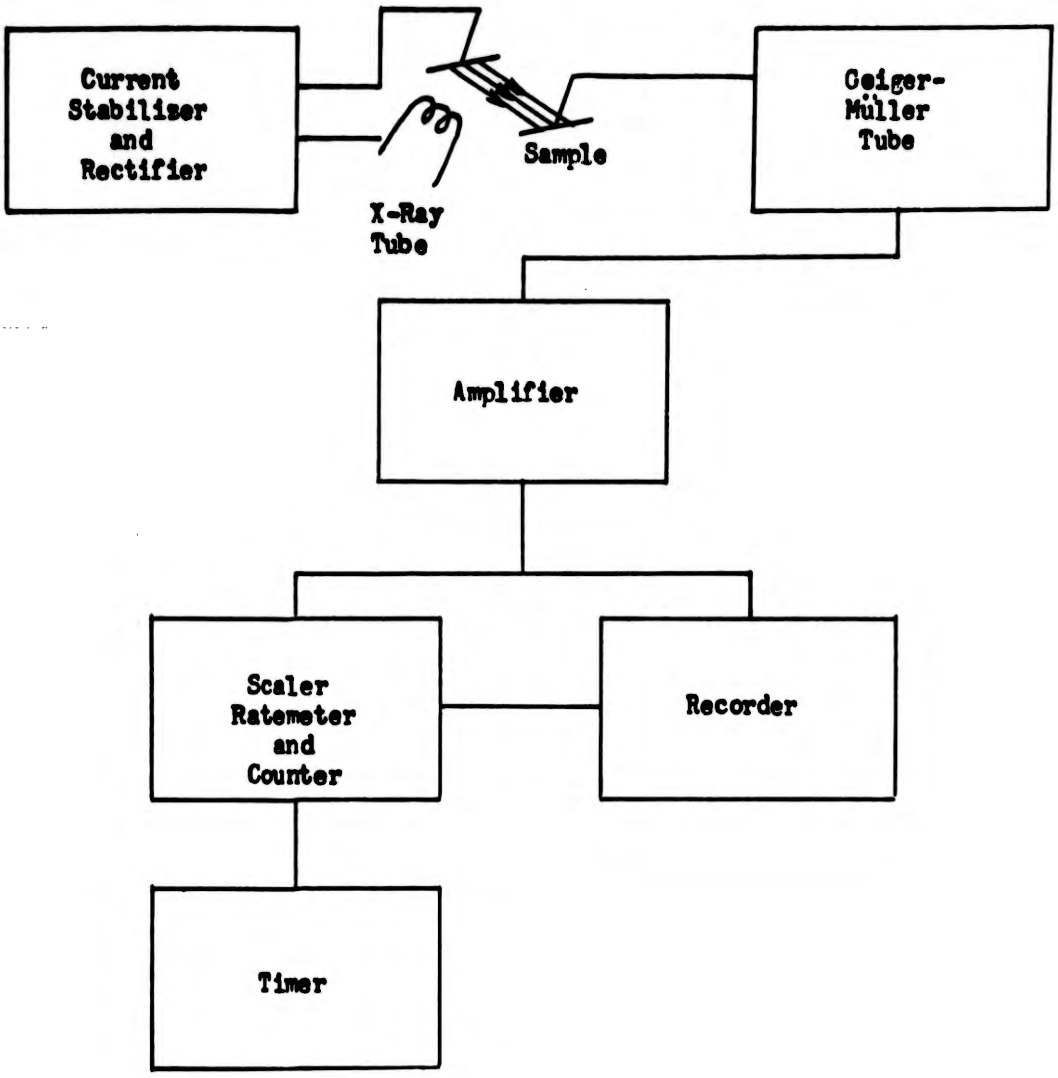

Figure 31. Diagram of X-Ray Diffraction Test Apparatus

Figure 32. View of X-Ray Diffraction Transverse Loading Device With Specimen In Place

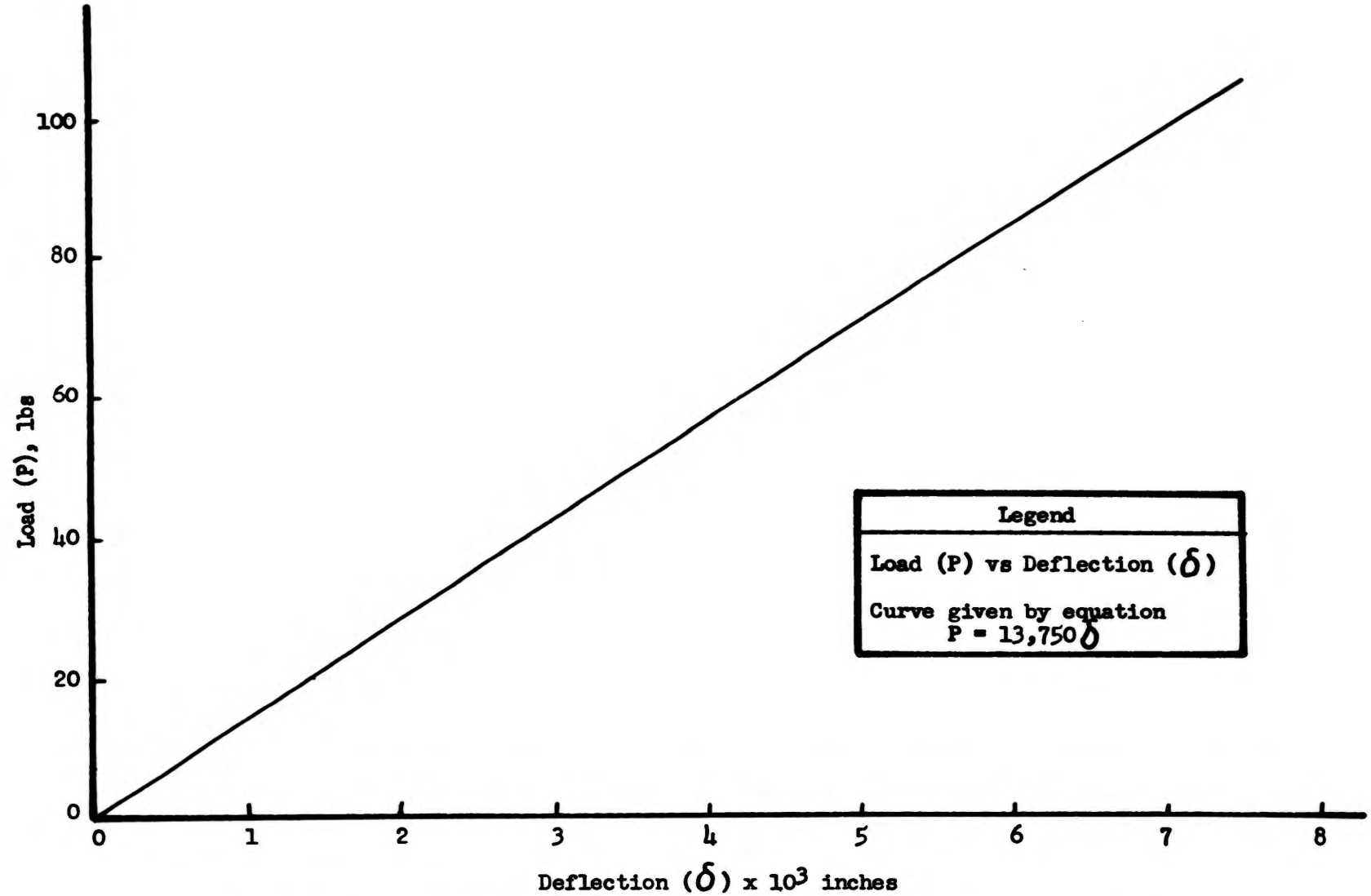

Figure 33. Load-Deflection Curve For X-Ray Diffraction Loading Apparatus

TABLE IV

X-RAY DIFFRACTION DATA FOR KT SILICON CARBIDE SPECIMEN NUMBER 1

Reading	Deflection (inches)	P Load (lbs.)	S_{max} Stress (psi)	d Interplanar Spacing (Angstroms)	2θ Degrees
1	0	0	0	.837020	133.916
2	.0013	17.9	4,278	.837015	133.920
3	.0020	27.5	6,572	.836985	133.930
4	.00265	36.4	8,700	.836925	133.950
5	.00335	46.1	11,018	.836865	133.970
6	.00385	52.9	12,643	.836865	133.970
7	.00450	61.9	14,794	.836835	133.980
8	.00535	73.6	17,590	.836800	133.992
9	.00565	77.7	18,570	.836800	133.992
10	.00600	82.5	19,718	.836800	133.992
11	.00635	87.3	20,865	.836800	133.992
12	.00670	92.1	22,012	.836780	133.998
13	.00700	96.3	23,016	.836780	133.998
14	.00730	100.4	23,996	.836740	134.010

TABLE V

X-RAY DIFFRACTION DATA FOR KT SILICON CARBIDE SPECIMEN NUMBER 2

Reading	Deflection (inches)	P Load (lbs.)	S_{max} Stress (psi)	d Interplanar Spacing (Angstroms)	2θ Degrees
1	0	0	0	.837045	133.912
2	0	0	0	.837045	133.912
3	.00065	8.9	2,130	.836985	133.930
4	.0010	13.8	3,300	.836985	133.930
5	.00165	22.7	5,425	.836985	133.930
6	.0020	27.5	6,570	.837015	133.920
7	.00200	27.5	6,570	.836925	133.932
8	.00235	32.3	7,720	.836925	133.932
9	.00285	39.2	9,370	.836925	133.932
10	.00285	39.2	9,370	.836865	133.936
11	.00335	46.1	11,020	.836835	133.946
12	.00365	50.2	12,000	.836835	133.946
13	.00400	55.0	13,150	.836800	133.958
14	.00420	57.8	13,810	.836800	133.958
15	.00420	57.8	13,810	.836835	133.956
16	.00450	61.9	14,790	.836740	134.038

VI ELECTRICAL RESISTIVITY

A. General

A study was undertaken to determine whether a change would occur in the electrical resistivity of silicon carbide when the material is subjected to mechanical loads such as compression and transverse loading. It was anticipated that data collected may enable the correlation of change in electrical resistivity with mechanical stress.

Data obtained from the Carborundum Company for KT silicon carbide shows a rapid decrease in electrical resistivity from room temperature to 400 F. The rate of decrease levels off until 2400 F. Above this temperature, the rate of decrease of resistivity increases.

Compression testing was selected for experimental purposes as test equipment requirements would be at a minimum.

B. Test Apparatus and Method

A number of techniques were evaluated to insure intimate contact between the specimen and the resistance measuring instrument.

In the early stages of the program, the current was passed through the specimen by means of copper plates mounted on the specimen. The pick up leads were wrapped around the specimen as shown in Figure 34 below.

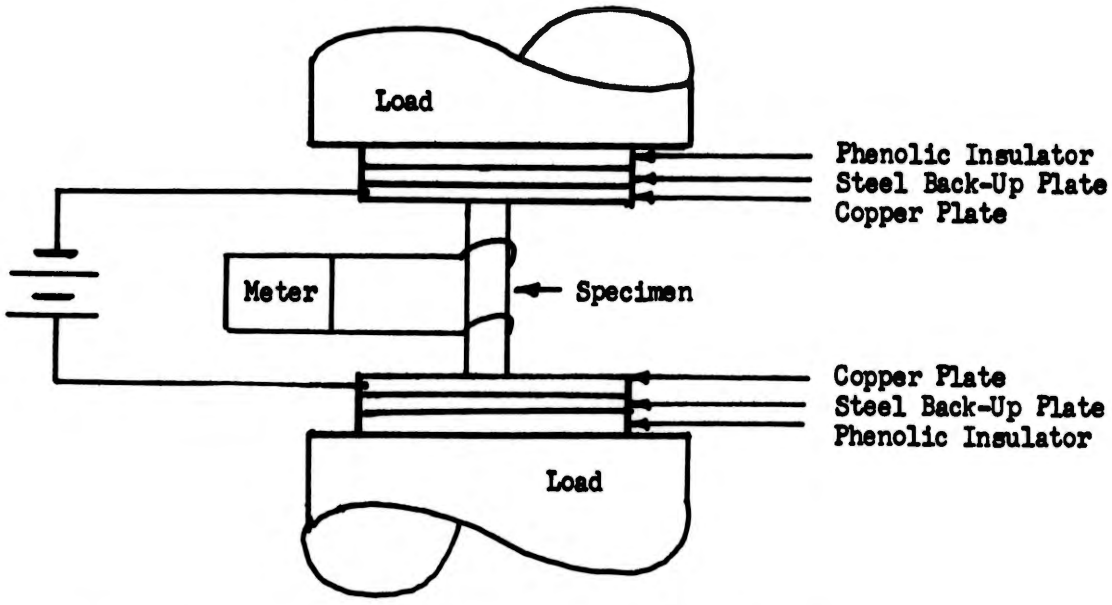

Figure 34. First Electrical Resistivity Test Assembly

The values obtained were erratic. This was attributed to poor electrical contact and the change in contact resistance. Wrapping the pick up leads around the specimen resulted only in point contact due to the rough surface finish of the specimen. It was observed that as the specimen was being compressed, the specimen was deforming the copper plate. This affected the contact resistance between the silicon carbide specimen and the plate.

In the next approach, the copper plates were eliminated and the current was applied directly to the specimen as shown in Figure 35. To obtain a relatively uniform specimen surface and maximum contact areas, the ends of the specimen and the areas where the pick up leads were to be positioned were painted with an electrically conductive silver paint. However, it was found that the resistance of the paint, due to the resin content, was higher than that of the specimen.

A method was evaluated by which strips of malleable conductive metals such as copper and lead were wrapped around the silicon carbide. Intimate contact was not obtained. The most successful approach evaluated was by copper electroplating the desired areas of the specimen. The leads were wrapped around and soldered to these copper electroplated areas.

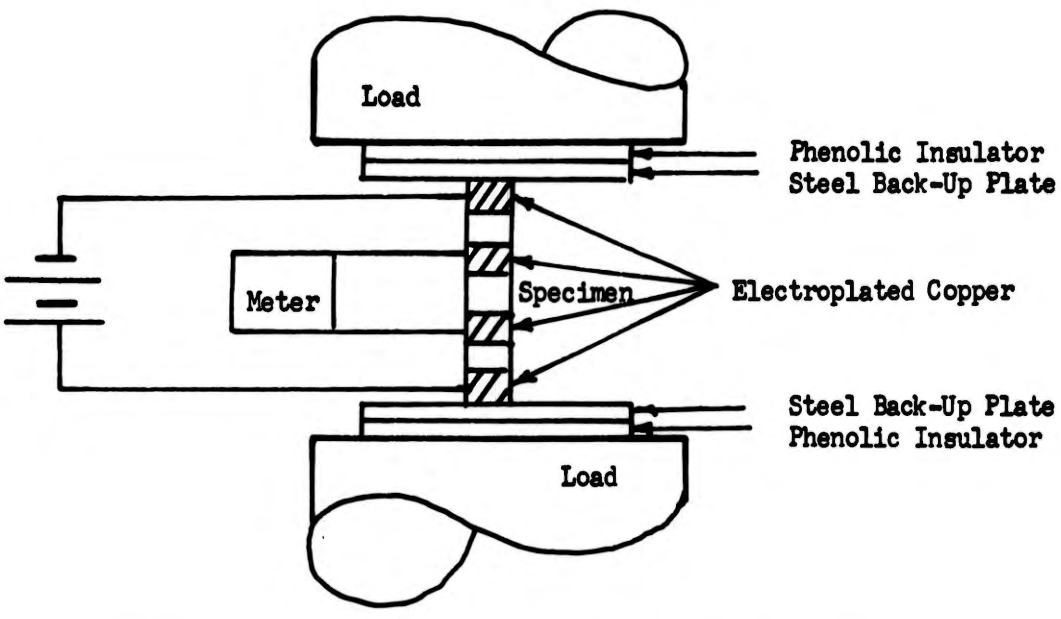

Figure 35. Modified Electrical Resistivity Test Set-Up

The loading mechanism was the Baldwin Universal Testing Machine, having a maximum load capacity of 60,000 pounds. A Rubicon Kelvin Bridge Model 1622 was used to apply the current and measure the resistance in ohms. On the low range the instrument can detect resistances to 0.0001 ohm, ±0.1%, ±20 micro-ohms.

Electrical resistivity of silicon carbide decreases with an increase in temperature. Current flowing through silicon carbide for any length of time, would heat the specimen and decrease the resistivity. To overcome or minimize this heating effect, the current was applied and removed momentarily while the resistance readings were taken.

C. Results

Observations made during this study indicate a slight decrease of electrical resistivity with increase of compressive load and an increase of resistivity with a decrease of load. The applied load was increased and decreased in equal increments. The change in resistivity however, was not linear.

The over-all change in resistivity noted when load was increased from 5,000 psi to 40,000 psi was 0.0124 ohm using the method shown in Figure 34. The over-all change in resistivity from 9,000 psi to 130,000 psi was 0.0009 ohm using the method shown in Figure 35.

Although the resistivity increased as the load was decreased, the resistivity did not recover to the same value it was during the application of the original load. For example: when a load of 5,000 pounds was applied to a specimen, a value "X" for electrical resistivity was obtained. As the load was increased to 10,000 lbs, we obtained another value "Y" ("Y" was less than "X") for the electrical resistivity. When the load was decreased to 5,000 pounds, the value for the electrical resistivity was not equal to "X" but was less than "X". If the load was then increased to 10,000 pounds again, the value for electrical resistivity was less than "Y".

Using a standard volt-ohm meter, it was observed that the silicon carbide specimen exhibited the property of electrical absorptivity. For example: when the instrument leads were first attached to the specimen a reading of 4 ohms would be obtained. This value would gradually drift down to 2 ohms. When the leads were removed and attached several additional times, a reading of 2 ohms would still be obtained. However, if the specimen were shorted out and the instrument leads attached again, a reading of 4 ohms was observed.

D. Conclusions

Since the changes of electrical resistivity with compressive load were small and gradual and contained hysteresis loops the only conclusion which may be made at this time is that there is a decrease of resistivity with compressive load. No correlation can be attempted between resistivity and a given amount of load change based upon this limited study. However, it is believed further study in this area is warranted. The effects may be more pronounced at a particular temperature.

VII DYNAMIC MODULUS - SONIC TECHNIQUE

A. General

The modulus of elasticity is the constant which expresses the ratio of unit stress to unit deformation for all values of unit stress not exceeding the proportional limit of the material (Reference 28). Young's modulus is used to express this ratio.

The modulus of elasticity is usually determined by two different methods: (1) dynamic and (2) static. KT silicon carbide specimens have been tested by both methods during this program.

By the dynamic method - sonic technique, the specimen is set into vibration and from the resonance frequency and the geometry of the specimen, the modulus can be determined. The modulus of elasticity in bending as determined by the static method is discussed later in this report.

B. Test Apparatus and Method

The apparatus and method of exciting flexural vibrations and measuring the amplitude of vibrations at room temperature are shown in Figures 36, 37, and 38. For the 2200 F tests, the specimen was suspended in a Marshall furnace designed for this purpose and shown in Figure 39.

The specimen was suspended horizontally by two Nichrome wires (0.0126 inch, B and S 28). One of these wires was attached to a University PA 50 speaker driven through a power amplifier by a signal generator. The vibration of the specimen was transmitted through the other suspension wire which was attached to an astatic standard groove crystal pick-up. The resulting signal was amplified and displayed on an oscilloscope. The frequencies, impressed and resultant, were measured by an electronic frequency counter which has an accuracy of ± 1 cycle from 10 cycles to 10 KC.

C. Results

The values of Young's modulus in flexure for KT silicon carbide as determined by the sonic technique are given in Table VI. The average values obtained are 10 to 20 million psi lower than the figures reported by the Carborundum Company for modulus of elasticity in flexure determined by mechanical means. The average values however, are in agreement with those reported by the National Bureau of Standards for KT silicon carbide of comparable dimension and surface finish determined by sonic techniques. Wachtman and Lam of the Bureau (Reference 29) report a value of 56.1×10^6 psi at room temperature and 51.5×10^6 psi at 2200 F. Bell test results show a dynamic modulus of 53.7×10^6 psi (average of 24 specimens) at room temperature and 50.3×10^6 psi (average of 5 specimens) at 2200 F for polished (60 rms) 6" x 1/2" x 1/4" bars.

The dynamic modulus of the "as fabricated" bars having the same nominal dimensions showed lower values. The room temperature (average of 16 specimens) was 47.4×10^6 psi, and the 2200 F value (average of 5 specimens) was 43.3×10^6 psi.

There was no appreciable difference due to size observed for the dynamic modulus of KT silicon carbide. Polished specimens 5" x 1/4" x 1/4" had dynamic modulus values of 55.9×10^6 psi (average of 8 specimens) at room temperature and 50.9×10^6 psi (average of 5 specimens) at 2200 F.

The dynamic modulus of elasticity determined by the sonic technique is calculated using the formula $E = CWn^2$ where

E = Young's modulus

W = Weight of the specimen

C = A factor which is dependent upon specimen geometry, mode of vibration, and Poisson's ratio.

n = Resonant frequency (f_R)

For the first mode of flexural vibration the formula becomes

$$E = C_1 W f_R^2$$

The resonant frequency for the specimens used in this study was approximately 3KC for the 6" x 1/2" x 1/4" specimens and about 4KC for the 5" x 1/4" x 1/4".

As noted above the results obtained on the "as fabricated" (unground) specimens were lower than those for the ground specimens. It is believed that this may be attributed to (1) surface finish and (2) magnitude of dimensional variation observed. The dimensions on a single specimen varied by as much as 5 to 6%. In some instances the dynamic modulus could not be determined for the "as fabricated" specimens because of excess warpage.

The following equation was used to calculate C_1, the shape factor:

$$C_1 = \frac{\text{constant}}{b} \times \left|\frac{\ell}{t}\right|^3 \quad \text{where}$$

b = width

constant = 0.002452 as determined by Pickett (Reference 30) for rectangular bars.

ℓ = length of specimen

t = thickness in direction of vibration

It can be seen that any variation in t will influence C_1. The other sources of error are additive. Since ℓ/t is approximately 24 for a 6" x 1/2" x 1/4" specimen, the small variations observed in ℓ from specimen to specimen was considered to have a negligible effect on C_1.

A typical calculation follows:

Measurements taken on specimen D-2 before fastening to the wire suspension were:

W = weight of bar = 37.9156 grams = 0.0836 pounds

ℓ = length of bar = 6.00 inches

t = average thickness of bar in direction of vibration = 0.250 inch

b = average width of bar = 0.500 inch

The specimen was then fastened to the support wires at the proper location and the resonant frequencies found at room temperature and at 2200 F. The resonant frequencies were determined by reading the maximum amplitude on the scope and cross checking with maximum deflection of the voltmeter.

The following information was compiled:

f_{R_1} = 3061 cps at room temperature

f_{R_1} = 2944 cps at 2200 F

r/ℓ = ratio of gyration of cross-section to length of bar =

$$\frac{\frac{1}{\sqrt{12}} \times t}{\ell} = \frac{0.289 \times t}{\ell} = 0.012$$

T_1 = Goen's correction factor

A correction factor T_1 of 1.0125 was used in calculating the modulus of elasticity (E) in bending using sonic techniques. This correction factor assumes a Poisson's ratio (μ) of zero. The error in calculating E introduced by this assumption is relatively insignificant as shown below. Tabular values of T_1 (Reference 30) are:

r/ℓ	Correction Factor T_1	
	$\mu = 0$	$\mu = 1/3$
.01	1.0079	1.0088
.02	1.0314	1.0350

The calculated r/ℓ for the specimens tested is 0.012. The correction factor T_1 for this ratio would be 1.0125 assuming $\mu = 0$, and 1.0140 assuming $\mu = 1/3$. Since KT silicon carbide has a reported $\mu = 0.27$ the correction factor would be less than 1.0140. Typical calculation for E using $T_1 = 1.0125$ and $T_1 = 1.0140$ follow.

$$E = C_1 W f_R^2$$

where $C_1 = \frac{.002452}{b}\left(\frac{\ell}{t}\right)^3 T_1 = \text{sec}^2/\text{in}^3$

(a) $$E = \frac{.002452}{b}\left(\frac{6.00}{0.25}\right)^3 \left(1.0125\right)\left(.0836\right)\left(3061\right)^2$$

$$E = 53.77 \times 10^6 \text{ psi using } T_1 = 1.0125$$

(b) $$E = \frac{.002452}{b}\left(\frac{6.00}{0.25}\right)^3 \left(1.0140\right)\left(.0836\right)\left(3061\right)^2$$

$$E = 53.85 \times 10^6 \text{ psi using } T_1 = 1.0140$$

At 2200 F the effect of change in length of the specimen is compensated for by multiplying the shape factor C, by $\frac{1}{\left[1 + \alpha\,(T_2 - T_1)\right]}$

where α equals the mean coefficient of linear expansion. The value of the linear coefficient of expansion was determined by Bell Aircraft (Reference 31).

$\alpha = 2.6 \times 10^{-6}$ in/in/°F, mean value from room temperature to 2200 F. Thus at 2200 F the corrected shape factor is now

$$C_1 = \frac{.0024523}{b} \times \left(\frac{\ell}{t}\right)^3 T_1 \times \frac{1}{\left[1 + \alpha\,(\theta_2 - \theta_1)\right]}$$

where θ_1 = temperature$_1$

θ_2 = temperature$_2$

and the Young's modulus is

$$E = \frac{.0024523}{0.500} \times \left(\frac{6.00}{0.250}\right)^3 \times T_1 \times \frac{1}{\left[1 + 2.6 \times 10^{-6} (2200-75)\right]} \times$$

$$.0836 \times (2944)^2$$

$$E = 49.47 \times 10^6 \text{ psi}$$

D. Conclusions

The non-destructive method of determining the dynamic modulus of Young's modulus of silicon carbide by the sonic technique is feasible. However, the method of using free - free flexural vibration is limited to rectangular and cylindrical geometry and critical dimensional tolerances. To determine the dynamic modulus of various other shapes of silicon carbide, it is believed that vibration excitation by wave velocity propagation should be investigated.

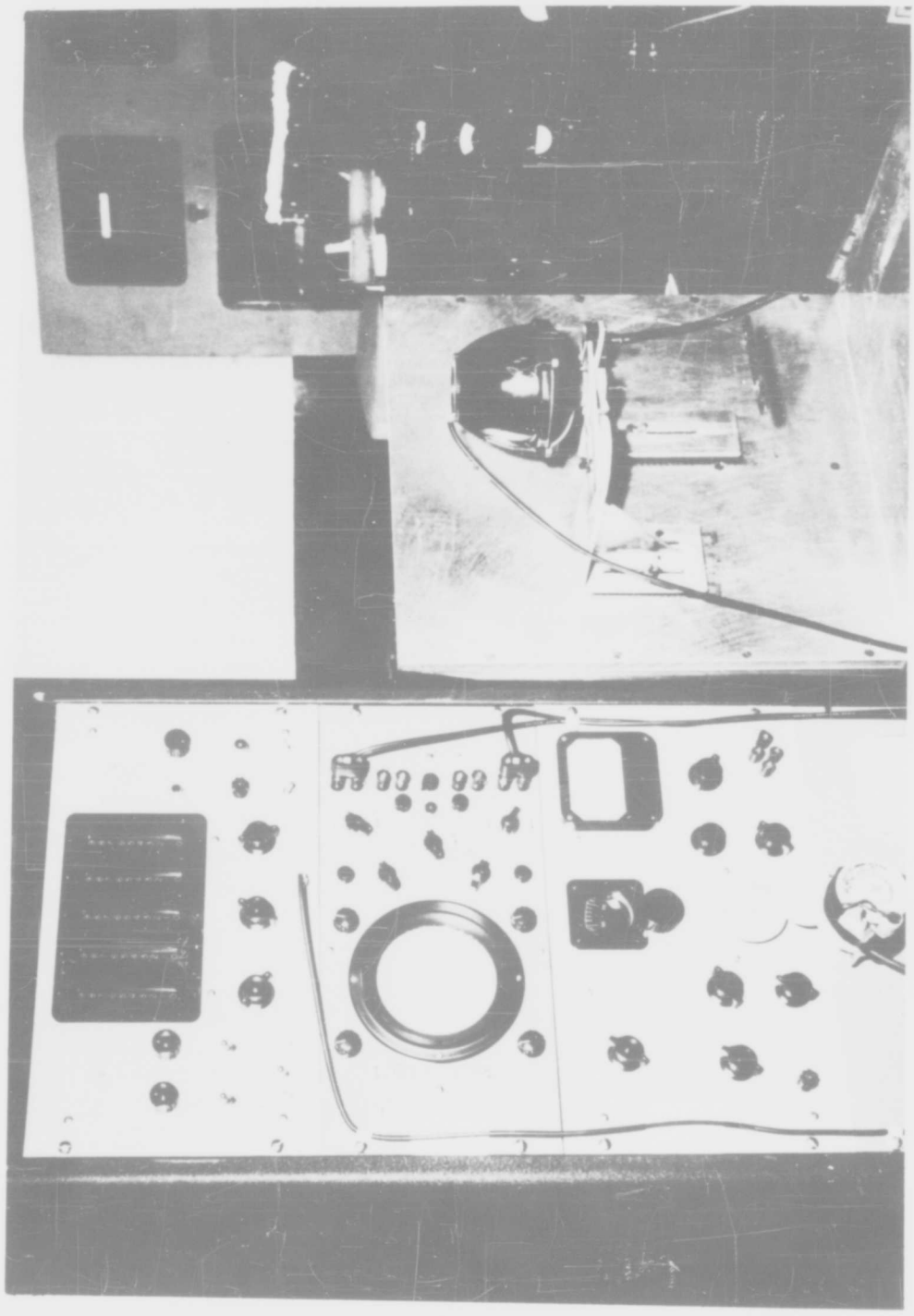

Figure 36. Dynamic Modulus Test Apparatus - Sonic

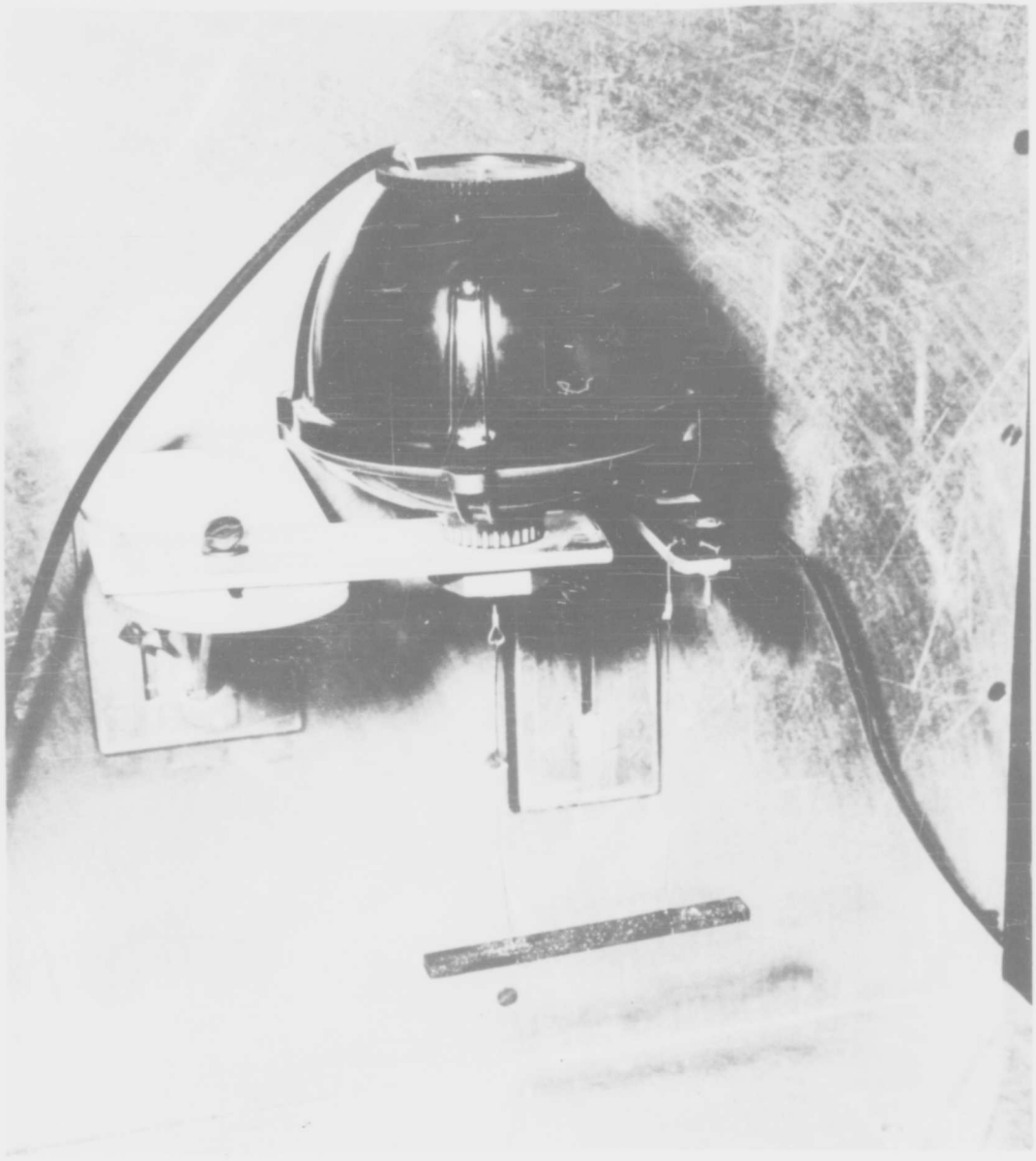

Figure 37. Close Up View of Dynamic Modulus Electro-Magnetic Driver, Crystal Pick-Up, and Specimen

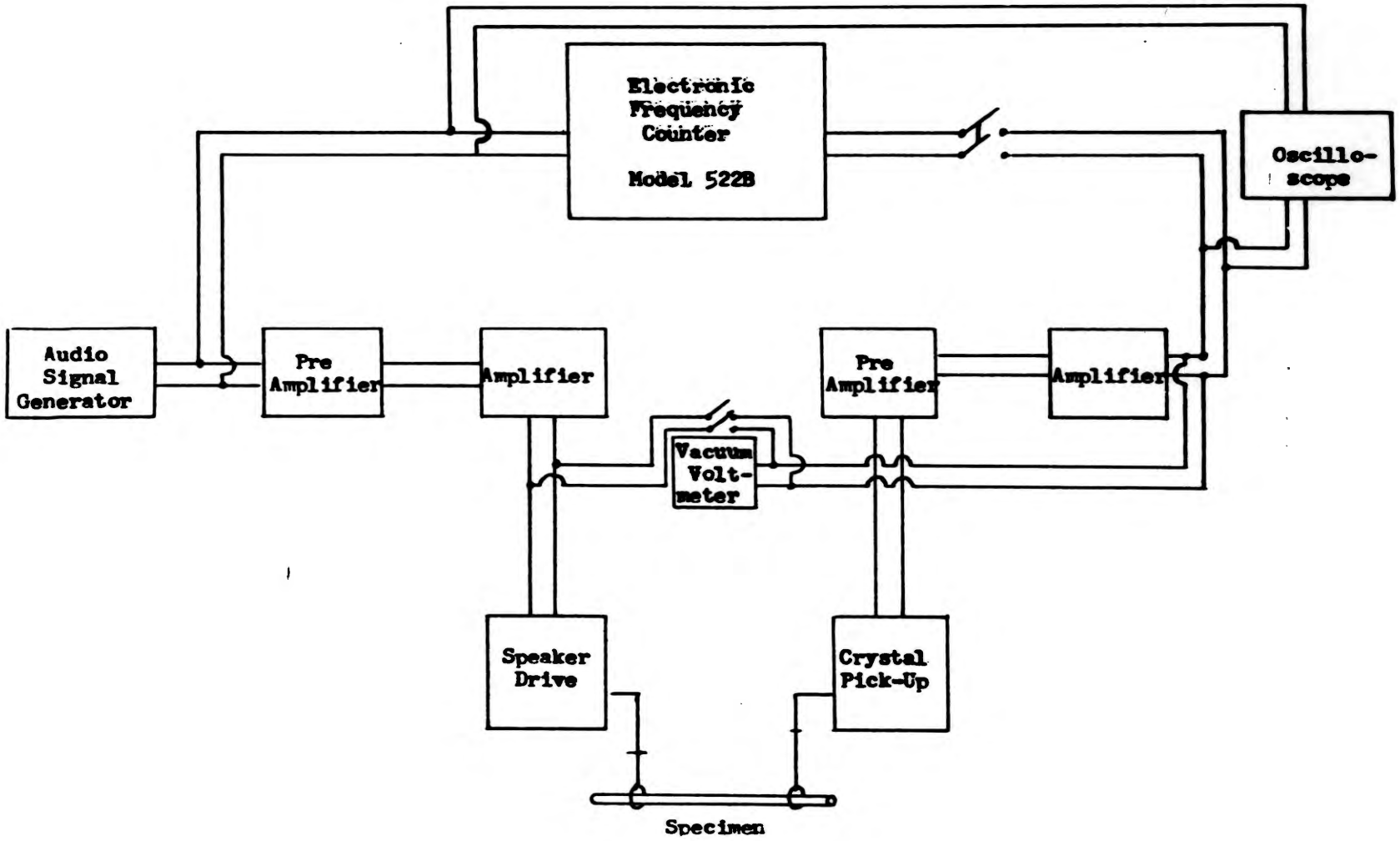

Figure 38. Block Diagram of Dynamic Modulus Test Apparatus As Constructed by Bell Aircraft Corporation

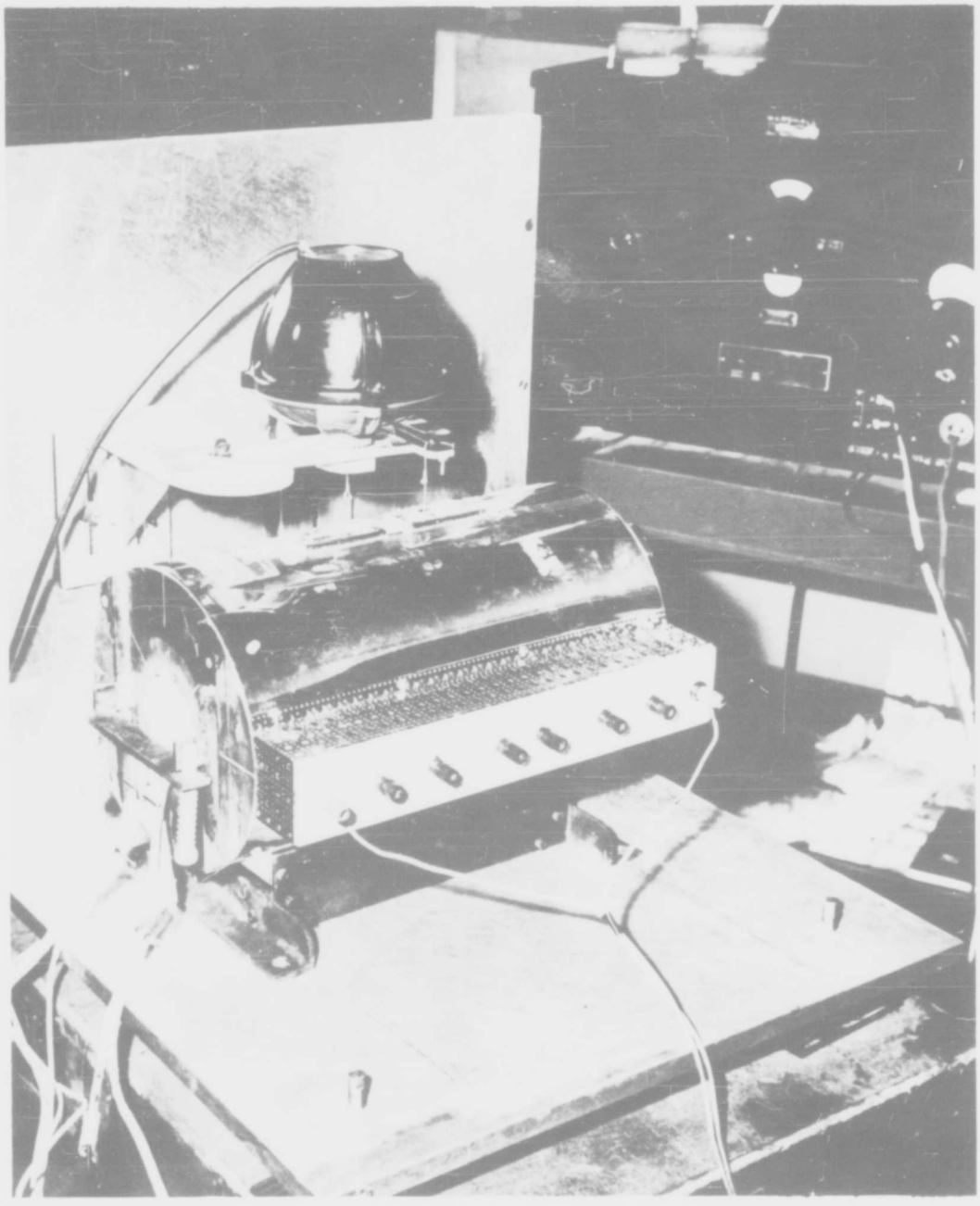

Figure 39. Marshall Furnace Used For Determining Dynamic Modulus at 2200 F

TABLE VI

DYNAMIC MODULUS OF FLEXURE FOR KT SILICON CARBIDE

Specimen 6" x 1/2" x 1/4" Ground	E x 10^{-6} psi		Specimen 6" x 1/2" x 1/4" "As Fabricated"	E x 10^{-6} psi		Specimen 5" x 1/4" x 1/4" Ground	E x 10^{-6} psi	
	80F	2200F		80F	2200F		80F	2200F
D-1	53.82		H-2	49.08		G-1	55.99	52.02
D-2	53.77	49.47	H-3	46.63		G-2	55.06	49.00
D-3	54.77	50.54	H-4	45.88		G-3	54.34	48.80
D-5	55.67	51.40	H-5	48.09		G-4	56.60	52.89
D-6	54.32	49.99	H-6	46.07		G-5	56.35	52.05
D-7	53.91		H-8	49.54		G-6	59.17	
D-8	55.61		H-9	45.53		G-7	56.98	
D-9	53.82		H-10	51.00		G-8	52.94	
D-10	54.51	50.07	H-11	44.61				
D-11	54.07		H-12	46.79	43.65			
D-12	52.96		H-13	47.34				
D-13	53.00		H-14	47.07	43.25			
D-14	51.97		H-16	49.18	45.46			
D-15	53.85		H-17	47.86	44.66			
D-16	54.66		H-20	50.70				
D-17	53.69		H-21	42.96	39.58			
D-18	52.53							
D-19	53.14							
D-20	52.12							
D-21	52.48							
D-22	53.91							
D-23	52.89							
D-24	53.02							
D-25	53.38							
Average	53.66	50.29	Average	47.40	43.32	Average	55.93	50.95

VIII INTERNAL FRICTION

A. General

The standard theory of elasticity implies a direct relationship between stress and strain. Also applied force and deformation are directly related provided that the applied force is varied slowly so that no vibrations result.

However, if the load is applied rapidly additional effects appear. It has been found (Reference 33) that when a load is applied suddenly the resulting strain does not appear instantaneously but approaches its final value exponentially as in the curve OA of Figure 40 below. Also if the load is removed, the strain approaches zero exponentially as in curve AB.

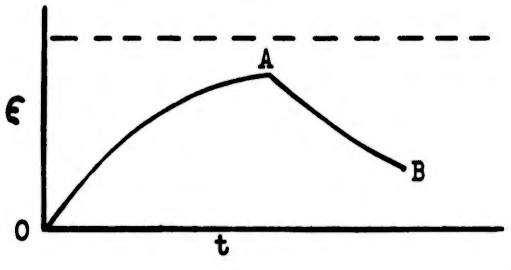

Figure 40. Strain vs Time

In the elastic range, these additional effects are described as time-dependent elasticity or anelasticity. Zener (Reference 32) states that anelasticity denotes that property of solids in virtue of which stress and strain are not single-valued functions of one another in that low stress range in which no permanent set occurs and in which the relation of stress to strain is still linear.

One of the manifestations of anelasticity is internal friction. Internal friction is a term used to denote, in an oscillating system, the rate at which energy is transferred from the vibrational energy of the system into irrecoverable thermal energy (Reference 34).

B. Test Apparatus and Method

Using the equipment described in Section VII of this report, the internal friction Q^{-1} may be determined in two ways. By the first method, the peak width Δf can be measured by finding the two values of frequency at which the amplitude of vibration is one half the value at resonance (Reference 32). Then

$$Q^{-1} = \frac{\Delta f}{\sqrt{3} f} \qquad \text{(equation 1) where}$$

f = resonant frequency

Δf = peak width

This method is most effective for specimens having values of Δf of several cycles per second. A second method is more effective for specimens having smaller values of internal friction. By this method, the internal friction Q^{-1} is determined by stopping the drive and measuring the time, t_n, for the amplitude to decay to $\frac{1}{n}$ of its value at the beginning of the measurement (Reference 32).

$$Q^{-1} = \frac{\ell n\, n}{\pi f\, t_n} \qquad \text{(equation 2)}$$

These two methods are considered indirect in that only relative values of amplitude are determined and not absolute values.

C. Results

The value of internal friction, Q^{-1} for specimen D-24 (6" x 1/2" x 1/4", ground) was approximately 3×10^{-4} determined by the band width technique. The measurements were made in air utilizing wire suspensions located at a distance of 1.350 - 1.400 inches from the end. The change in the location of supports did not appreciably affect the band width.

However, it is believed that the value $Q^{-1} = 3 \times 10^{-4}$ is not indicative of the true value of the internal friction of KT silicon carbide. It is believed that the value obtained is more representative of the dampening capacity of the suspension system and the surrounding atmosphere in which the tests were conducted.

The above assumptions are based on the fact that equation 1 assumes some of the energy dissipation takes place in the specimen. In practice, however, the method for exciting flexural vibrations used in this work necessitates that the support wires be located off the nodes so that the driver and pick-up may operate effectively. Therefore, some energy will be dissipated into the suspension system and into the surrounding atmosphere.

Zener (Reference 32) has pointed out that for internal friction on the order of magnitude of 10^{-4}, it is necessary to place the specimen in an evacuated chamber to eliminate energy dissipation to the surrounding atmosphere. Wachtman and Lam (Reference 29) have determined the internal friction of various ceramic and cermet bodies and conducted their tests in a vacuum at pressures of approximately one micron in order to eliminate energy losses resulting from acoustical radiation. Wachtman and Teft (Reference 35) have developed a method for compensating for the effect of suspension damping.

The band widths obtained for KT silicon carbide during this study were about 1.5 - 1.9 cycles. The accuracy of the electron counter used to measure the output frequency is ±1 cycle for 10 cycles to 10 KC. This accuracy is sufficient for determining the resonant frequency for dynamic modulus measurements, but for the precise determinations necessary for band width measurement, a frequency counter with an accuracy of ±0.1 cycle is mandatory.

D. Conclusions

This study was a feasibility study. Time did not permit extensive and detailed experimental determination or modification of existing equipment. Internal friction measurement made with equipment described are tentative and the results are preliminary only.

It was believed that the initial study in determining the internal friction of silicon carbide be conducted in a normal atmosphere (instead of a vacuum) since that would be the environment in which silicon carbide would be utilized in an aircraft or missile.

IX MODULUS OF RUPTURE AND DEFLECTION

A. General

The determination of the modulus of rupture and the modulus of elasticity in bend (bending modulus) by loading specimens to failure was the only destructive test conducted in this program. The objectives of this test were as follows:

1. Possible correlation of data obtained by non-destructive and destructive tests.

2. Reproducibility and/or scatter of data under identical conditions of loading.

3. Comparing data obtained using one point loading and two point loading.

4. Temperature effect on the modulus of rupture of silicon carbide.

5. Effect of test specimen geometry.

The number of tests conducted was limited by the number of specimens available.

B. Test Apparatus and Method

Modulus of rupture tests were conducted on KT silicon carbide specimens in a silicon carbide electrical resistance heated furnace shown in Figure 43. The specimen was supported on a KT silicon carbide base plate shown in Figure 45. This plate had two parallel semi-circular ridges (1/4 inch radius) spaced 4 inches center to center. Each ridge was terminated at the back by a short KT silicon carbide rod. The two vertical rods served to properly position the specimen with respect to the loading block. The base plate had a 3 inch long, 1 inch wide, 1/2 inch deep (at the center) groove directly under the loading area with a hole to provide passage for the deflection rod. For two point loading tests a top load block of KT silicon carbide was used as shown in Figure 45. This block had two parallel semi-circular ridges (1/4 inch radius) spaced 1 inch center to center. The block also had two semi-circular grooves at the back which served as positioning guides against the two vertical rods of the base plate. A 1 inch diameter KT silicon carbide push rod with a chisel point transmitted the load from loading mechanism to the top load block. Specimen deflection was transmitted to the deflection measuring system by means of a 3/8 inch diameter KT silicon carbide rod shown in Figure 45.

The positioning of the test bars to provide a 1 inch overlap for the 6 inch specimens and a 1/2 inch overlap for the 5 inch specimens on each side of the two parallel semi-circular ridges of the base plate was accomplished by visual observation. The horizontal movement of the push rod is limited to ±0.03 inch by the collar bushing diameter in the metal frame work through which the push rod travels. This results in a possible movement of ±0.16 inch of the chisel point. However, the push rod is visually aligned so that the chisel point rests directly above the deflection rod, is perpendicular to the top load block, and equidistant and parallel to the load and support ridges.

The loading of the specimen was accomplished by a spring loaded cantilever beam. The spring, to which a load cell was attached, was driven in tension by a motor which imparted a rate of loading of approximately 50 pounds per minute. The load applied was transmitted to the specimen by the push rod and top block. The load applied was measured by the load cell. The electrical output of the cell was fed to the Y axis of an X-Y recorder. The deflection of the specimen was transmitted by the deflection detector rod to a strain gauge cantilever beam which in turn fed electrical information to the X axis of the X-Y recorder. The applied load and deflection were plotted simultaneously. The deflection assembly was mounted on an adjustable channel beam which assured contact of the detector rod with specimen.

For one point loading system the apparatus and loading was the same except the top load block was not used.

Figure 43 is a general view of the test apparatus showing the cantilever load beam and drive motor. Figure 44 is a view of the strain gauge cantilever deflection assembly. Figure 45 shows the specimen, an earlier designed base plate and top block, and push rod in position. Figure 46 shows a modified base plate and top block which permits testing of material up to 3/4 inch deflection. In Figure 46 the two outer lines represent the support points and the two inner lines the load points (for two point load).

For the elevated temperature tests, the specimens were inserted directly into the furnace at the test temperature without preheating. All specimens were soaked at the test temperature for one hour before application of the loading force. To facilitate testing, specimens were inserted into the furnace at 20 minute intervals. As each specimen was broken, another from the supply within the furnace was positioned for the next test. Broken specimens were removed from the furnace and allowed to cool in still air to room temperature. Fractures were examined and location of fractures were compared with the X-rays of the specimens in an attempt to determine the influence of possible flaws.

Most of the available specimens were tested under two point load at 80 F, 2200 F, and 2400 F. The test specimens which had been previously used for the determination of dynamic modulus at 2200 F were tested for modulus of rupture and elasticity under two point load at 80 F. In order to obtain limited insight into the two point versus one point loading system, a few remaining specimens were tested under one point loading at 80 F.

For one point load the following were used for calculating the modulus of rupture and modulus of bending elasticity:

$$\text{Modulus of Rupture} = \frac{3P\ell}{2bd^2}$$

$$\text{Modulus of Elasticity} = \frac{P\ell^3}{4bd^3y} \quad \text{where}$$

P = load, lbs.

ℓ = span, inches

b = width, inches

d = depth, inches

y = deflection, inches

For two point load, referring to figure - below, the following were used for calculations.

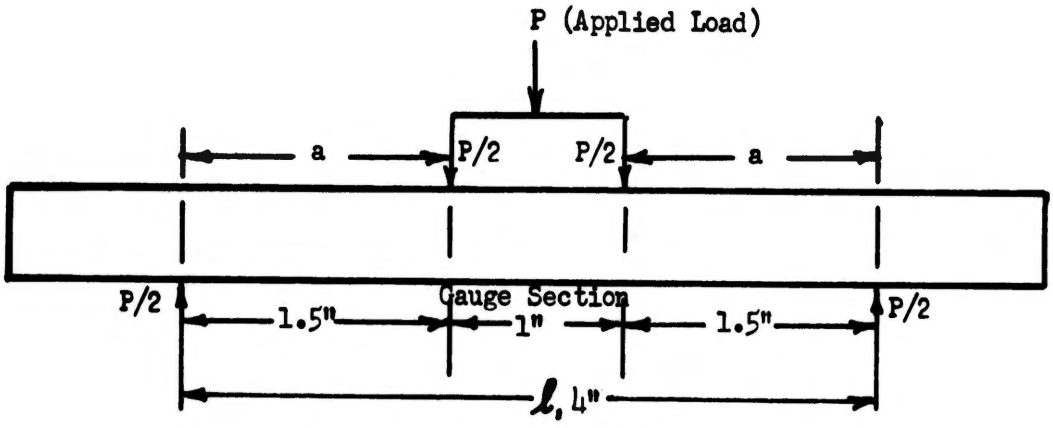

Figure 41. Forces Acting On Modulus of Rupture Bar In Two Point Load

Modulus of Rupture = $\frac{3Pa}{bd^2}$

Bending Modulus of Elasticity (E_b) = $\frac{Pa}{4ybd^3}\left[3\ell^2 - 4a^2\right]$ where

a = nominal distance from point of load to point of reaction

If the load deflection curve is a straight line $\frac{P}{y}$ will be a constant resulting in a constant bending modulus of elasticity. With the bending stress calculated from the beam formula $f_b = \frac{Mc}{I}$ for any load, and E_b calculated from the above equation for the same load and the corresponding deflection, the bending strain may be determined from Hooke's Law. The resulting stress - strain curve will be a straight line.

For the case when the load deflection curve is not a straight line as shown in Figure 42 below, $\frac{P}{y}$ will not be a constant.

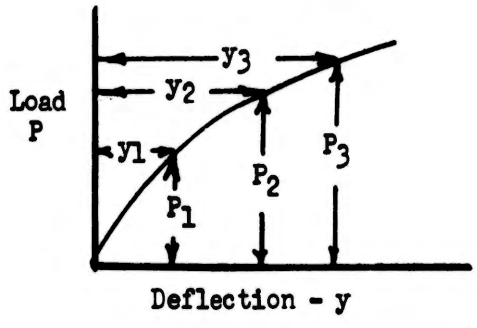

Figure 42. Load vs Deflection

The curve is broken up into load increments P_1, P_2, P_3, etc., with the corresponding deflection y_1, y_2, y_3, etc. For a load increment P_1 the bending stress is determined and with the same load increment and the corresponding deflection, the modulus of elasticity is calculated. This is the secant bending modulus. The tangent bending modulus can be found by taking tangents to the bending stress - bending strain curve determined as explained previously. The tangents are obtained by visual alignment and a slight readjustment of the tangent to the stress-strain curve results in a significant change in the tangent bending modulus. Therefore, the bending modulus of elasticity is somewhat approximate when the load deflection curve is not a straight line. The load deflection curves obtained during this study were essentially straight lines.

In the above, if "a" was greater than 1.5 inches, 1.5 was used in the calculations. If "a" was less than 1.5 inch, then the actual measurement was used.

C. Results

The modulus of rupture, deflection at failure, and modulus of elasticity in bend at failure data for KT silicon carbide are given in Table VII.

Figures 47, 48, and 49, show the broken bars. As in Figure 46, the background lines indicate the support points and load points. The bars are positioned in the figures in the same manner as on the test fixture in the furnace (left side of bar in the figure was also on the left side in the furnace).

The fracture areas of the specimens are indicated on the composite X-ray photographs of the specimens in Figures 50 through 61.

The modulus of rupture, two point load, of the specimens not previously exposed to elevated temperature, versus temperature is shown in Figure 62.

The average tangent modulus versus temperature and the stress versus strain curves for the bars tested during this program are shown in Figures 63 through 75.

Concurrent with this study, Bell Aircraft was conducting a material evaluation program as part of Contract No. AF33(616)-6034, Investigation of Feasibility of Utilizing Available Heat Resistant Materials For Hypersonic Leading Edge Applications. Modulus of rupture and deflection tests were conducted on 5" x 1/4" x 1/4" ground KT silicon carbide specimens. The modulus of rupture versus temperature, the average tangent modulus versus temperature, and stress versus strain curves collected under AF33(616)-6034 are reproduced in this report as Figures 76 through 82.

D. Conclusions

The slightly higher average modulus of rupture obtained by the one point load tend to support the theory that the two point method is more indicative of the strength of a material system. In the two point method a greater portion of the specimen is subjected to a high stress level. Thus the effect of inherent characteristic flaws of the material may be reflected to a greater degree in the test results obtained using the two point loading technique.

Tests indicate that the ground bars have a lower average modulus of rupture than the "as fabricated" bars. This may be attributed to stresses induced by polishing.

Room temperature modulus of rupture values obtained from tests on silicon carbide specimens heat soaked at 2200 F did not show any appreciable difference from rupture values obtained on specimens not exposed to temperature.

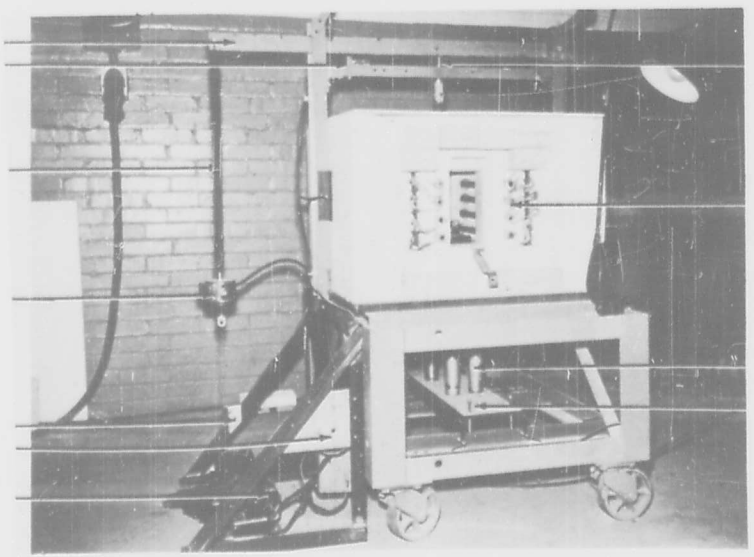

Figure 43. General View of Modulus of Rupture and Deflection Test Apparatus

Figure 44. Close-Up View of Deflection Assembly

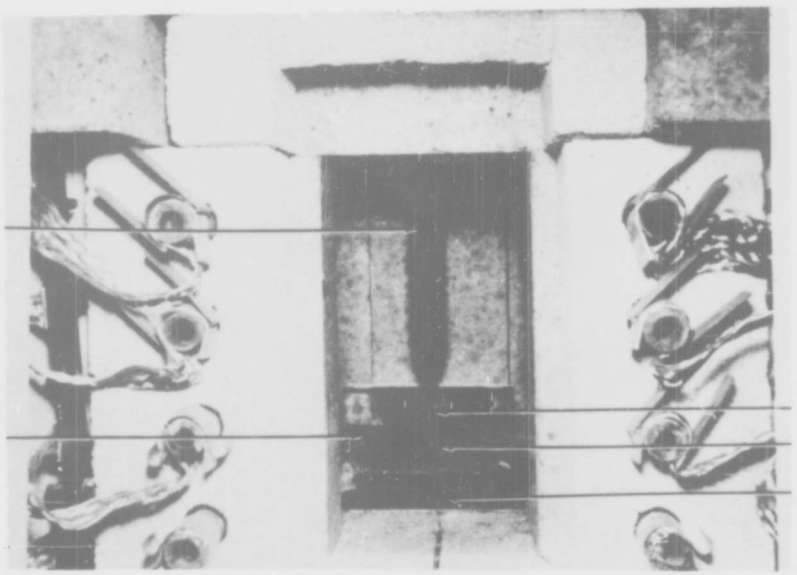

Figure 45. Close-Up View of Specimen Under Load and First Base Plate and Top Block

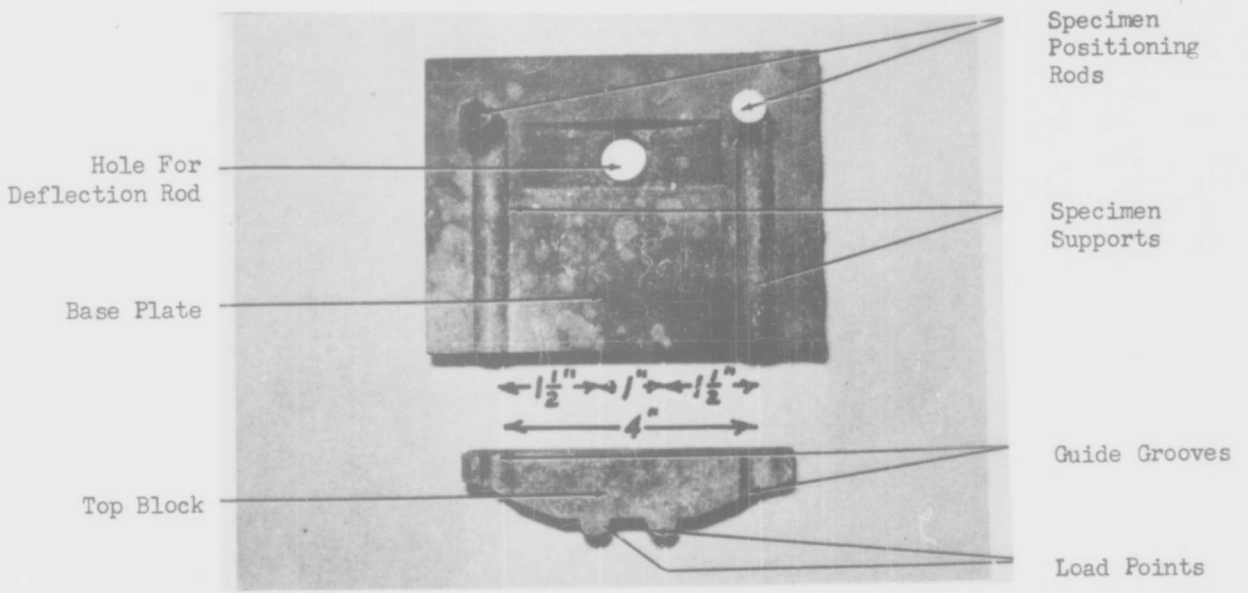

Figure 46. Redesigned Modulus of Rupture Test Fixture Base Plate and Top Block

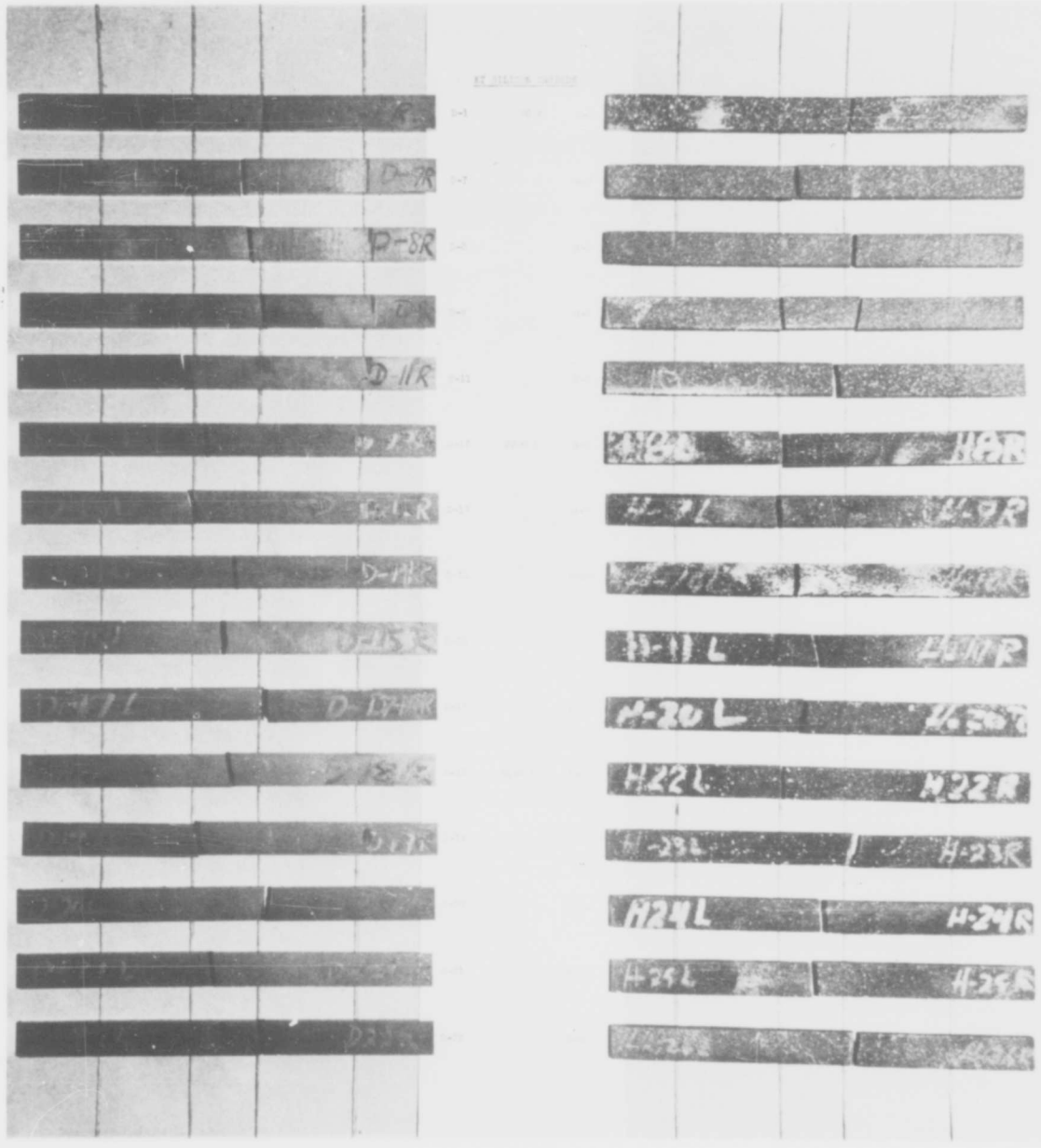

Figure 47. KT Silicon Carbide Modulus of Rupture Test Specimen Failures - Two Point Load

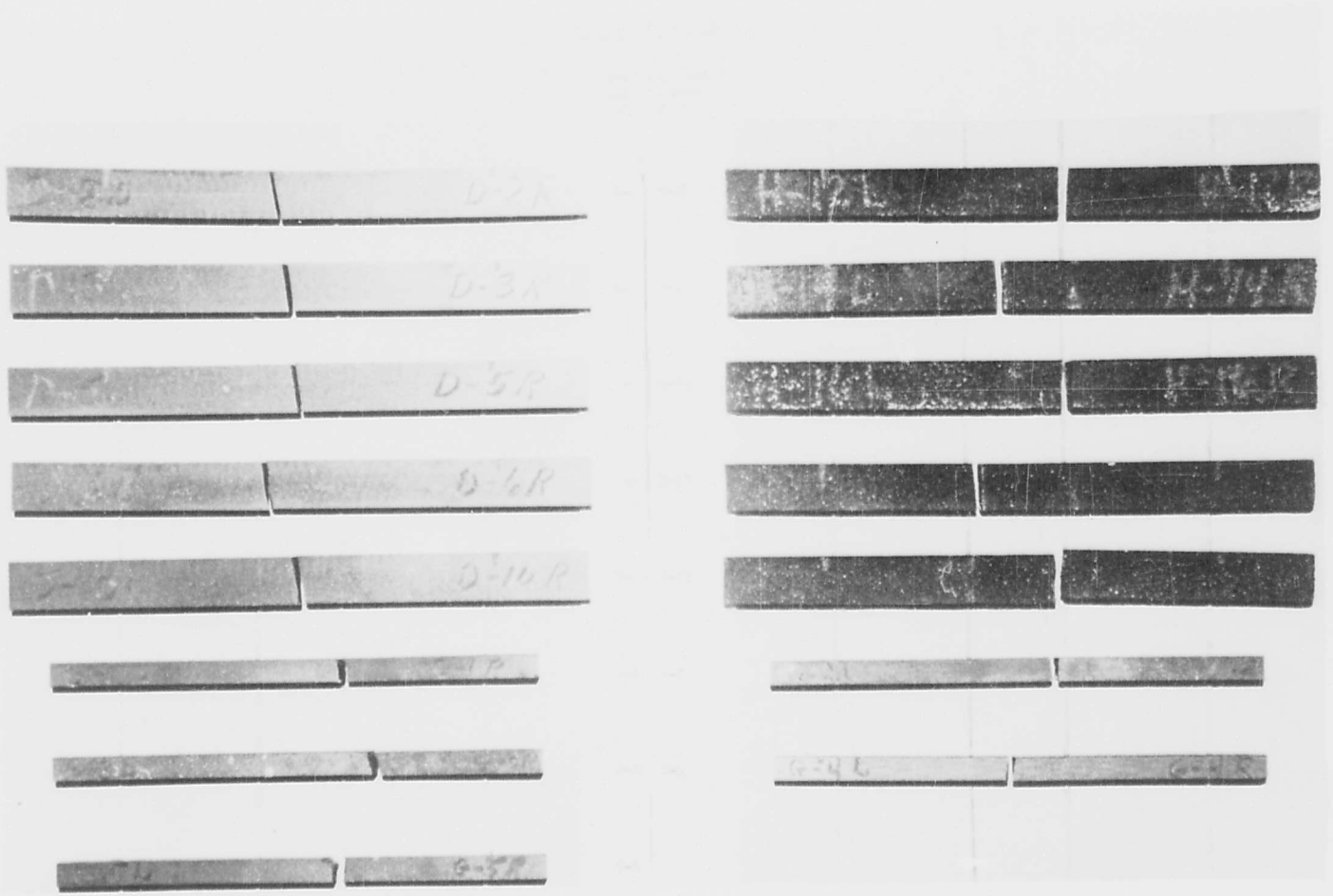

Figure 48. Previously Heat Soaked KT Silicon Carbide Modulus Of Rupture Test Specimen Failures - Two Point Load

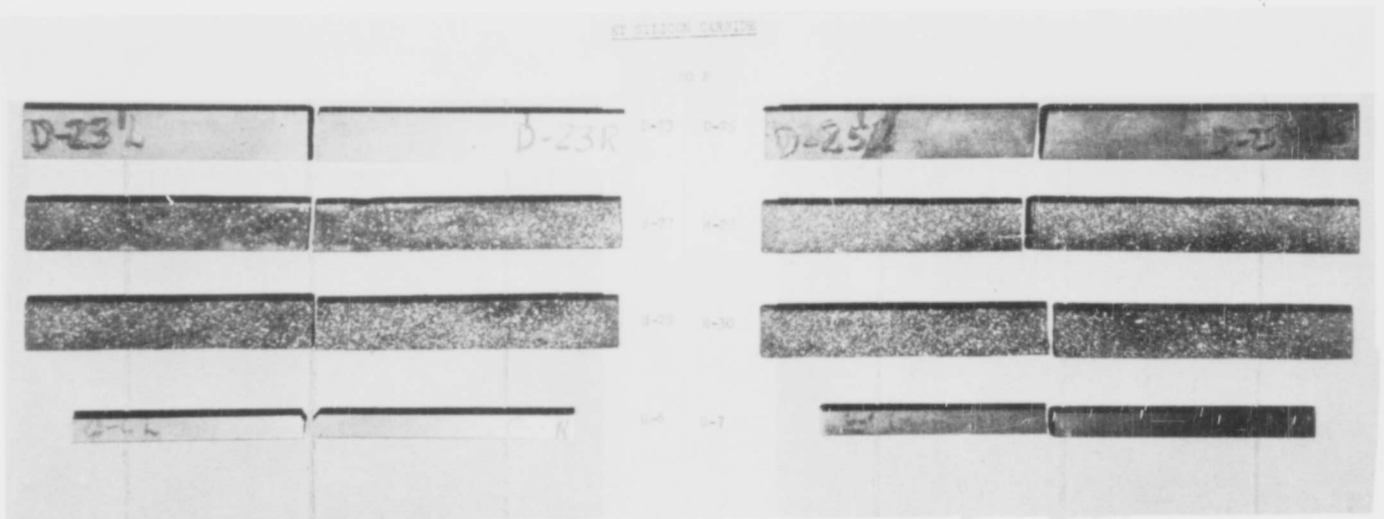

Figure 49. KT Silicon Carbide Modulus of Rupture Test Specimen Failures - One Point Load

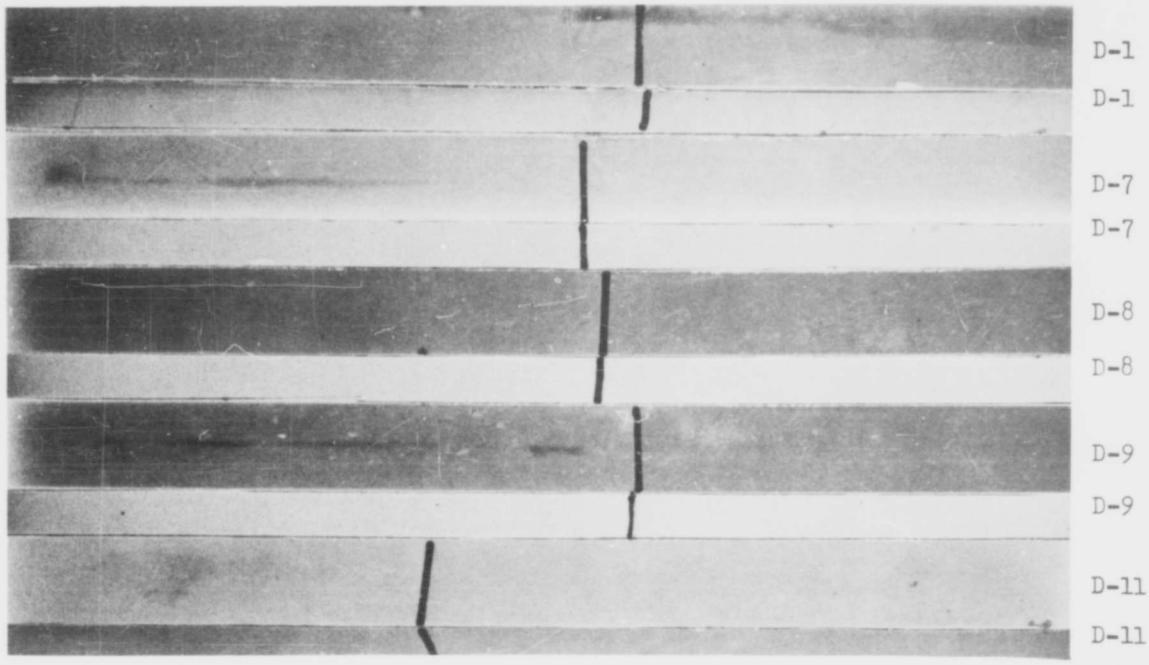

Figure 50. X-Ray Photographs of Ground KT Silicon Carbide Modulus of Rupture Specimens D-1, D-7 to D-9, D-11 with Fracture Noted - Two Point Load, 80 F

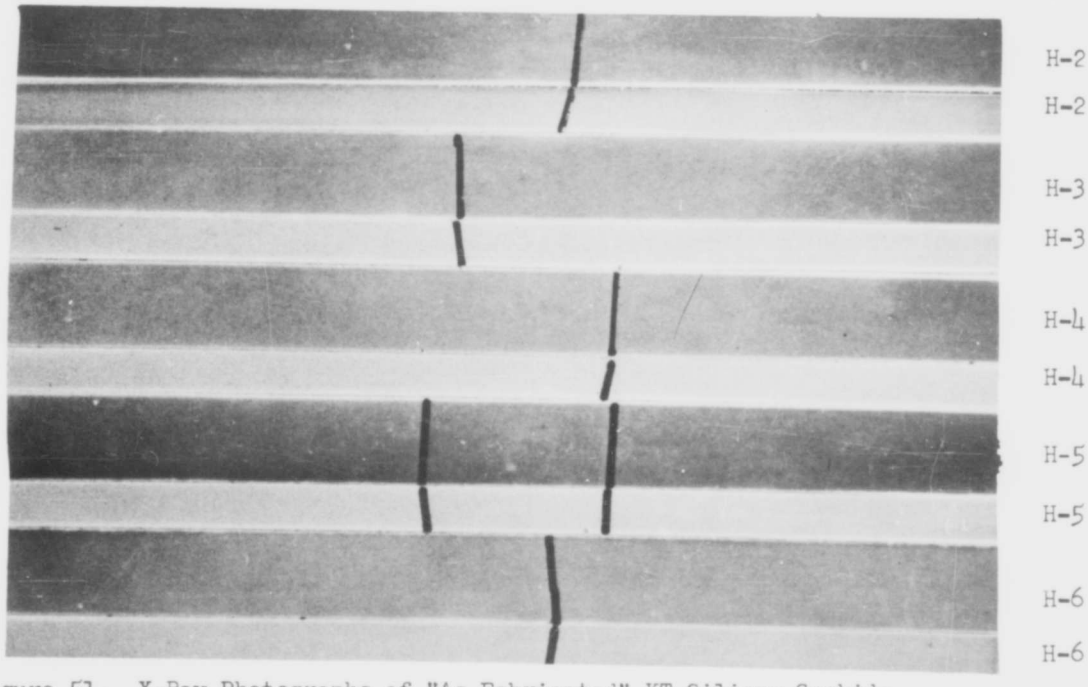

Figure 51. X-Ray Photographs of "As Fabricated" KT Silicon Carbide Modulus of Rupture Specimens H-2 to H-6 with Fracture Noted - Two Point Load, 80 F

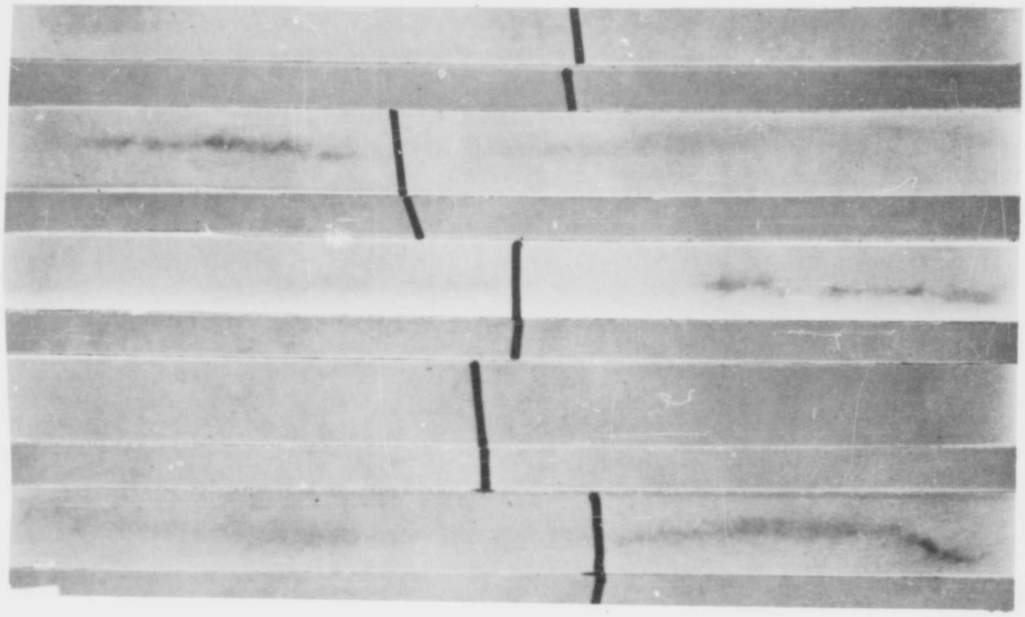

Figure 52. X-Ray Photographs of Ground KT Silicon Carbide Modulus of Rupture Specimens D-12 to D-15, D-17 with Fracture Noted - Two Point Load, 2200 F

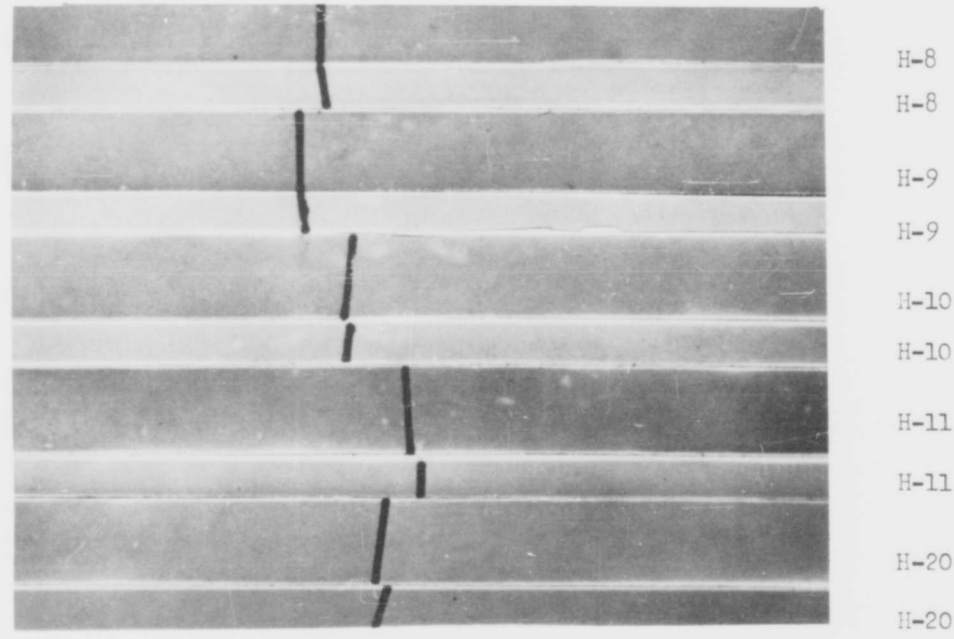

Figure 53. X-Ray Photographs of "As Fabricated" KT Silicon Carbide Modulus of Rupture Specimens H-8 to H-11, H-20 with Fracture Noted - Two Point Load, 2200 F

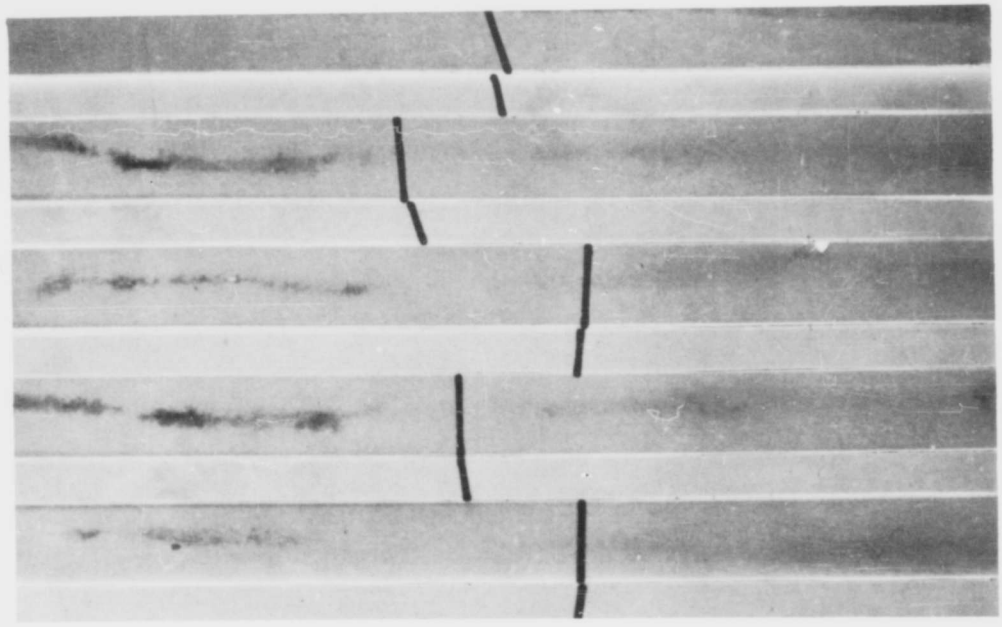

Figure 54. X-Ray Photographs of Ground KT Silicon Carbide Modulus of Rupture Specimens D-18 to D-22 with Fracture Noted - Two Point Load, 2400 F

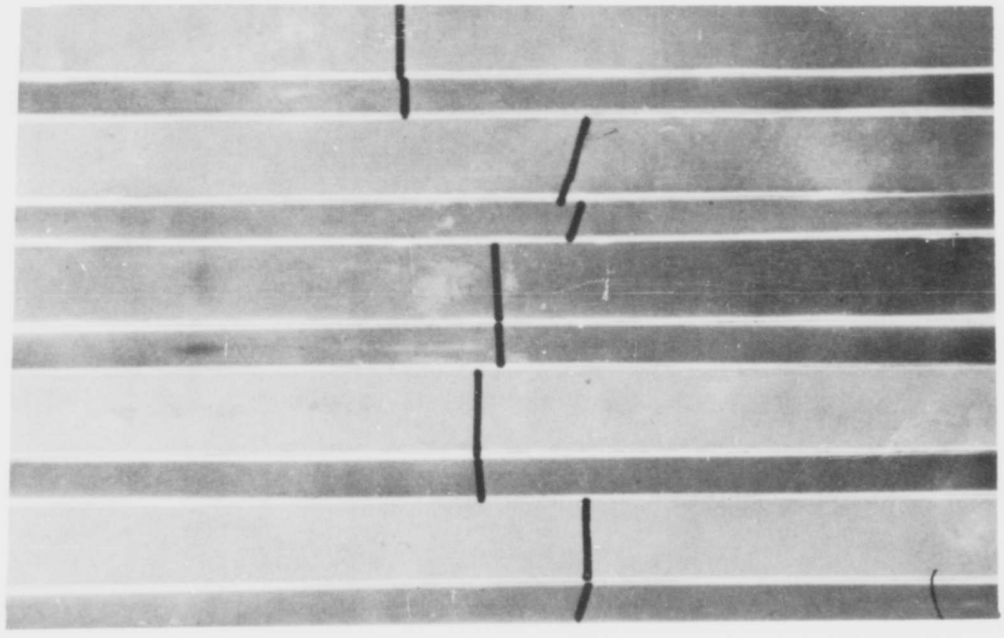

Figure 55. X-Ray Photographs of "As Fabricated" KT Silicon Carbide Modulus of Rupture Specimens H-22 to H-26 with Fracture Noted - Two Point Load, 2400 F

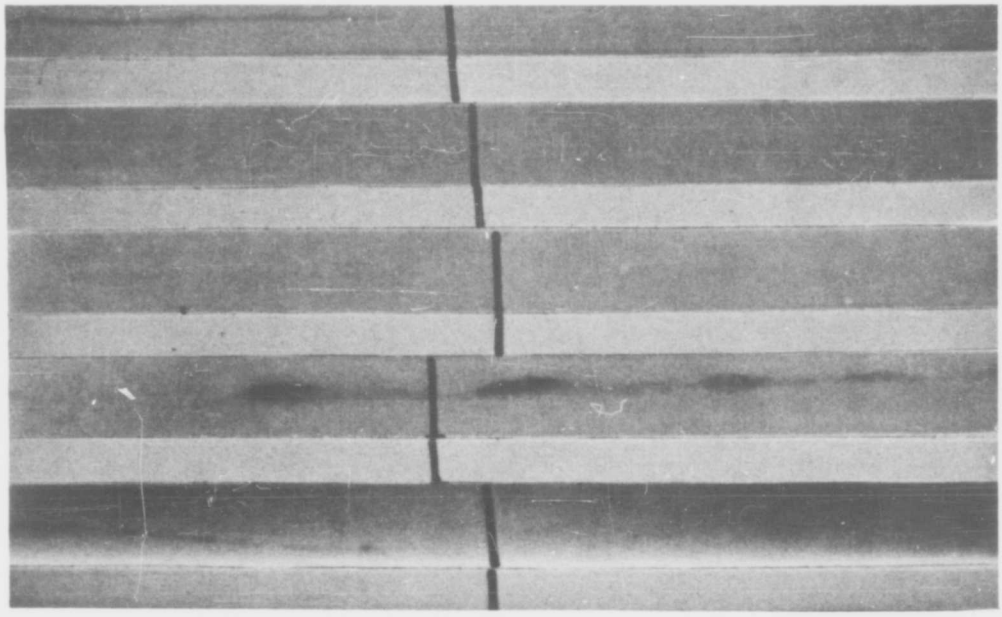

Figure 56. X-Ray Photographs of Ground KT Silicon Carbide Modulus of Rupture Specimens D-2, D-3, D-5, D-6, D-10 with Fracture Noted, Previously Heat Soaked 1 Hour at 2200 F - Two Point Load, 80 F

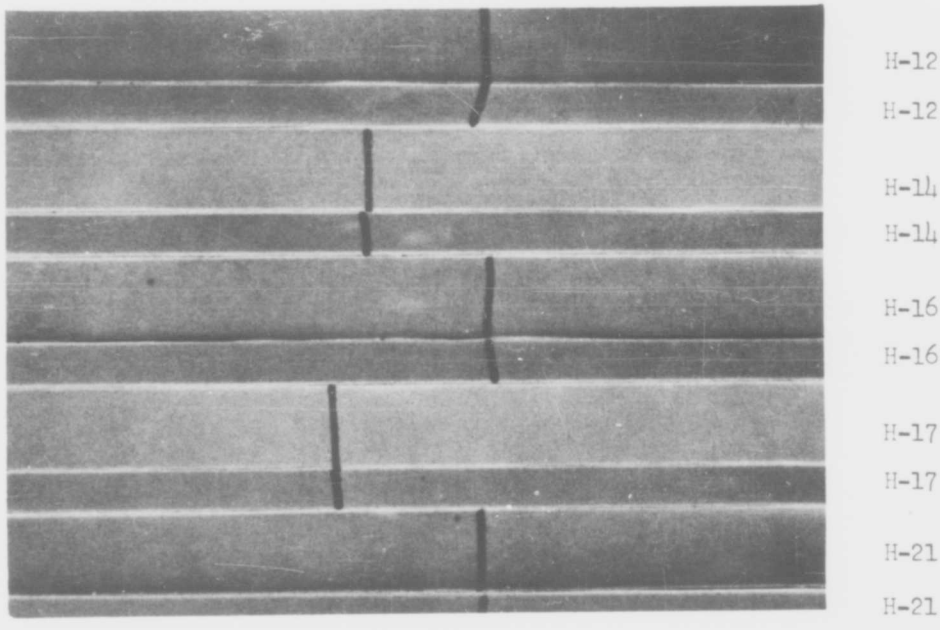

Figure 57. X-Ray Photographs of "As Fabricated" KT Silicon Carbide Modulus of Rupture Specimens H-12, H-14, H-16, H-17, H-21, with Fracture Noted, Previously Heat Soaked 1 Hour at 2200 F - Two Point Load, 80 F

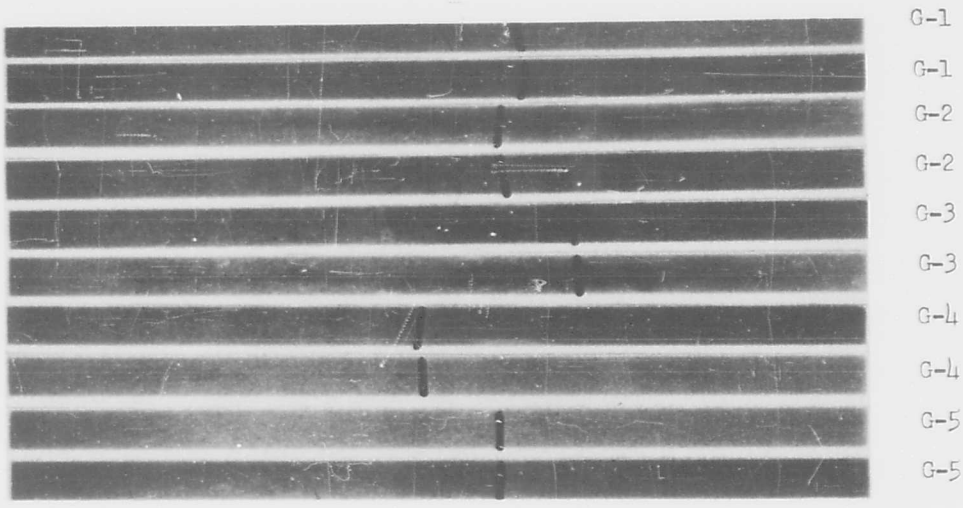

Figure 58. X-Ray Photographs of Ground KT Silicon Carbide Modulus of Rupture Specimens, G-1 to G-5 with Fracture Noted, Previously Heat Soaked 1 Hour at 2200 F - Two Point Load, 80 F

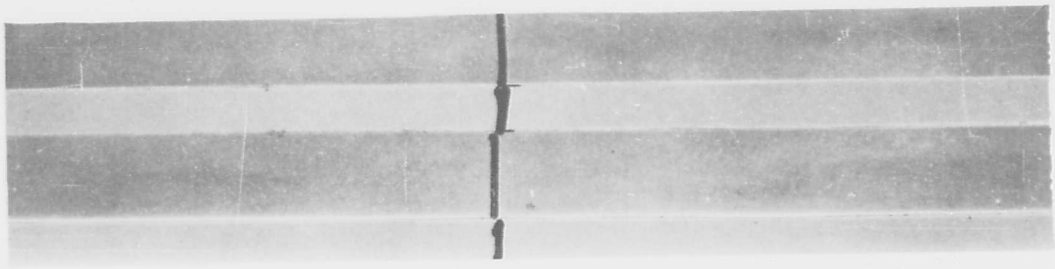

Figure 59. X-Ray Photographs of Ground KT Silicon Carbide Modulus of Rupture Specimens D-23, D-25 with Fracture Noted - One Point Load, 80 F

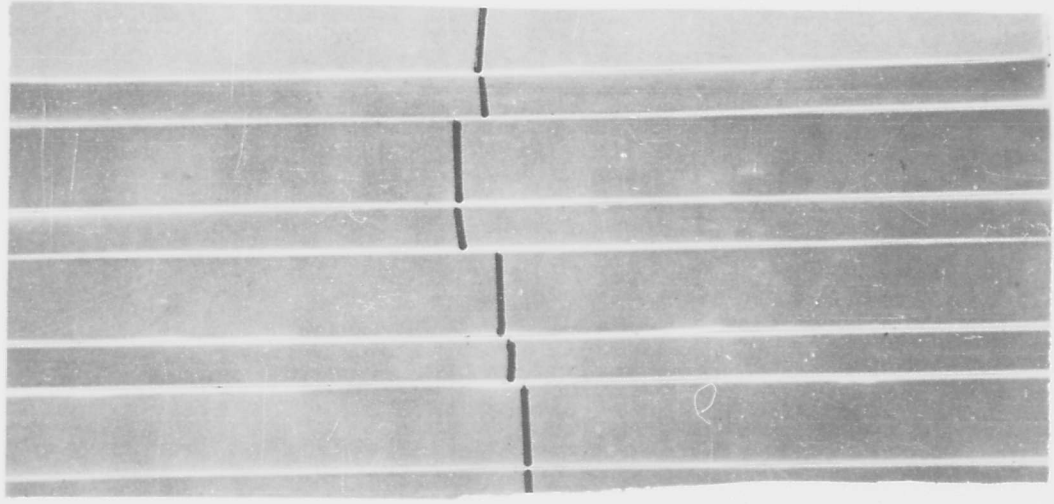

Figure 60. X-Ray Photographs of "As Fabricated" KT Silicon Carbide Modulus of Rupture Specimens H-27 to H-30 with Fracture Noted - One Point Load, 80 F

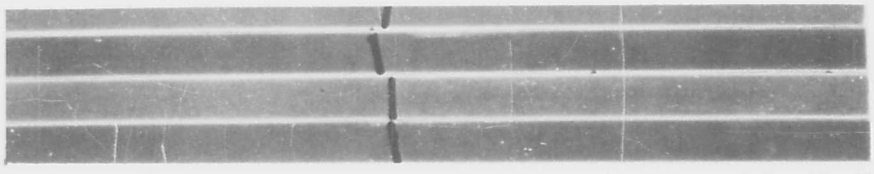

Figure 61. X-Ray Photographs of Ground KT Silicon Carbide Modulus of Rupture Specimens G-6, G-7 with Fracture Noted - One Point Load, 80 F

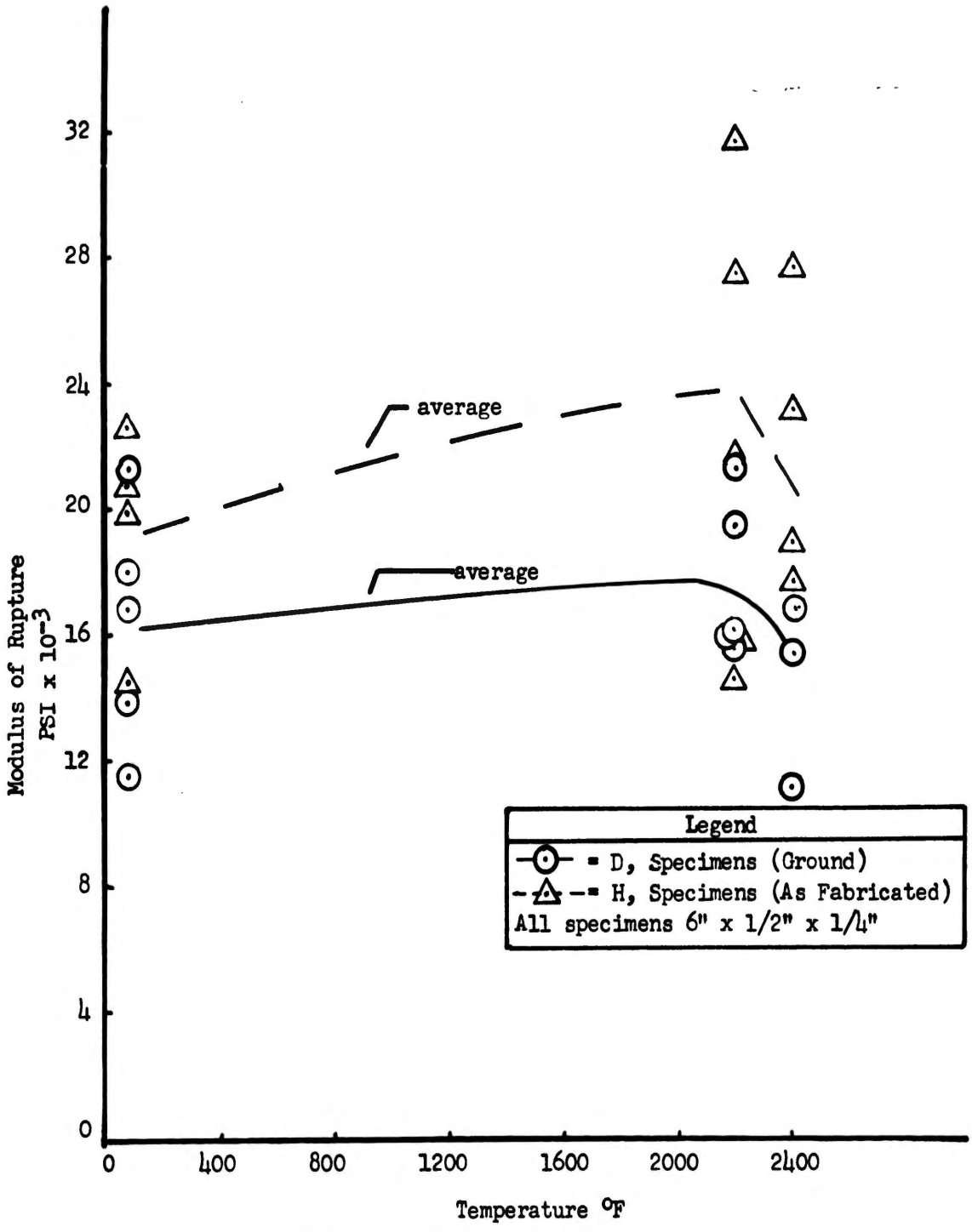

Figure 62. Modulus of Rupture of KT Silicon Carbide (Two Point Load) vs Temperature

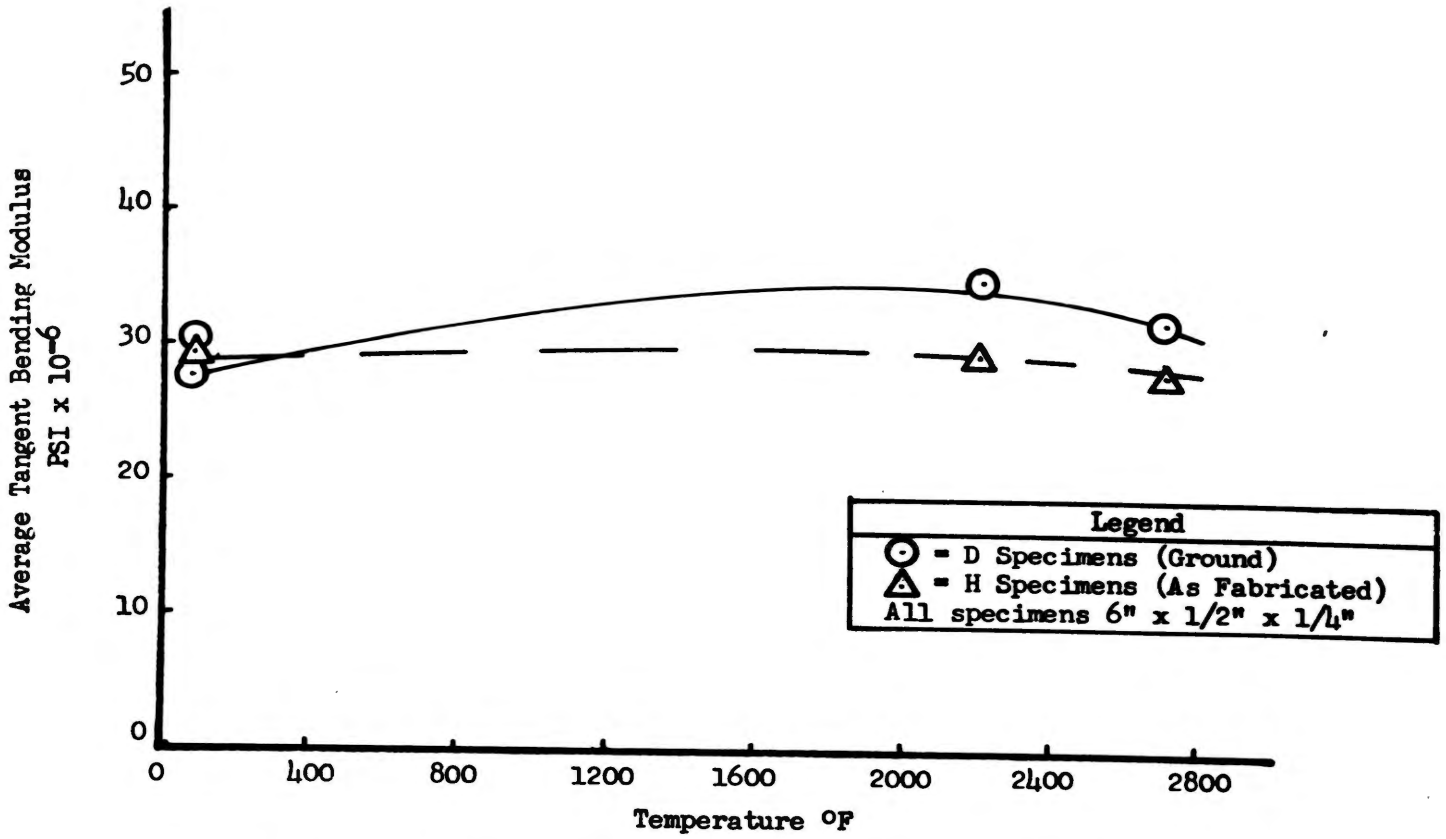

Figure 63. KT Silicon Carbide Average Tangent Bending Modulus vs Temperature (Two Point Load)

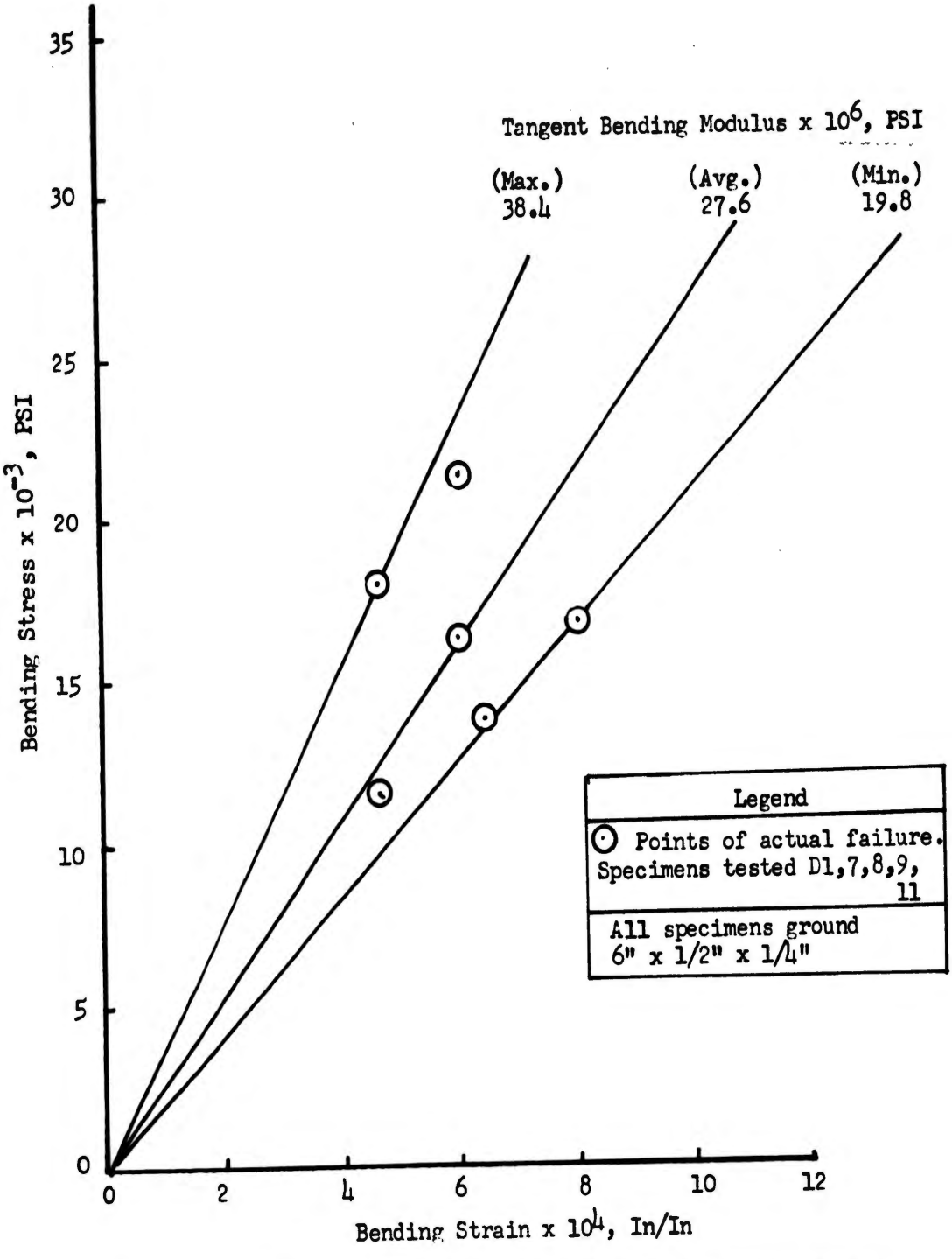

Figure 64. Stress-Strain Curves for Ground KT Silicon Carbide at 80 F (Two Point Load)

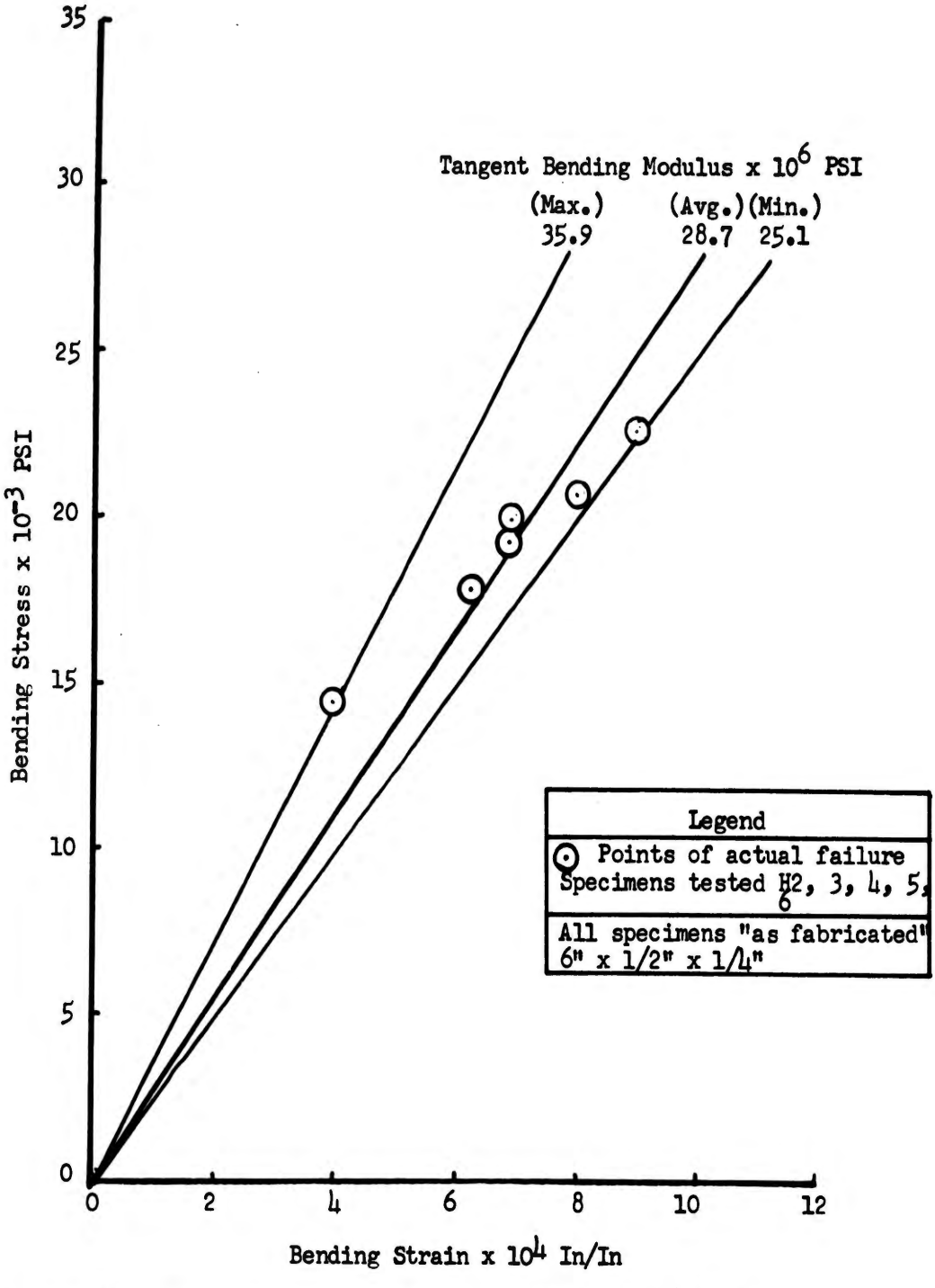

Figure 65. Stress-Strain Curves For "As Fabricated" KT Silicon Carbide at 80 F (Two Point Load)

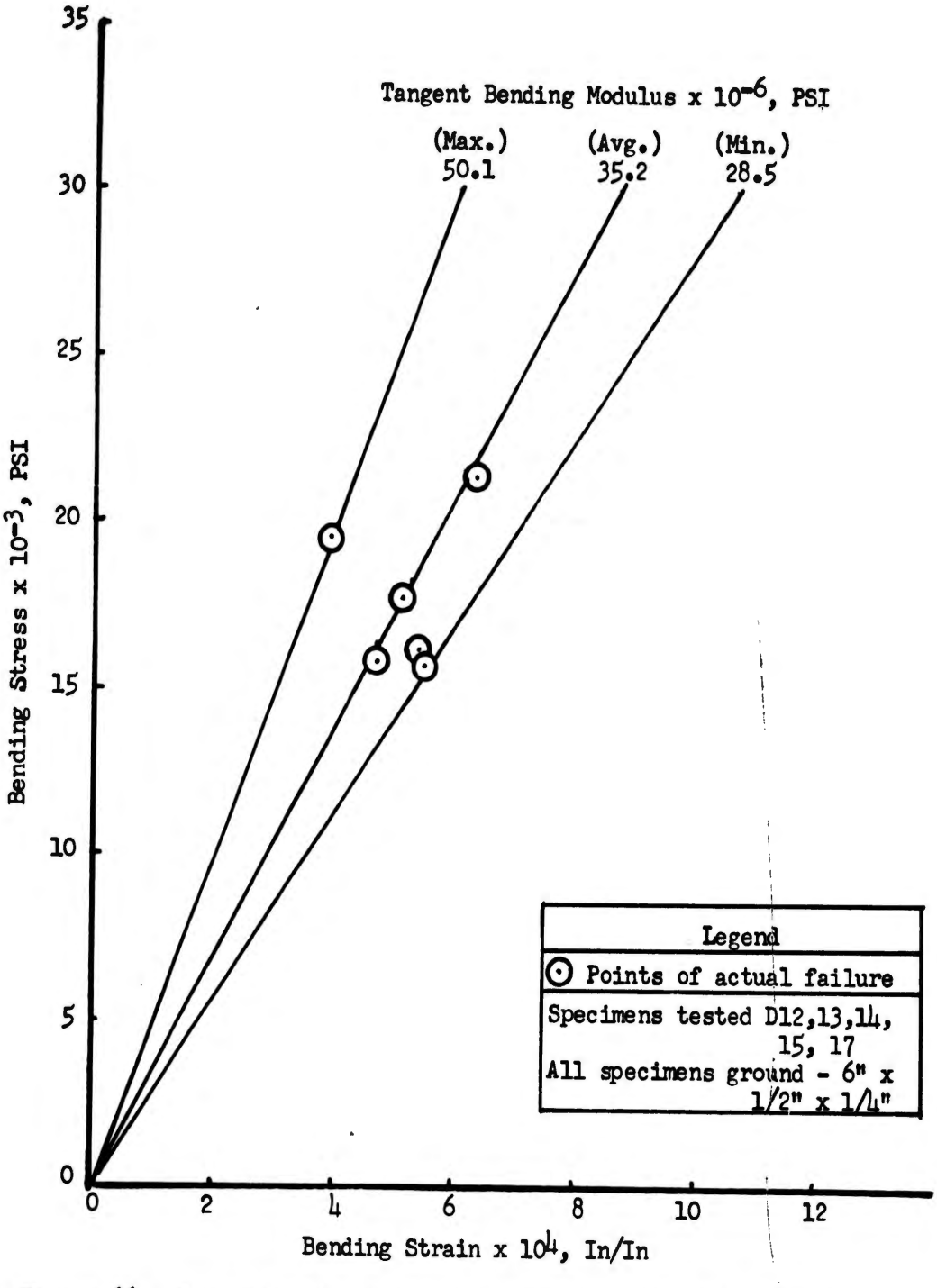

Figure 66. Stress-Strain Curves for Ground KT Silicon Carbide at 2200 F (Two Point Load)

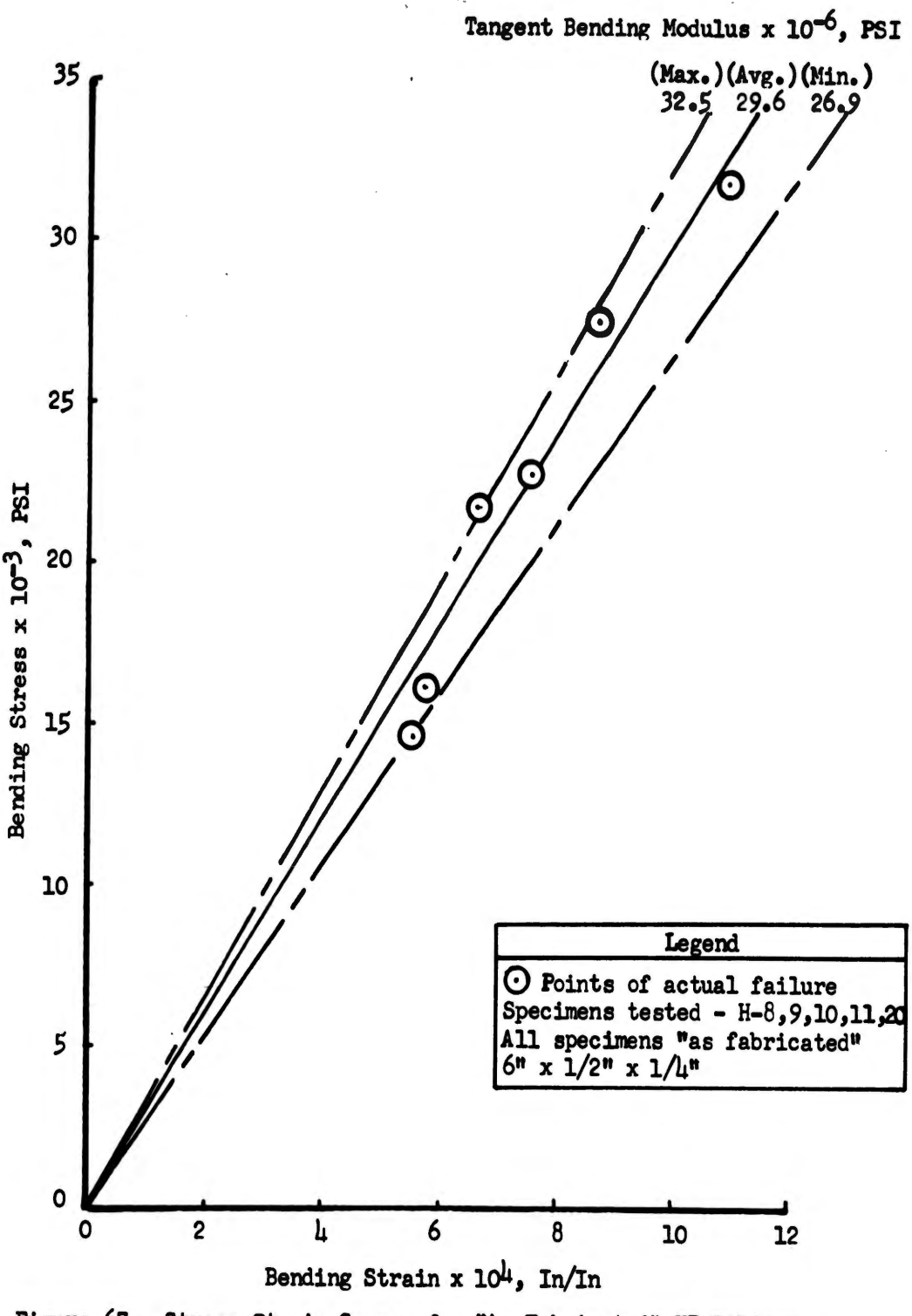

Figure 67. Stress-Strain Curves for "As Fabricated" KT Silicon Carbide at 2200 F (Two Point Load)

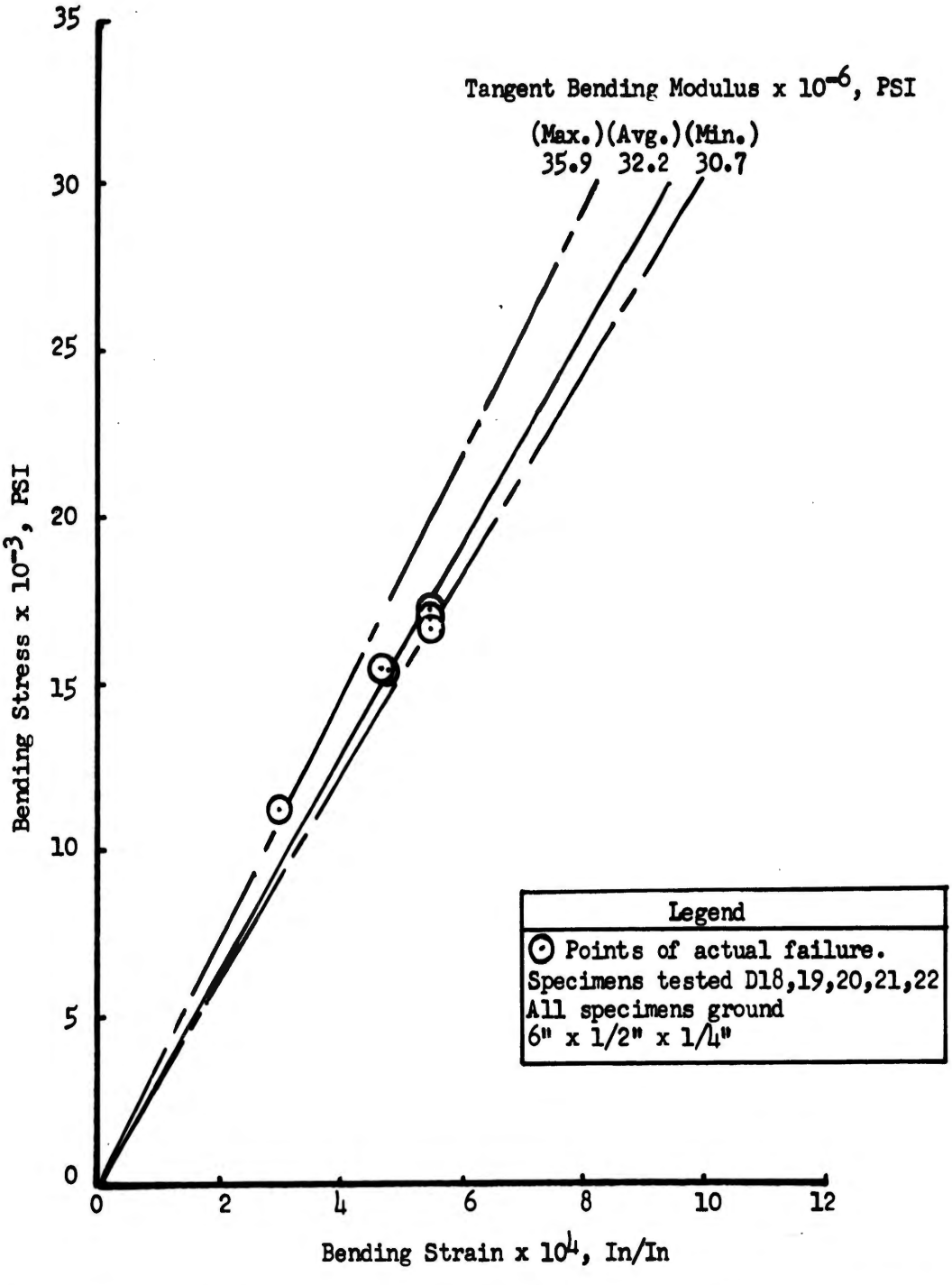

Figure 68. Stress-Strain Curves for Ground KT Silicon Carbide at 2400 F (Two Point Load)

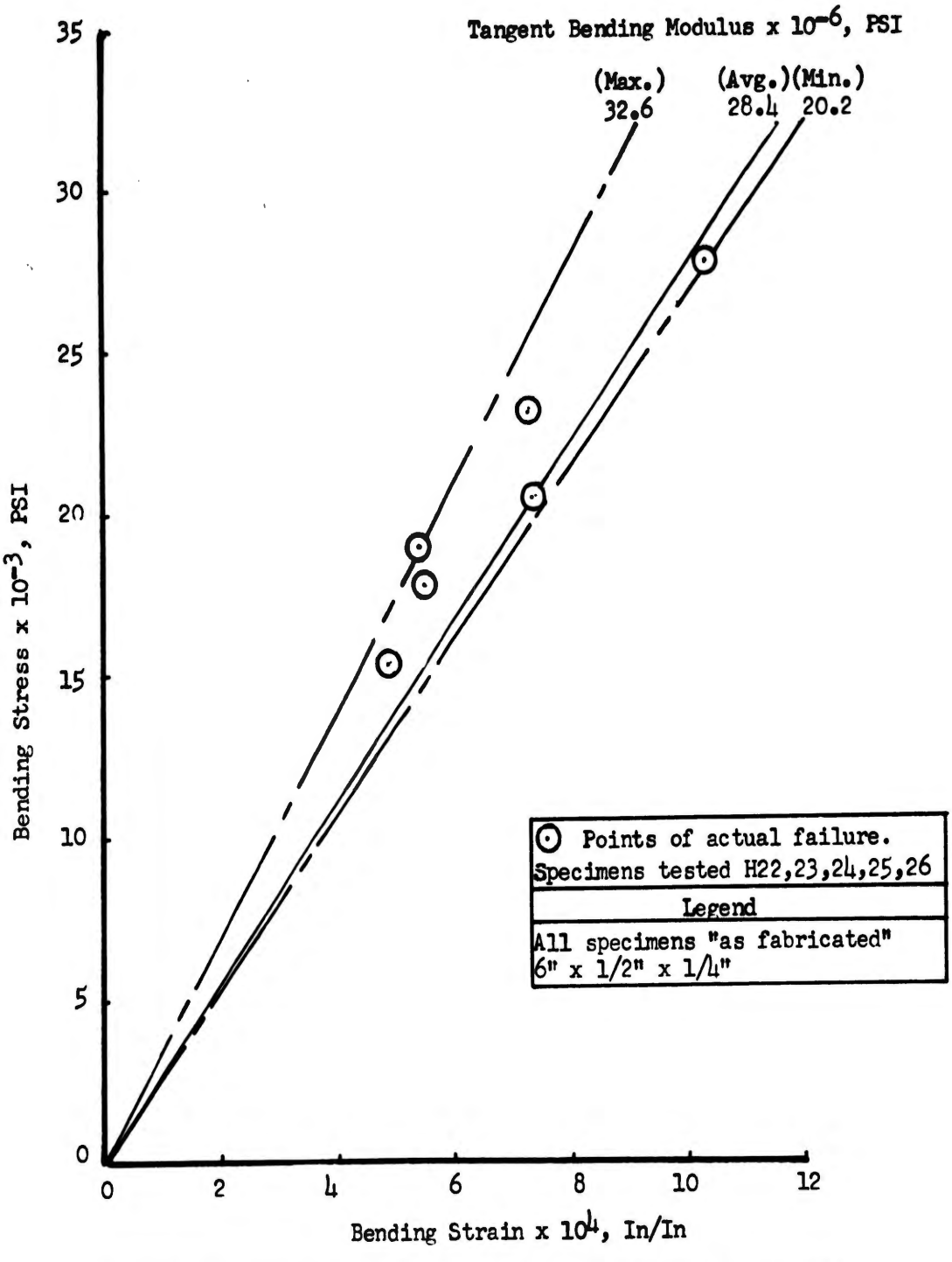

Figure 69. Stress-Strain Curves for "As Fabricated" KT Silicon Carbide at 2400 F (Two Point Load)

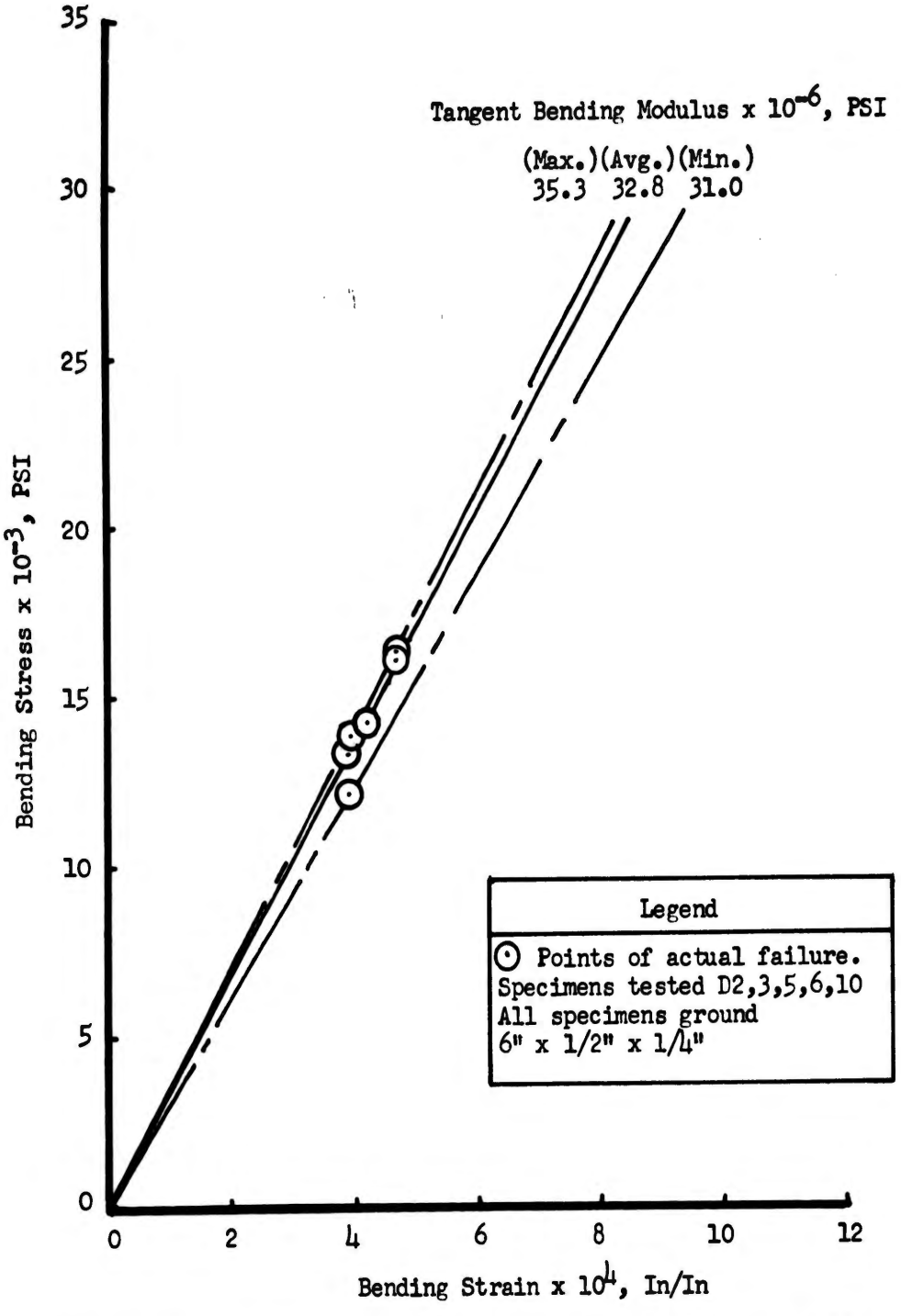

Figure 70. Stress-Strain Curves for Ground KT Silicon Carbide at 80 F (Previously Heat Soaked 1 Hour at 2200 F. Two Point Load)

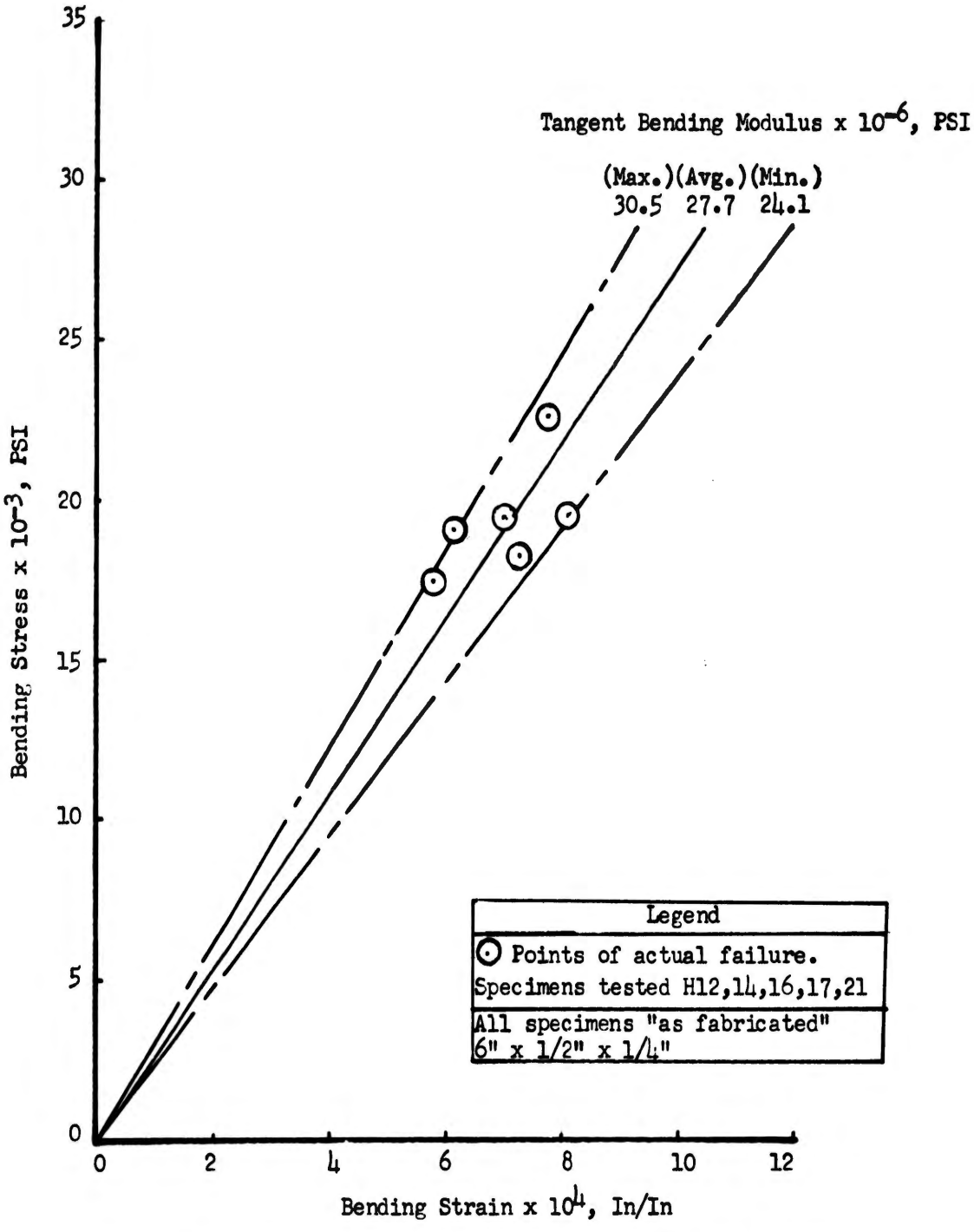

Figure 71. Stress-Strain Curves for "As Fabricated" KT Silicon Carbide at 80 F (Previously Heat Soaked 1 Hour at 2200 F. Two Point Load)

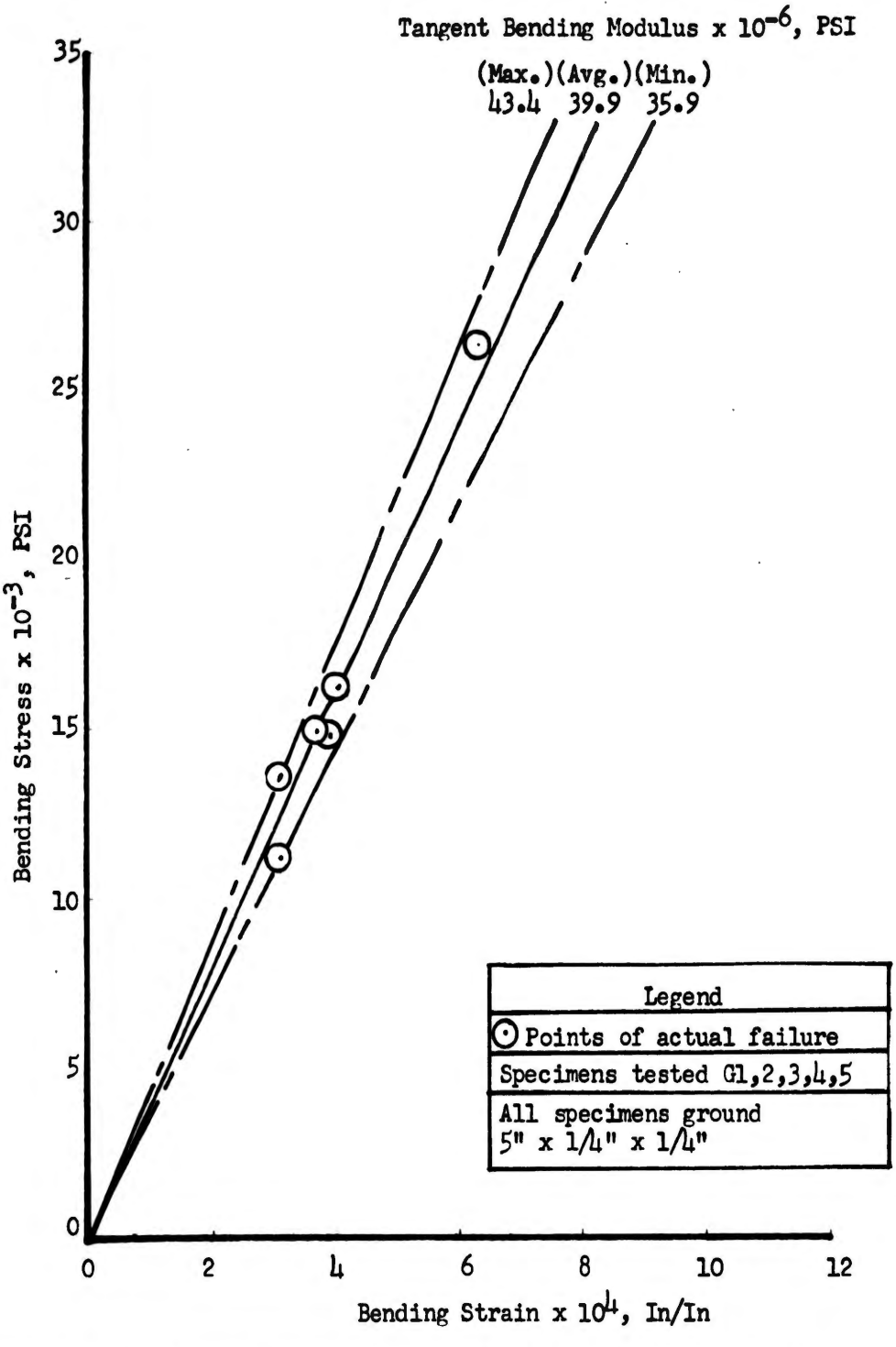

Figure 72. Stress-Strain Curves for Ground KT Silicon Carbide at 80 F (Previously Heat Soaked 1 Hour at 2200 F. Two Point Load)

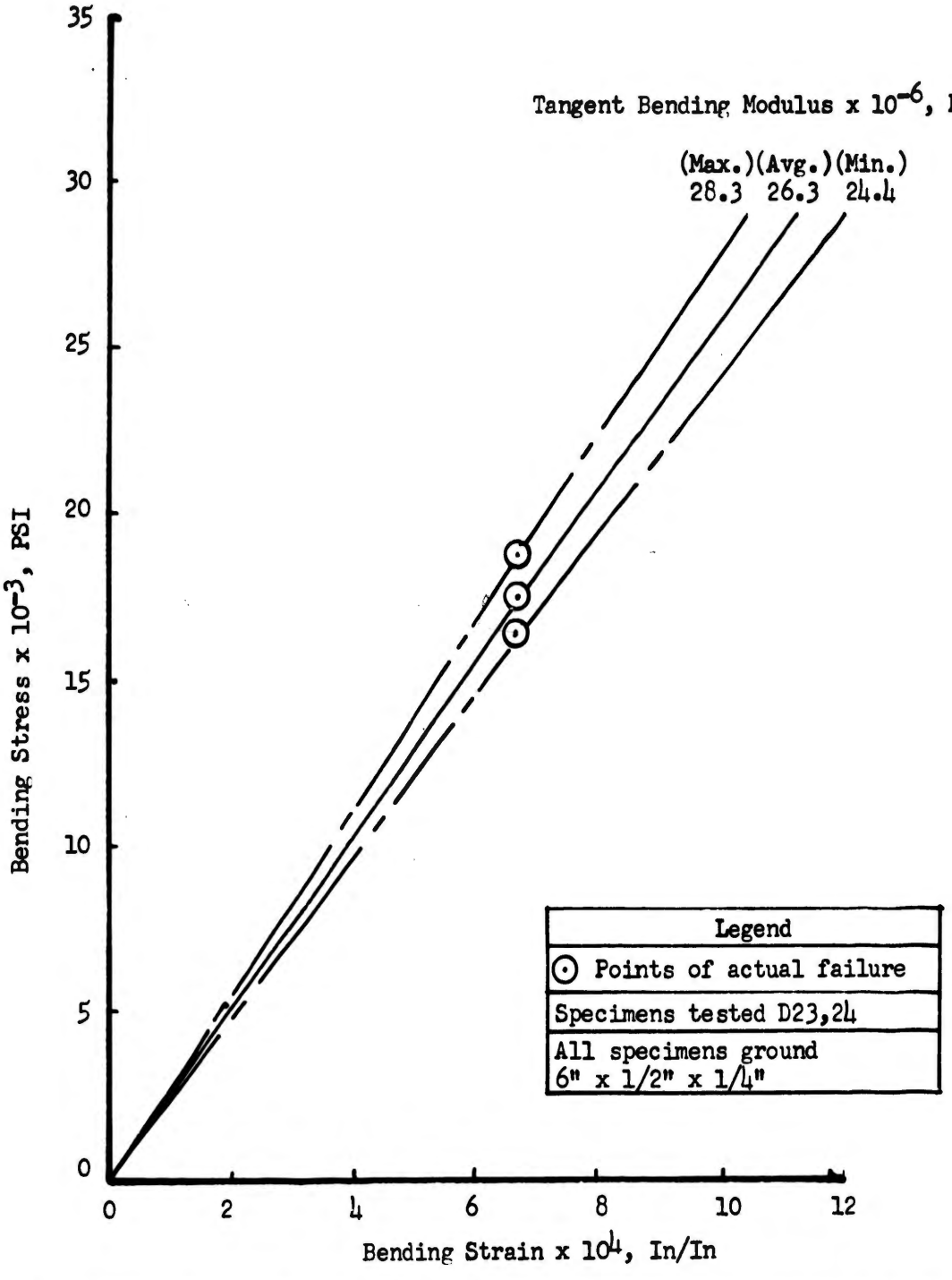

Figure 73. Stress-Strain Curves for Ground KT Silicon Carbide at 80 F (One Point Load)

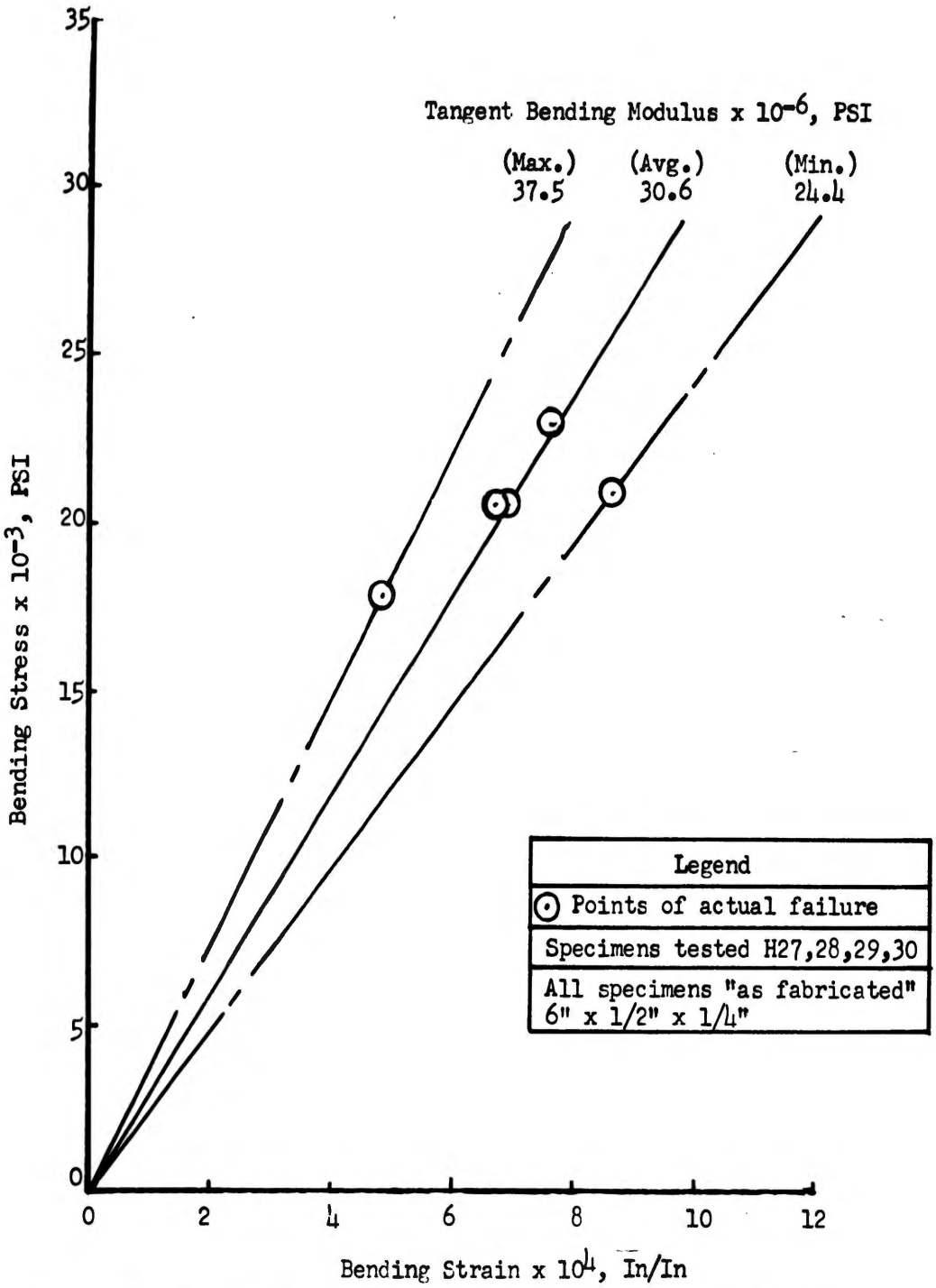

Figure 74. Stress-Strain Curves for "As Fabricated" KT Silicon Carbide at 80 F (One Point Load)

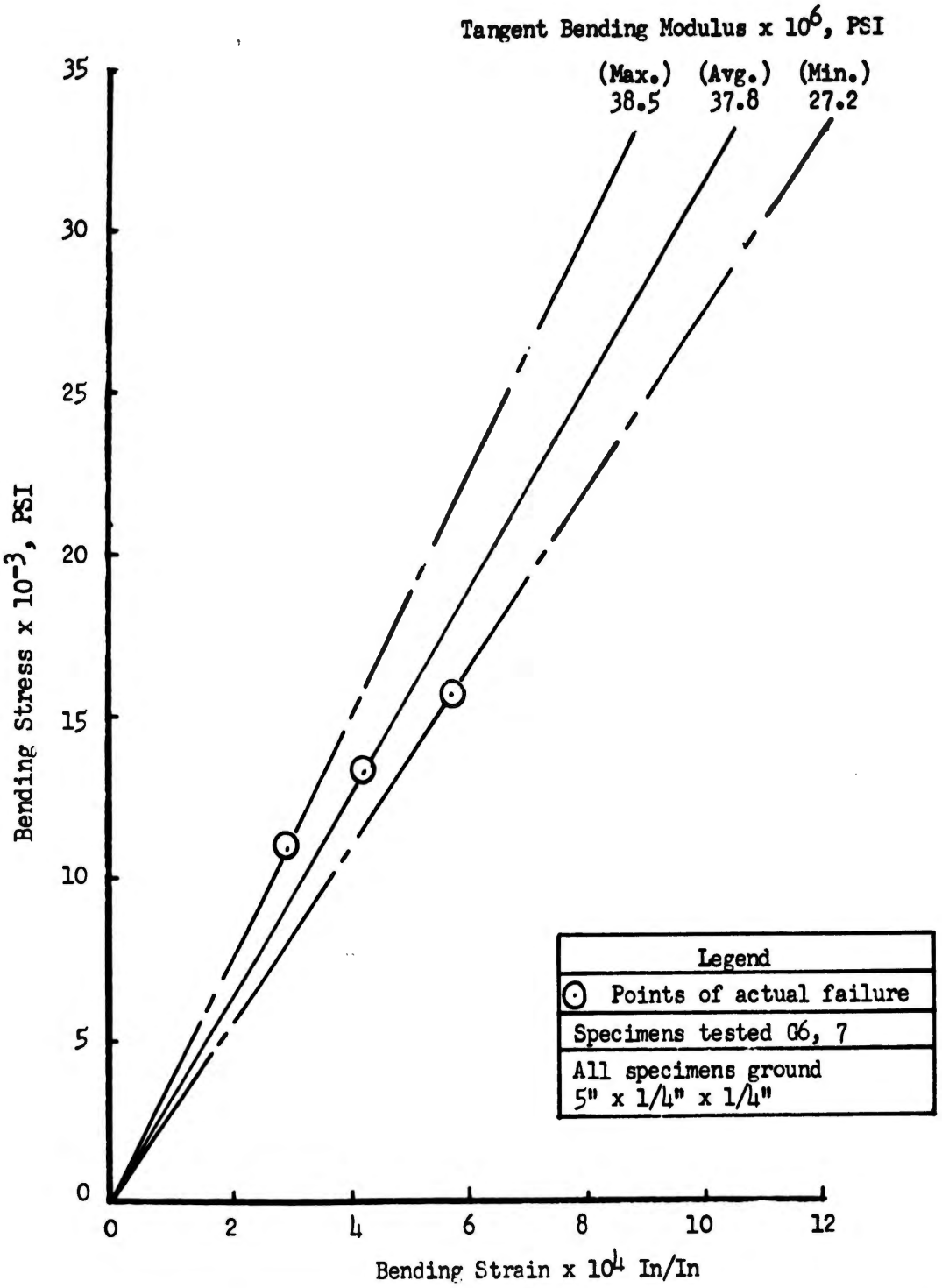

Figure 75. Stress-Strain Curves for Ground KT Silicon Carbide at 80 F (One Point Load)

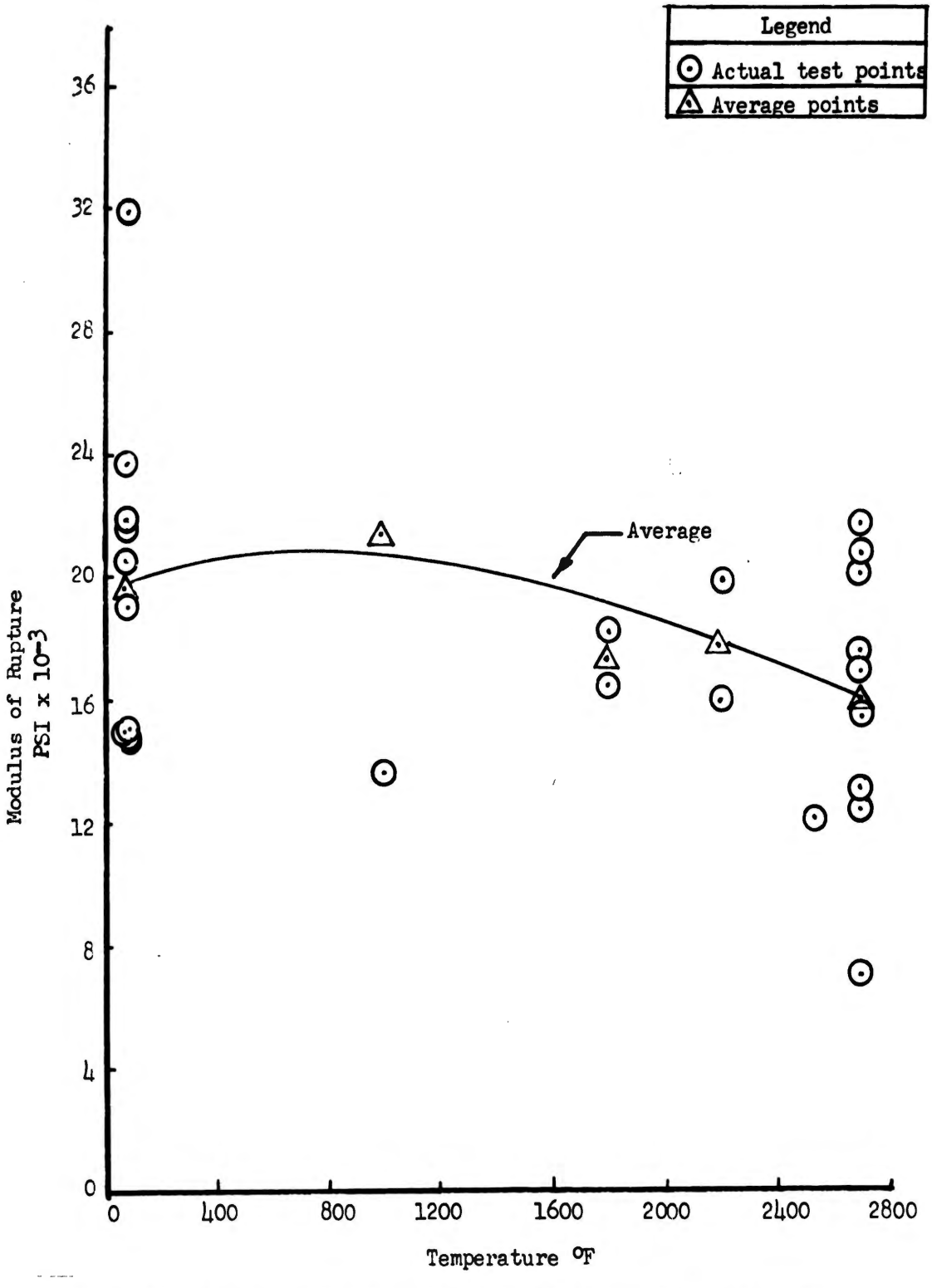

Figure 76. Modulus of Rupture (Two Point Load) vs Temperature For 5" x 1/4" x 1/4" Ground KT Silicon Carbide Specimens (Source Reference 31)

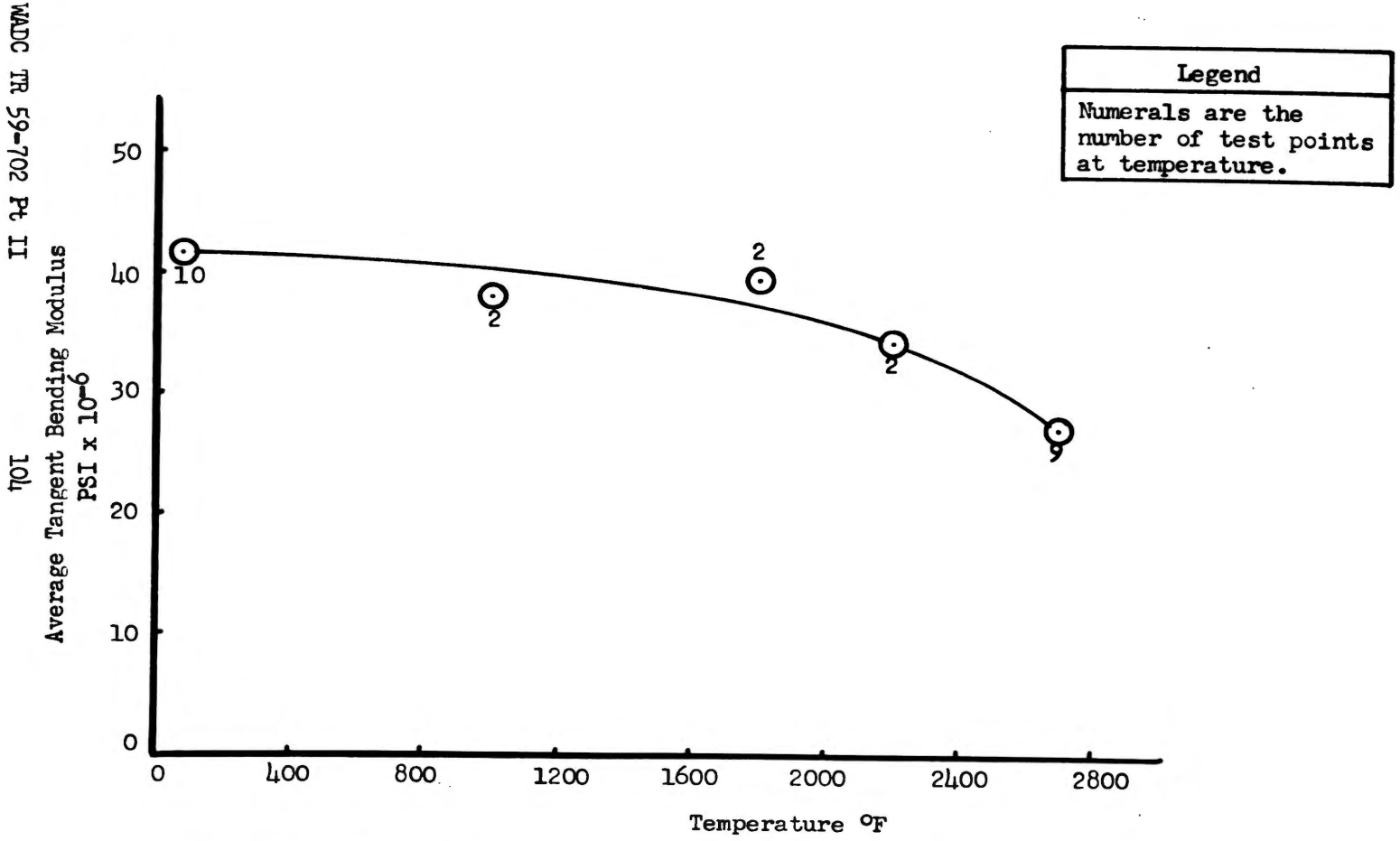

Figure 77. KT Silicon Carbide Average Tangent Bending Modulus vs Temperature for 5" x 1/4" x 1/4" Ground Specimens (Two Point Load) (Source: Reference 31)

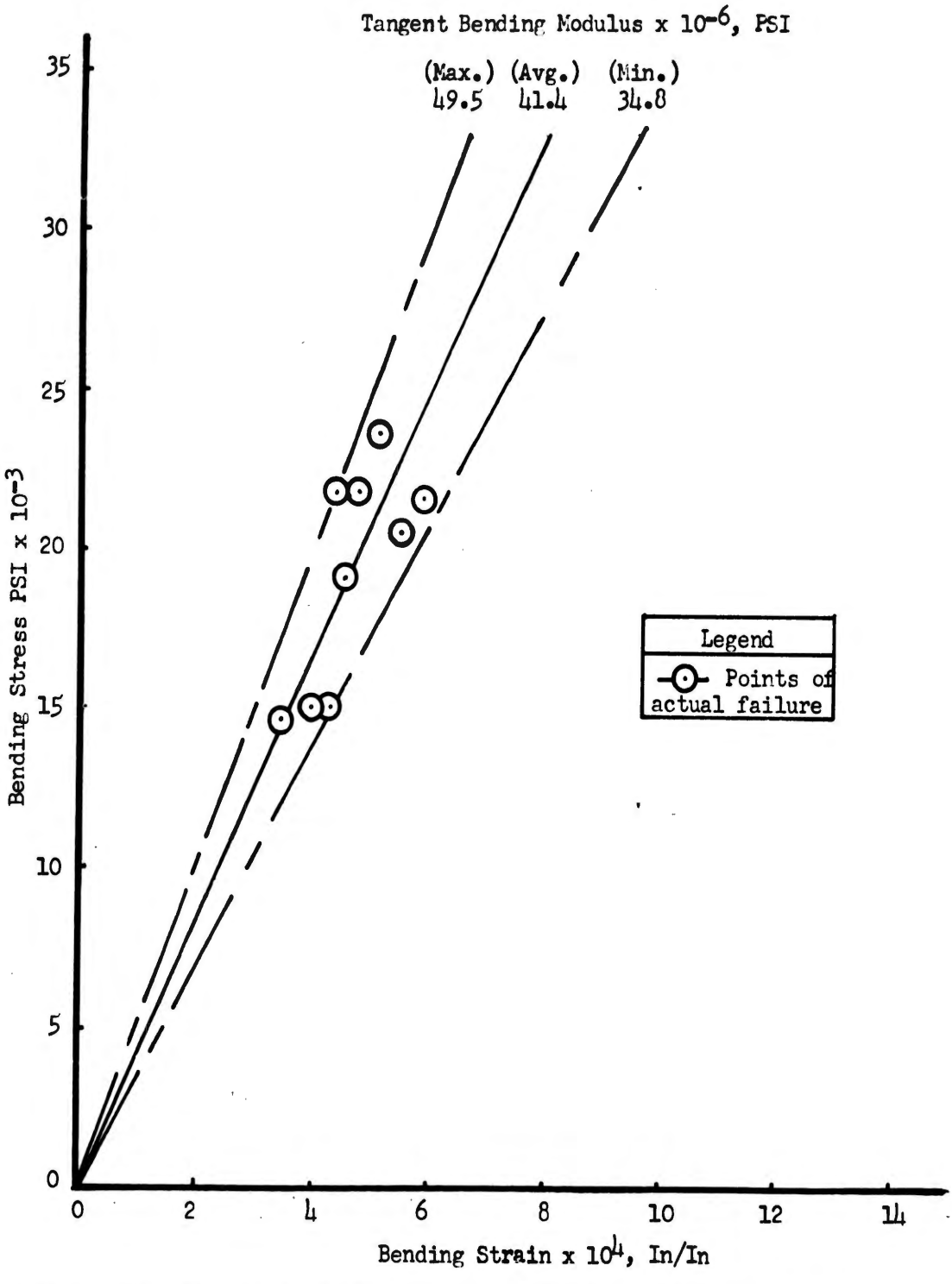

Figure 78. Stress-Strain Curves for 5" x 1/4" x 1/4" Ground KT Silicon Carbide Specimens at 80 F (Two Point Load) (Source: Reference 31)

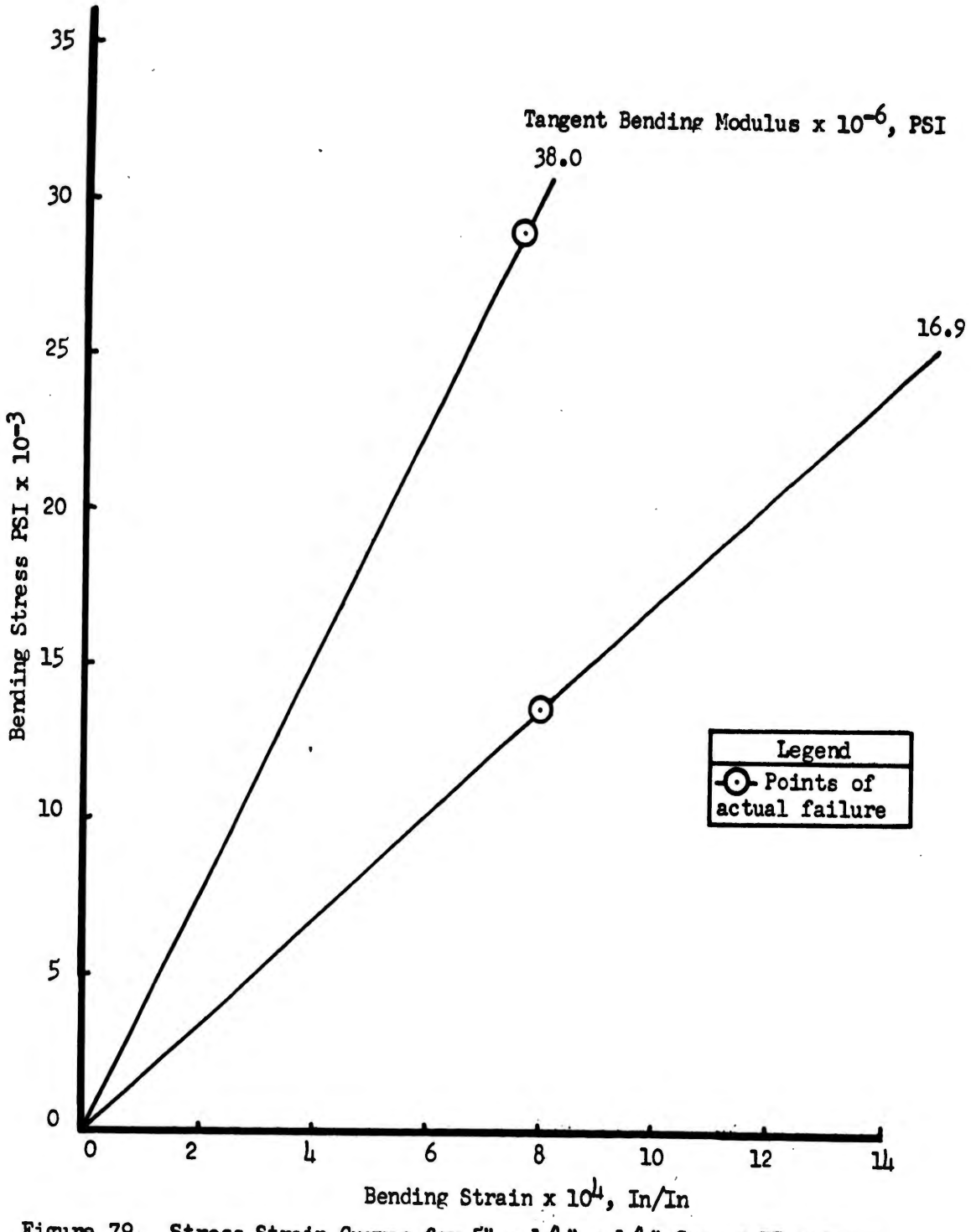

Figure 79. Stress-Strain Curves for 5" x 1/4" x 1/4" Ground KT Silicon Carbide Specimens at 1000 F (Two Point Load) (Source: Reference 31)

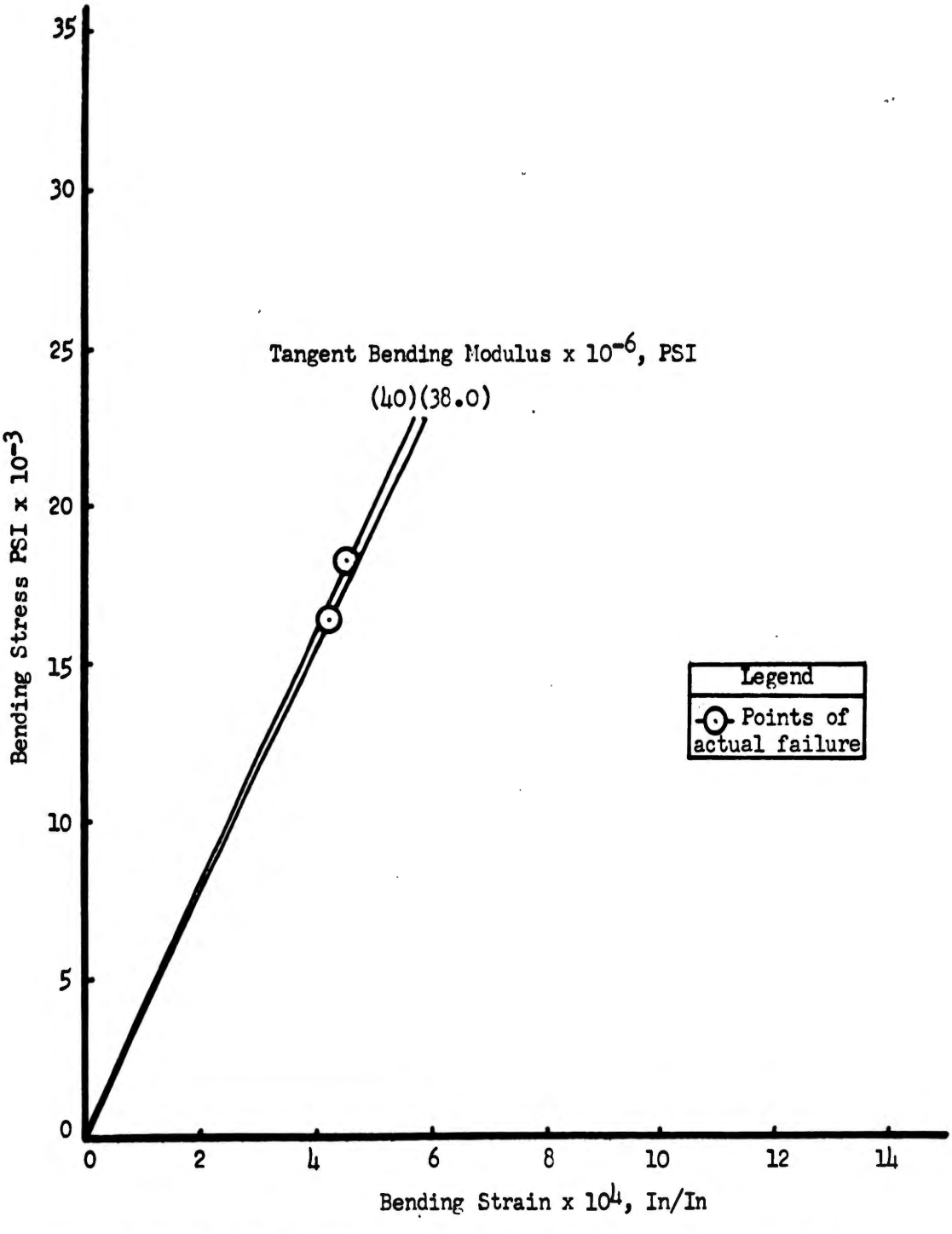

Figure 80. Stress-Strain Curves for 5" x 1/4" x 1/4" Ground KT Silicon Carbide Specimens at 1800 F (Two Point Load) (Source: Reference 31)

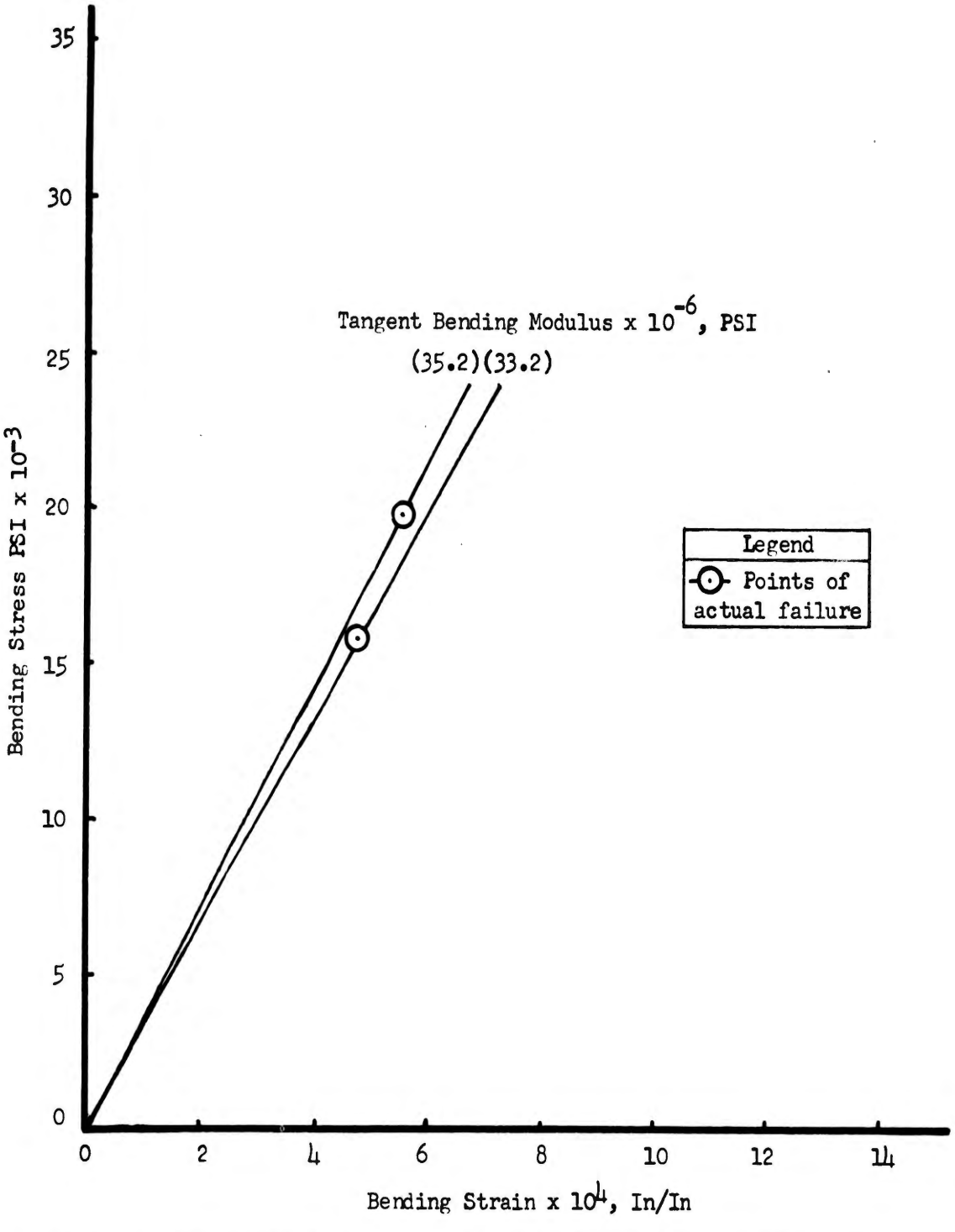

Figure 81. Stress-Strain Curves for 5" x 1/4" x 1/4" Ground KT Silicon Carbide Specimens at 2200 F (Two Point Load)(Source: Reference 31)

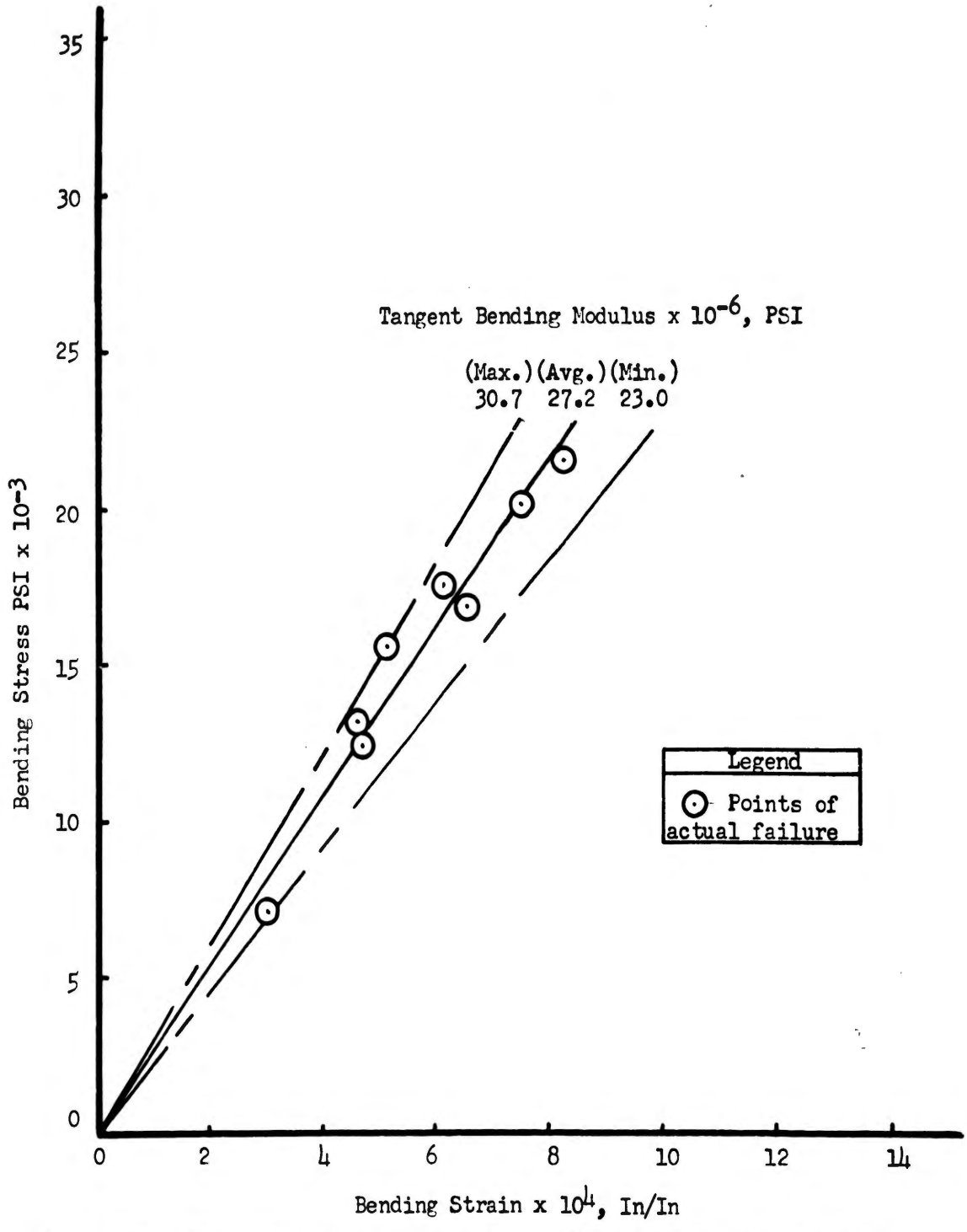

Figure 82. Stress-Strain Curves for 5" x 1/4" x 1/4" Ground KT Silicon Carbide Specimens at 2700 F (Two Point Load) (Source: Reference 31)

TABLE VII

BELL AIRCRAFT TEST DATA ON KT SILICON CARBIDE

Test Temp.	No.	Specimen Size	Specimen Finish	Density gms/cc	Modulus of Rupture (psi x 10^{-3}) 1 Point Load Results	1 Point Load Average	2 Point Load Results	2 Point Load Average	Deflection at Failure (inches) 1 Point Load Results	1 Point Load Average	2 Point Load Results	2 Point Load Average	Bending Modulus of Elasticity (psi x 10^{-6}) 1 Point Load Results	1 Point Load Average	2 Point Load Results	2 Point Load Average	Dynamic Modulus (psi x 10^{-6}) 80 F Results	80 F Average	2200 F Results	2200 F Average
	D-1	6" x 1/2" x 1/4"	Ground	3.12			11.5				0.006				24.6		53.8			
	D-7	↑	↑	3.09			13.9				0.007				19.8		53.9			
	D-8	↓	↓	3.11			18.0	16.3			0.006	0.007			38.4	27.6	55.6			
	D-9			3.10			16.8	(Av of 5)			0.007	(Av of 5)			20.6	(Av of 5)	53.8	53.9		
	D-11			3.12			21.3				0.006				34.8		54.1	(Av of 7)		
	D-23			3.11	16.3	17.5			0.007	0.007			24.4	26.3			52.9			
	D-25	6" x 1/2" x 1/4"	Ground	3.11	18.8	(Av of 2)			0.007	(Av of 2)			28.3	(Av of 2)			53.4			
	H-2	6" x 1/2" x 1/4"	As Fabricated	3.10			14.5				0.005				35.9		49.1			
80 F	H-3	↓	↑	3.12			17.8	19.2			0.008	0.009			28.3	26.7	46.6	47.1		
	H-4			3.12			20.0	(Av of 5)			0.010	(Av of 5)			28.7	(Av of 5)	45.9	(Av of 5)		
	H-5			3.10			22.7				0.012				25.1		48.1			
	H-6			3.10			20.8				0.010				25.4		46.1			
	H-27			3.12	20.5				0.007				30.7							
	H-28			3.11	22.9	20.5			0.008	0.008			30.0	30.6						
	H-29	↓	↓	3.11	20.9	(Av of 4)			0.009	(Av of 4)			24.4	(Av of 4)						
	H-30	6" x 1/2" x 1/4"	As Fabricated	3.10	17.8				0.008				37.5							
	G-6	5" x 1/4" x 1/4"	Ground	3.14	15.6	13.3			0.006	0.004			27.2	32.8			59.2	58.1		
	G-7	5" x 1/4" x 1/4"	Ground	3.12	11.0	(Av of 2)			0.003	(Av of 2)			38.5	(Av of 2)			57.0	(Av of 2)		
	D-12	6" x 1/2" x 1/4"	Ground	3.11			15.8				0.006				33.8		53.0			
	D-13	↑	↑	3.11			16.2	17.7			0.007	0.006			30.3	35.4	53.0	53.1		
	D-14	↓	↓	3.10			15.7	(Av of 5)			0.006	(Av of 5)			28.5	(Av of 5)	52.0	(Av of 5)		
	D-15			3.11			21.4				0.008				38.1		53.9			
	D-17	6" x 1/2" x 1/4"	Ground	3.11			19.5				0.005				50.1		53.7			
2200 F	H-8	6" x 1/2" x 1/4"	As Fabricated	3.11			23.7				0.009				32.5		49.5			
	H-9	↓	↑	3.10			16.1	22.8			0.008	0.010			27.8	29.6	45.5	48.2		
	H-10			3.11			27.5	(Av of 5)			0.011	(Av of 5)			31.9	(Av of 5)	51.0	(Av of 5)		
	H-11			3.12			14.7				0.007				26.9		44.6			
	H-20	6" x 1/2" x 1/4"	As Fabricated	3.11			31.8				0.014				29.1		50.7			
	D-18	6" x 1/2" x 1/4"	Ground	3.10			16.9				0.007				30.9		52.5			
	D-19	↑	↑	3.11			15.4	15.4			0.006	0.006			32.8	32.2	53.1	52.8		
	D-20	↓	↓	3.10			16.8	(Av of 5)			0.007	(Av of 5)			30.7	(Av of 5)	52.1	(Av of 5)		
	D-21			3.10			11.2				0.004				35.9		52.5			
	D-22	6" x 1/2" x 1/4"	Ground	3.11			16.9				0.007				30.8		53.9			
2400 F	H-22	6" x 1/2" x 1/4"	As Fabricated	3.11			23.2				0.010				31.7					
	H-23	↑	↑	3.11			19.0	20.6			0.012	0.010			20.2	28.4				
	H-24	↓	↓	3.12			27.8	(Av of 5)			0.013	(Av of 5)			26.2	(Av of 5)				
	H-25			3.13			15.4				0.006				31.5					
	H-26	6" x 1/2" x 1/4"	As Fabricated	3.11			17.8				0.007				32.6					
		Previously Heated One (1) Hour at 2200 F																		
	D-2	6" x 1/2" x 1/4"	Ground	3.09			13.3				0.005				34.2		53.8		49.5	
	D-3	↑	↑	3.10			12.1	14.3			0.005	0.005			33.0	33.8	54.8	54.6	50.5	50.3
	D-5	↓	↓	3.10			14.1	(Av of 5)			0.006	(Av of 5)			34.0	(Av of 5)	55.7	(Av of 5)	51.4	(Av of 5)
	D-6			3.09			13.8				0.005				35.3		54.3		50.0	
	D-10	6" x 1/2" x 1/4"	Ground	3.10			16.2				0.006				34.3		54.5		50.1	
	H-12	6" x 1/2" x 1/4"	As Fabricated	3.11			19.0				0.008				30.5		46.8		43.7	
80 F	H-14	↑	↑	3.08			22.6	19.4			0.010	0.009			28.9	27.7	47.1	46.8	43.2	43.3
	H-16	↓	↓	3.15			17.4	(Av of 5)			0.008	(Av of 5)			30.1	(Av of 5)	49.2	(Av of 5)	45.5	(Av of 5)
	H-17			3.12			18.2				0.009				24.8		47.9		44.7	
	H-21	6" x 1/2" x 1/4"	As Fabricated	3.09			19.6				0.010				24.1		43.0		39.6	
	G-1	5" x 1/4" x 1/4"	Ground	3.12			13.6				0.004				43.4		56.0		52.0	
	G-2	↑	↑	3.11			11.2	16.2			0.004	0.005			35.9	39.9	55.1	55.6	49.0	50.9
	G-3	↓	↓	3.12			14.9	(Av of 5)			0.005	(Av of 5)			40.4	(Av of 5)	54.3	(Av of 5)	48.8	(Av of 5)
	G-4			3.14			14.8				0.005				37.7		56.6		52.9	
	G-5	5" x 1/4" x 1/4"	Ground	3.11			20.3				0.008				42.0		56.3		52.0	

X TEST SPECIMEN GEOMETRY

A. General

One of the problems related to the use of brittle materials such as silicon carbide is the lack of adequate technical data. Available property data on brittle materials is generally directed to applications such as refractory brick for metal industries, abrasive wheels, enamels, whitewares, etc. More detailed mechanical and thermal data are required to provide a basis for possible selection of brittle materials as structural and semi-structural elements for aircraft and missiles. Test data must be evaluated in terms of the test procedures. To more fully evaluate the possible use of brittle materials such as silicon carbide, an understanding is required of the effect test specimen geometry has on test results.

The most common mechanical test conducted on brittle (ceramic) materials is modulus of rupture. This test was selected for the study on test specimen geometry because of the relatively large amount of data available on dense silicon carbide. Table VIII lists some of the modulus of rupture test results available on one commercial grade of dense silicon carbide.

B. Results

The following results are based on available test data given in Table VIII.

1. Higher modulus of rupture values were obtained using a one point loading technique as compared to a two point loading technique.

2. Higher modulus of rupture values were obtained using a shorter span.

3. Polishing or grinding test specimens results in lower modulus of rupture values.

4. Specimens having smaller cross sections will have higher modulus of rupture values.

C. Theoretical Analysis

1. Modulus of Rupture Calculations

The two basic test systems used in determining modulus of rupture employ a one point loading technique and a two point loading technique. The techniques are illustrated in the figures shown in Section IX of this report. The formulas used in calculating the modulus of rupture are developed as follows.

One Point Technique

Simple Beam - Concentrated Load at Center

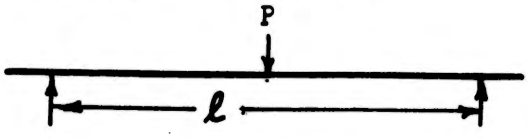

Bending Moment $M = \frac{P\ell}{4}$

Flexure Formula

σ (unit stress) $= \frac{Mc}{I}$

Section modulus for rectangular beam

$\frac{I}{c} = \frac{bd^2}{6}$

Thus

σ = Modulus of Rupture $= \left(\frac{P\ell}{4}\right)\left(\frac{6}{bd^2}\right)$

Modulus of Rupture $= \frac{3\,P\ell}{2\,bd^2}$

Two Point Technique

Simple Beam - Two Equal Concentrated Loads at Equal Distances from Supports

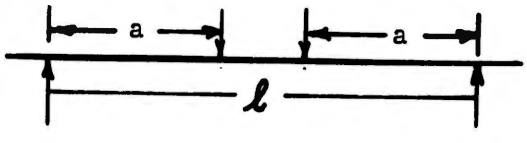

Bending Moment = Pa

Flexure formula

σ (unit stress) $= \frac{Mc}{I}$

Section modulus for rectangular beam

$$\frac{I}{c} = \frac{bd^2}{6}$$

Thus

$$\sigma = \text{Modulus of Rupture} = (Pa)\left(\frac{6}{bd^2}\right)$$

$$\text{Modulus of Rupture} = \frac{6\ Pa}{bd^2}$$

The two point formula given in Section IX differs from the above since the method of applying the load in tests conducted and reported therein assumes a total load of P. Half of this load $\frac{P}{2}$ is assumed to be acting at each of the load points in the illustration above. Thus the modulus of rupture would be

$$\text{M of R} = \frac{6\left(\frac{P}{2}\right)a}{bd^2} = \frac{3\ Pa}{bd^2}$$

2. Volume of Test Specimen Under Stress

The moment diagrams applicable to the two loading technique are illustrated below:

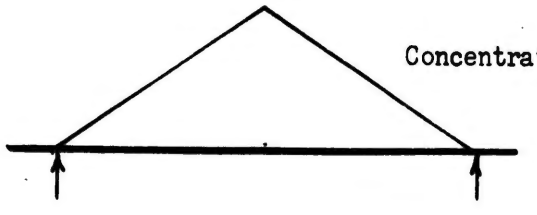

Concentrated Load at Center

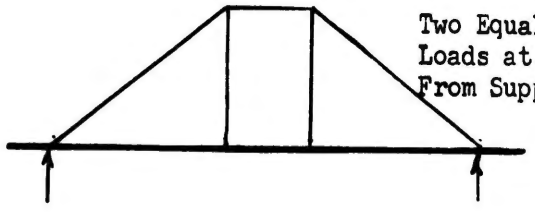

Two Equal Concentrated Loads at Equal Distances From Supports

A greater volume of the specimen under test is subjected to stress using the two point technique. It may be assumed that the results obtained using the two point technique will reflect to a greater degree flaws that may exist in the material being tested. The flaws will result in lower strength values. This theory is supported by data shown in Table VIII. Test results on dense silicon carbide specimens 6" x 1/2" x 1/4" both "as fabricated" and ground, show that the two point technique results in lower modulus of rupture values than the one point technique.

In the same manner a greater volume of material is subject to stress when larger test specimens are used. Thus average modulus of rupture values obtained using a two point technique on ground 6" x 1/2" x 1/4" specimens (16,300 psi) was less than obtained on ground 5" x 1/4" x 1/4" specimens (19,800 psi) using the same span (Table VIII).

The span of the specimen under test influences the modulus of rupture value obtained. The loading technique used in determining modulus of rupture puts the test specimen under compression and under tension. As the span is increased, more of the cross section of the specimen is subject to tension. Since ceramic materials are usually considerably weaker in tension than compression, increasing the span results in a lower average modulus of rupture. This is illustrated in Table VIII by the data on specimens having the same cross section. It is shown that the 3" x 1/2" x 1/4" specimens tested at a span of 2" had an average modulus of rupture of 36,100 psi. Specimens 6" x 1/2" x 1/4" tested at a span of 4" had an average modulus of rupture of 17,500 psi.

3. Surface Finish

It is believed important to establish the effect of surface finish on the strength of brittle materials. Fabrication may involve some grinding or polishing operation. Based on rather limited data it appears that polishing or grinding dense silicon carbide lowers the strength as reflected by average modulus of rupture values. Tests conducted in this program show that lower values are obtained on ground specimens regardless whether one point or a two point loading technique is used. This is illustrated by data given in Table VIII. The ground 6" x 1/2" x 1/4" test specimens had average modulus of rupture values of 17,500 psi and 16,300 psi using one point and two point loading techniques respectively. The "as fabricated" specimens had average modulus of rupture values of 20,500 psi and 18,800 psi using one point and two point loading techniques.

Although no positive explanation can be given at this time for this phenomena, it is theorized that polishing and/or grinding the dense silicon carbide induces stresses in the specimens resulting in a lower over-all strength.

D. Analysis of Test Data

Although no single theory of strength has been established for brittle materials, the flaw concept appears satisfactory to a number of investigators. Battelle Memorial Institute has conducted extensive studies related to the theories of strength and their applicability to brittle materials (References 36 and 37). Although the mechanism responsible for failure cannot be adequately defined, the strength characteristics observed can be approximated to the first degree by statistical methods. For apparently identical specimens tested under identical conditions, it is possible that no two specimens would fail under the same load but that the scatter of the results could be defined statistically and the probability of failure occurring under a given loading could be predicted. The probability fraction found most useful in Battelle studies was one proposed by Weibull:

$$S = 1 - e^{-V\left(\frac{\sigma - \sigma_u}{\sigma_o}\right)^m}$$

S = probability of failure at stress σ

e = Napierian logarithm 2.71828

V = volume or area subjected to stress

σ = stress level of interest

σ_u = stress at which there is zero probability of failure

σ_o = constant characteristic of the material which may be considered as a reference stress level

m = constant characteristic of the material which indicates the number and severity of flaws. Increasing values of m indicate decreasing variability in strength data.

A basic variation of the Weibull theory follows:

$$\left(\frac{X_1}{X_2}\right)_{\text{bending}} = \left(\frac{X_1}{X_2}\right)_{\text{tension}} = \left(\frac{N_2}{N_1}\right)^{\frac{1}{m}}$$

X = mean fracture strength

1, 2 = refer to specimen size

N = specimen size (volume or surface area)

m = Weibull material constant

Since it is not known whether fracture is volume or surface sensitive the following equations are used to determine the Weibull constant m:

$$\left|\frac{X_1 \text{ bending}}{X_1 \text{ tension}}\right| = \left|\frac{X_2 \text{ bending}}{X_2 \text{ tension}}\right| = (2m + 2)^{\frac{1}{m}}$$

Although the number of test points was very limited, the material constant m was calculated in this study for the "as fabricated" KT SiC and the ground KT SiC. The method employed to calculate the constant m was to plot the log log $\left|\frac{1}{1 - \text{Probability}}\right|$ against the log of failure stress. The slope of the line was taken to be the constant m. The number of test points available does not allow a conclusion on the material constant m. However, for exploratory purposes a constant m of 1.99 was obtained on ground KT specimens, and a constant m of 4.70 was obtained on "as fabricated" KT specimens. Data available on the 6" x 1/2" x 1/4" specimens was used (see Table VIII).

The constant m was also calculated as follows:

$$\left|\frac{X_1}{X_2}\right| = \left|\frac{N_2}{N_1}\right|^{\frac{1}{m}}$$

$$\left|\frac{16{,}300 \text{ psi}}{19{,}800 \text{ psi}}\right| = \left|\frac{\frac{1}{16} \text{ cu.in.}}{\frac{1}{8} \text{ cu.in.}}\right|^{\frac{1}{m}}$$

$$0.824 = (0.5)^{\frac{1}{m}}$$

$$\log 0.824 = \frac{1}{m} \log 0.5$$

$$(9.9159\text{-}10) = \frac{1}{m} (9.6989\text{-}10)$$

$$m = \frac{9.6989\text{-}10}{9.9159\text{-}10} = \frac{-.3011}{-.0841} = 3.58 \quad \text{if material is volume sensitive}$$

$$\left|\frac{X_1}{X_2}\right| = \left|\frac{N_2}{N_1}\right|^{\frac{1}{m}}$$

$$\left|\frac{16{,}300 \text{ psi}}{19{,}800 \text{ psi}}\right| = \left|\frac{1.0 \text{ sq.in.}}{1.5 \text{ sq.in.}}\right|^{\frac{1}{m}}$$

$$0.824 = 0.667^{\frac{1}{m}}$$

$$\log 0.824 = \frac{1}{m} \log 0.667$$

$$m = \frac{\log 0.667}{\log 0.824} = \frac{9.8241-10}{9.9159-10}$$

$$m = \frac{-0.1759}{-0.0841} = 2.09 \text{ assuming material is surface sensitive.}$$

The value of m = 2.09 based on ground KT silicon carbide data compares very favorably with the theoretical m = 1.99 obtained in evaluating the ground KT specimens. Based on this very limited data it appears that the KT silicon carbide specimens which have been ground may be surface sensitive if the m values are assumed to be correct. However, using a larger number of specimens under Contract AF33(616)-6034 a value of m = 4.75 was obtained on a series of ground specimens. This discussion is based on a limited number of tests. The results must be considered exploratory. A more comprehensive test program would undoubtedly yield data which would be more reliable.

The variability of crystalline forms and sizes; the variability of number, shape, size and location of surface and volume flaws; the variability introduced by impurities; the variability introduced by machining and other fabrication techniques; - plus brittleness - reflect in the lack of a simple correlation between the properties and geometry of silicon carbide. A statistical approach appears feasible and the most practical way of dealing with such brittle material.

A detailed statistical evaluation will be made to evaluate the properties of coated graphite, in partial fulfillment of Contract AF33(616)-6034.

TABLE VIII

ROOM TEMPERATURE MODULUS OF RUPTURE - DENSE SILICON CARBIDE

Specimen Size	Source of Data	Specimen Finish	Modulus of Rupture			
			One Point Load	Span	Two Point Load	Span
6" x 1/2" x 1/4"	Bell, Contract AF33(616)-5760	As Fabricated	20,500 psi	4"	19,200 psi	4"
6" x 1/2" x 1/4"	Bell, Contract AF33(616)-5760	Ground	17,500	4"	16,300	4"
5" x 1/4" x 1/4"	Bell, Contract AF33(616)-6034	Ground	No data	-	19,800	4"
3" x 1/2" x 1/4"	Bell, Contract AF18(600)-1607	Ground	36,100	2"	No data	-
3" x 1/2" x 1/4"	NAA (Reference 38)	Ground	No data	-	27,000	2-1/2"
3" x 1/2" x 1/4"	NAA (Reference 38)	As Fabricated	No data	-	16,000 ①	2-1/2"

Note ① Data is not considered reliable by Mr. Chipman, engineer conducting the test. Apparently samples supplied were not representative.

XI REFERENCES AND BIBLIOGRAPHY

1. Anon: "Durby" (Silicon-Bonded Silicon Carbide), Technical Data Sheet (no number), Carborundum Company, Niagara Falls, New York, November 1958

2. W. L. Wroten: Nitride-Bonded Silicon Carbide, Product Engineering, Vol. 28, McGraw-Hill Publishing Company, Incorporated, New York, New York, February 1957

3. Anon: Silicon Carbide-Bonded Graphite, Technical Data Sheet (no number), Carborundum Company, Niagara Falls, New York, 1958

4. Anon: "GRB" Silicon Carbide, Technical Data Sheet (no number), Carborundum Company, Niagara Falls, New York, 1958

5. Anon: "GRB" Silicon Carbide (Silicon Carbide Bonded Graphite), Advanced Materials Technology, Vol. 1, No. 5, Carborundum Company, Niagara Falls, New York, December 1958

6. K. M. Taylor: Improved Silicon Carbide for High Temperature Parts, Materials and Methods, Vol. 44, No. 10, Reinhold Publishing Company, New York, New York, October 1958

7. K. M. Taylor: KT Silicon Carbide, A New High Density Silicon Carbide Body, Technical Paper, Carborundum Company, Niagara Falls, New York

8. L. D. Loch: Above 2500 F, What Material to Use?, Chemical Engineering, Vol. 65, No. 13, McGraw-Hill Publishing Company, Incorporated, New York, New York, June 1958

9. Anon: KT Silicon Carbide, Technical Bulletin (no number) Carborundum Company, Niagara Falls, New York

10. R. W. Brown: High Temperature Nonmetallics, Chemical Engineering, Vol. 65, No. 8 McGraw-Hill Publishing Company, Incorporated, New York, New York, April 1958

11. Anon: Mechanical and Electrical Properties of Alsimag Ceramics, Technical Data Chart 591, American Lava Corporation, Chattanooga, Tennessee

12. E. D. Bell: Silicon Carbide - Alsimag 687, letter to J. M. Nowak, Bell Aircraft Corporation from American Lava Corporation, Chattanooga, Tennessee, July 8, 1958

13. E. D. Bell: Silicon Carbide Materials - Alsimag 539 and Alsimag 687, letter to H. G. DeBan, Bell Aircraft Corporation from American Lava Corporation, Chattanooga, Tennessee, April 7, 1959

14. Anon: Stabilized Crystolon Ceramics, Technical Bulletin 686 NP-1, New Products Department, Norton Company, Worcester, Massachusetts

15. Anon: Silicon Carbide Foam, Technical Data Sheet (no number), Carborundum Company, Niagara Falls, New York 1959

16. Anon: Silicon Carbide, Materials in Design Engineering, Materials Selector Reference Issue, Vol. 48, No. 5, Reinhold Publishing Company, New York, New York, 1958

17. V. E. Wolkodoff: Letter to R. Horwath, Bell Aircraft Corporation from Carborundum Company, Niagara Falls, New York, October 1, 1958

18. Anon: Protection for Silicon Carbide at 3000 F, Product Engineering, Vol. 29, No. 14, McGraw-Hill Publishing Company, Incorporated, New York, New York, April 1958

19. C. C. Kane: Letter to H. G. DeBan, Bell Aircraft Corporation from Product Engineering, McGraw-Hill Publishing Company, Incorporated, New York, New York, May 21, 1959

20. W. C. Riley, W. G. Coppins, W. A. Hedden, W. H. Duckworth: The Effect Of Nuclear Radiation on Ceramic Materials, REIC Report No. 2-C, The Radiation Effects Information Center, Battelle Memorial Institute, Columbus, Ohio, June 1958 - (SECRET)

21. Anon: Typical High Temperature Material Erosion Test Data, Carborundum Company, Niagara Falls, New York, October 1958

22. Anon: Typical High Temperature Material Surface Ablation Test Data, Carborundum Company, Niagara Falls, New York

23. Anon: Non-Destructive Testing, Part I: Developments in the Application of Ultrasonic Flaw-Detection to Raw Material Inspection, Correlation of Data and Coding of Defective Materials, Aircraft Production, Vol. 20, No. 8, Iliffe and Sons Limited, London, England, August 1958

24. H. P. Klug, L. E. Alexander: X-Ray Diffraction Procedures for Polycrystalline and Amorphous Materials, John Wiley and Sons Incorporated, New York, New York, 1954

25. S. R. Maloof, H. R. Erard: Critical Evaluation of the Norelco High Anode X-Ray Spectrometer for Elastic Strain Measurements, The Review of Scientific Instruments, Vol. 23, No. 12, December 1952

26. H. R. Erard, G. L. Underhill: Residual Stress Analysis by X-Ray Diffractometer, Report SA-TR20-2403, Springfield Armory Research and Development Division, Springfield, Massachusetts, August 1954

27. H. S. Peiser, H. P. Rooksby, A. J. C. Wilson: X-Ray Diffra
Polycrystalline Materials, Reinhold Publishing Company, New
New York, 1955

28. O. W. Eshbach: Handbook of Engineering Fundamentals, John
and Sons Incorporated, New York, New York, 1952

29. J. B. Wachtman, Jr., D. C. Lam, Jr.: Young's Modulus of Va
Refractory Materials As A Function Of Temperature, Journal
American Ceramic Society, May 1959

30. G. Pickett: Equations for Computing Elastic Constants From
and Torsional Resonant Frequencies of Vibration of Prisms an
Cylinders, ASTM Proceedings, Vol. 45, 1945

31. W. H. Dukes, F. M. Anthony, H. A. Pearl: Investigation of F
of Utilizing Available Heat Resistant Materials for Hyperson
Edge Applications, Third Quarterly Progress Report, Report N
7008-0252-009, Bell Aircraft Corporation, Buffalo, New York,
1959

32. C. Zener: Elasticity and Anelasticity of Metals, University
Press, Chicago, Illinois, 1948

33. J. C. Jaeger: Elasticity, Fracture and Flaw, John Wiley an
Incorporated, New York, New York, 1956

34. C. West: The Metallurgical Use of Anelasticity, Modern Res
Techniques in Physical Metallurgy, American Society for Met
Cleveland, Ohio, 1953

35. J. B. Wachtman, Jr., W. E. Teft: Effect of Suspension Positi
Apparent Values of Internal Friction Determined by Forster's
The Review of Scientific Instruments, Vol. 29, No. 6, June 19

36. O. K. Salmasey, E. G. Bodine, W. H. Duckworth, G. K. Manning:
Behavior of Brittle-State Materials, WADC Technical Report 5
Part II, June 1955

37. W. H. Duckworth, A. D. Schwope, O. K. Salmasey, R. L. Carson,
H. Z. Schofield: Mechanical-Property Tests On Ceramic Bodies
WADC Technical Report 52-67, March 1952

38. R. D. Chipman: Stress-Strain-Temperature-Time Relationships
Refractory Materials, Technical Paper, no number, Atomic Inte
Division, North American Aviation Incorporated, Canoga Park,
California

UNCLASSIFIED